JPL PUBLICATION 77-41, VOLUME I

Voyager Electronic Parts Radiation Program

Volume I: Final Report

National Aeronautics and Space Administration

Jet Propulsion Laboratory
California Institute of Technology
Pasadena, California 91103

TECHNICAL REPORT STANDARD TITLE PAGE

1. Report No. JPL Pub. 77-41	2. Government Accession No.	3. Recipient's Catalog No.
4. Title and Subtitle Voyager Electronic Parts Radiation Program (Volume I)		5. Report Date September 15, 1977 6. Performing Organization Code
7. Author(s) A. G. Stanley/K. E. Martin/W. E. Price		8. Performing Organization Report No.
9. Performing Organization Name and Address JET PROPULSION LABORATORY California Institute of Technology 4800 Oak Grove Drive Pasadena, California 91103		10. Work Unit No. 11. Contract or Grant No. NAS 7-100 13. Type of Report and Period Covered JPL Publication
12. Sponsoring Agency Name and Address NATIONAL AERONAUTICS AND SPACE ADMINISTRATION Washington, D.C. 20546		14. Sponsoring Agency Code

15. Supplementary Notes

16. Abstract

In the final report for the Voyager parts radiation program, the program philosophy, radiation, environment, device hardening efforts, and radiation test methods are discussed in detail. In addition, the results of characterization testing and sample screening of over 200 device types, in a radiation environment, are summarized.

17. Key Words (Selected by Author(s))	18. Distribution Statement
Space Radiation	Unclassified - Unlimited

19. Security Classif. (of this report)	20. Security Classif. (of this page)	21. No. of Pages	22. Price
Unclassified	Unclassified	210	

HOW TO FILL OUT THE TECHNICAL REPORT STANDARD TITLE PAGE

Make items 1, 4, 5, 9, 12, and 13 agree with the corresponding information on the report cover. Use all capital letters for title (item 4). Leave items 2, 6, and 14 blank. Complete the remaining items as follows:

3. Recipient's Catalog No. Reserved for use by report recipients.

7. Author(s). Include corresponding information from the report cover. In addition, list the affiliation of an author if it differs from that of the performing organization.

8. Performing Organization Report No. Insert if performing organization wishes to assign this number.

10. Work Unit No. Use the agency-wide code (for example, 923-50-10-06-72), which uniquely identifies the work unit under which the work was authorized. Non-NASA performing organizations will leave this blank.

11. Insert the number of the contract or grant under which the report was prepared.

15. Supplementary Notes. Enter information not included elsewhere but useful, such as: Prepared in cooperation with... Translation of (or by)... Presented at conference of... To be published in...

16. Abstract. Include a brief (not to exceed 200 words) factual summary of the most significant information contained in the report. If possible, the abstract of a classified report should be unclassified. If the report contains a significant bibliography or literature survey, mention it here.

17. Key Words. Insert terms or short phrases selected by the author that identify the principal subjects covered in the report, and that are sufficiently specific and precise to be used for cataloging.

18. Distribution Statement. Enter one of the authorized statements used to denote releasability to the public or a limitation on dissemination for reasons other than security of defense information. Authorized statements are "Unclassified—Unlimited," "U. S. Government and Contractors only," "U. S. Government Agencies only," and "NASA and NASA Contractors only."

19. Security Classification (of report). NOTE: Reports carrying a security classification will require additional markings giving security and downgrading information as specified by the Security Requirements Checklist and the DoD Industrial Security Manual (DoD 5220.22-M).

20. Security Classification (of this page). NOTE: Because this page may be used in preparing announcements, bibliographies, and data banks, it should be unclassified if possible. If a classification is required, indicate separately the classification of the title and the abstract by following these items with either "(U)" for unclassified, or "(C)" or "(S)" as applicable for classified items.

21. No. of Pages. Insert the number of pages.

22. Price. Insert the price set by the Clearinghouse for Federal Scientific and Technical Information or the Government Printing Office, if known.

JPL PUBLICATION 77-41, VOLUME I

Voyager Electronic Parts Radiation Program

Volume I: Final Report

Alan G. Stanley
Keith E. Martin
William E. Price

September 15, 1977

National Aeronautics and
Space Administration

Jet Propulsion Laboratory
California Institute of Technology
Pasadena, California 91103

Prepared Under Contract No. NAS 7-100
National Aeronautics and Space Administration

PREFACE

The work described in this report was performed by the Information Systems Division of the Jet Propulsion Laboratory under the cognizance of the Voyager Project.

Documents outlining the conditions and requirements of the test program, which make up Appendixes A through E of this report, will be published as Volume II. These Appendixes are as follows:

Appendix A -- Electron Simulation Radiation Test Specification for Voyager Electronic Parts and Devices

Appendix B -- Electronic Piece-Part Testing Program for Voyager

Appendix C -- Test Procedure for Radiation Screening of Voyager Piece Parts

Appendix D -- Boeing In Situ Test Fixture

Appendix E -- Irradiate - Anneal (IRAN) Screening Documents

The Voyager Project was formerly designated the Mariner Jupiter/Saturn 1977 Project, and some of the publications cited in this report bear the earlier Project nomenclature.

DEFINITION OF IDENTIFICATION CODES

Subsystem Identification Codes

Abbreviation	Subsystem Name	Division
STRU	Structure	35
RFS	Radio Frequency	33
MDS	Modulation/Demodulation	33
PWR	Power	34
CCS	Computer Command	36
FDS	Flight Data	36
AACS	Attitude & Articulation Control	34
PYRO	Pyrotechnic	38
CABL	Cabling	35
PROP	Propulsion	38
TEMP	Temperature Control	35
DEV	Mechanical Devices	35
DSS	Data Storage	36
CRS	Cosmic Ray	29
PRA	Planetary Radio Astronomy	29
PWS	Plasma Wave	29
LECP	Low Energy Charged Particle	29
PPS	Photopolarimeter	29
PLS	Plasma	29
UVS	Ultraviolet Spectrometer	29
MAG	Magnetometer	29
ISS	Imaging Science	82
IRIS	Infrared Interferometer Spectrometer	29

Vendor Identification Codes

JPL Alphabetical Code	FSCM Number	Vendor
ADI	24355	Analog Devices, Inc., Norwood, Mass.
ANA	31855	Analog Technology Corporation
CAD	19647	Caddock Electronics, Division of Globe Union, Inc.
CRC	12517	Component Research Company, Inc.
CTI		Circuit Technology, Inc.
DAL	91637	Dale Electronics, Inc., Subsidiary of the Lionel Corporation
DIK	12954	Dickson Electronics Corporation
EXR	52063	Exar Integrated Systems, Inc.
FAS	07263	Fairchild Semiconductors, Division of Fairchild Camera and Instrument Corp.
GEC	09214	General Electric Company, Semiconductor Products Dept.
HAR	91417	Harris Semiconductor (Radiation, Inc.)
HON	91929	Honeywell, Inc., Microswitch Division
HPA	28480	Hewlett-Packard Company
INL	32293	Intersil Inc., Cupertino, Cal.
KMC	20754	KMC Semiconductor
MOT	14713	Motorola Semiconductor Products, Inc.
NSC	27014	National Semiconductor Corporation
PMI	06665	Precision Monolithics, Inc., Santa Clara, California

Vendor Identification Codes
(Continuation 1)

JPL Alphabetical Code	FSCM Number	Vendor
RAY	49956	Raytheon Company
RCA	02735	RCA Corp., Solid State Division, Somerville, N. J.
SET	14099	Semtech Corporation
SGN	18324	Signetics Corp., Subsidiary of Corning Glass Works
SIL	17856	Siliconix, Inc.
SOD	13327	Solitron Devices, Inc.
TIX	01295	Texas Instruments, Inc., Semiconductor Components Div.
TRW	01281	TRW Semiconductor, Inc., (PSI)
UTR	12969	Unitrode Corp.
WEC	05277	Westinghouse Electric Corp., Semiconductor Division

ABSTRACT

In the final report for the Voyager parts radiation program, the program philosophy, radiation, environment, device hardening efforts, and radiation test methods are discussed in detail. In addition, the results of characterization testing and sample screening of over 200 device types, in a radiation environment, are summarized.

CONTENTS

Figures

Tables

SECTION I

INTRODUCTION

This final report summarizes the parts radiation program for the Voyager spacecraft which will be launched in 1977 and will pass Jupiter in 1979. Pioneer spacecraft have measured large fields of electrons and protons trapped in Jupiter's magnetic field. Because these radiation fields are potentially damaging to the sophisticated electronic systems of Voyager, a program to radiation-harden the systems was necessary (see Section II, Radiation Environment, and Section VI, Device Hardening).

The purpose of the parts radiation program was to provide devices capable of meeting the environmental requirements or, if necessary, to provide data from which to determine how to harden the circuits or to shield the parts. In the device characterization tests, the general radiation sensitivity levels of approximately 200 different device types were determined under the specific bias conditions used in the spacecraft. More than 230 integrated circuit (IC) and transistor radiation screening tests were conducted, and more than 13,000 CMOS devices were radiation screened (see Section IV, Electronic Parts Radiation Program).

The electron radiation was provided by a 2.0- to 2.5-MeV Dynamitron, and in the case of the CMOS and the Irradiate-Anneal (IRAN) program, a cobalt 60 source was used (see Section V, Radiation Testing and Dosimetry). The devices were always electrically biased during irradiation, using the worst-case spacecraft circuit conditions and measured <u>in situ</u> within 5 min after the end of radiation exposure. The majority of the circuits had been designed before the necessity for considering the radiation environment was understood. Consequently, the first step was a worst-case analysis of the completed designs, making use of an existing radiation effects data base. This was supplemented as rapidly as possible by data from device characterization tests more representative of the Jupiter radiation environment.

The results of the analysis and characterization tests led to circuit redesign, the substitution of harder components, spot shielding, and a comprehensive screening program. This multifaceted screening program was designed to ensure that the flight devices performed in the same manner as the devices in the characterization tests (see Section III, Radiation Program Philosophy). Because of time and cost restraints, only those devices from the Voyager parts usage that were known to be sensitive to radiation were tested. Section VII covers the characterization test results, and Section VIII covers the screening test results.

Complete detailed test results for the individual device types are presented in Reference 1-1.

SECTION II

RADIATION ENVIRONMENT

A. INTRODUCTION

The Voyager spacecraft was designed to function within specification during and after exposure to Earth and Jupiter radiation belts, large solar proton events, solar wind protons, galactic cosmic radiation, and radiation from the Radioisotope Thermoelectric Generators (RTG) and Radioisotope Heater Units (RHU). The greatest radiation damage to the electronics is caused by the electrons of the Jupiter belts.

B. EXTERNAL NATURAL SPACE RADIATION

The Jupiter radiation model is based on the results of the three Pioneer 10 and 11 particle experiments.

The electron spectra were derived using the results of integrations along the Jupiter-Saturn-Io (JSI) trajectory including peak fluxes. The proton spectra were derived using the results of integrations along the Jupiter-Saturn-Ganymede (JSG) trajectory.

The Voyager program is oriented toward an equatorial flyby mission with perijove ≤ 5 R_J.

A definition of the environment is shown in Table 2-1. A more detailed description of the external radiation environment may be found in Reference 2-1.

The solar flare proton fluence made a negligible contribution to the total proton environment except at the very highest energies. The 95 percent probability solar flare fluence was considered in the characterization of the environment.

C. RTG AND RHU RADIATION

The RTG and RHU radiation models were based on the following nuclear characteristics:

RTG Power	2400 watt (th)
RHU power	1 watt (th)
Fuel age	10-year-old ^{238}Pu
Fuel form when manufactured	PPO with 1.2 ppm of ^{236}Pu, ^{232}U, and ^{228}Th
Neutron emission	7×10^3 n/s-g ^{238}Pu excluding self-multiplication

Table 2-1[a]. Charged Particle and Nuclear Radiation[a]

Environment	Bus-Mounted Electronics and Science Instruments		Non-Bus-Mounted Science Instruments	
	Peak Flux (cm^{-2}-s^{-1}) Unshielded	Fluence (cm^{-2}) Unshielded	Peak Flux (cm^{-2}-s^{-1}) Unshielded	Fluence (cm^{-2}) Unshielded
Proton[b]	9×10^7 E > 1 MeV	5×10^{12} (20 MeV Eq.)	9×10^7 E > 1 MeV	5×10^{12} (20 MeV Eq.)
Electron	2×10^8 E > 0.4 MeV	4×10^{12} (3 MeV Eq.)	2×10^8 E > 0.4 MeV	4×10^{12} (3 MeV Eq.)
RTG and RHU Neutron ($1.0 \leq E \leq 3.0$ MeV)	4 rad (Si)s 80	2×10^5rad(Si) 1×10^{10}	4 rad(Si)s 10	2×10^5rad(Si) 1×10^9
RTG and RHU Gamma ($0.3 \leq E \leq 3.0$ MeV)	3200	1×10^3[c]	350[d]	100[c]

[a]From Table 18, "Functional Requirement, Mariner Jupiter/Saturn 1977 Environmental Design Requirements," MJS77-3-240, Jet Propulsion Laboratory, Pasadena, Calif., March 14, 1975 (JPL Internal Document).

[b]Proton flux and fluence assume a 1-MeV cutoff. Proton levels for true external surface problems will be higher than those above. The level is 3.1×10^8 rad(Si).

[c]Ionization dose controlled by electron and proton environment.

[d]Value for scan platform instruments location.

The neutron fluence and gamma dose values shown in Table 2-1 are integrated values over 4 years and are total spectrum values having an average energy in the ranges of $0.3 \leq E \leq 3.0$ MeV for gammas and $1.0 \leq E \leq 3.0$ MeV for neutrons.

D. INTERNAL ENVIRONMENT

The internal environment is dominated by the penetrating electrons, which generate surface ionization effects in semiconductor devices as well as rate effects in sensitive optical devices. The contribution of the electrons to displacement damage is very small. The total internal proton fluence is insufficient to cause significant displacement damage, and the ionization effects caused by protons are much less than those caused by electrons. The neutron fluence from the RTG's and RHU's is insufficient to cause significant displacement damage. The ionization effect caused by the gamma-rays from the RTG's and RHU's is much less than that of the electrons.

The levels in Table 2-1 are external (unshielded) environments containing no margins. Parts environments were controlled by the application of shielding as required, to satisfy the established design margins. The radiation design margin is defined as the ratio of the part (or component) capability in a given current application to the local ambient environment. For Voyager, the radiation design margin for electrons was based strictly on dose, since ionization is the dominant damage mechanism. The electron dose radiation design margin was 2 for engineering subsystems and the imaging science subsystem and was a minimum of unity for all other science instruments. For protons, where displacement damage is of most concern (except for exterior spacecraft surfaces) the radiation design margin was based on displacement fluence and was the same as that applied to electron dose for the subsystems listed. The radiation design margin for interference effects was related to charged particle flux and is the same as is defined above for the engineering and science subsystems, except for the imaging subsystem, where the radiation design margin for flux was unity.

In addition, electronic parts had to be capable of operating within limits specified by the cognizant engineer for the particular functional application, during and after exposure to the radiation levels shown in Table 2-2.

If the electronic parts did not satisfy these requirements or if spot shielding had to be added to provide the radiation design margins, waivers were written by the cognizant engineer of the subsystem in which the discrepancy existed. The waiver contained the proposed design values for parts capability and shielded environment, and an estimate of added shielding mass, if any. These waivers provide a permanent record of special radiation design requirements, a control mechanism for shielding mass allocations, and a systematic method of reviewing and controlling special shielding requirements.

Table 2-2. Electronic Parts Capability

Environment	Displacement Damage	Ionization Damage
Proton	1 x 10^{10} p/cm^2 (20-MeV equivalent)	Electrons dominate[a]
Electron	Ionization dominates	60 krad(Si)
Neutron	1 x 10^{10} n/cm^2 (1-MeV equivalent)	Negligible effect
Gamma	Negligible effect	Electrons dominate

[a]Except for true external spacecraft surfaces.

SECTION III

RADIATION PROGRAM PHILOSOPHY

A. GENERAL CONSIDERATIONS

The Voyager radiation program was intended to provide confidence that the spacecraft will perform within acceptable limits during and after Jupiter encounter and at Saturn, within a limited allowance for radiation effects. This was achieved by limited investigations of known sensitive areas.

The investigations were conducted primarily at the parts level, with limited circuit tests to assess interference effects. Subsystem tests were not carried out except on a very limited basis during the early phases of the program. Subsystem tests are generally ineffective due to insufficient sample size, parametric variations with lot, and inadequate analysis of extreme conditions including minimum pre-irradiation specifications, temperature and aging effects.

Most of the characterization data were obtained with a monochromatic 2.5-MeV electron beam from a Dynamitron. Although this differs substantially from the exponential Jupiter spectrum, the effects are practically the same, since total dose effects depend only on the energy absorbed by the device in rad(Si). Although the tests were carried out at flux rates at least one order of magnitude greater than those experienced in the Jupiter environment, this fact does not in any way change the magnitude of the effects, and this was experimentally verified in several instances. Synergistic effects are not expected to play any role in the Jupiter environment.

The overall program was carried out in three phases as shown below:

Phase I - Circuit design analysis.

- Device radiation characterization.
- Shielding analysis.

Phase 2 - Substitution of components.

- Circuit redesign.
- Shielding analysis and additional shielding.
- Modification of components.

Phase 3 - Screening of sensitive flight devices.

The majority of circuits had been designed before the necessity for considering the radiation environment was understood. Consequently, the first step was an analysis of the completed designs, making use

of an existing radiation effects data base. This was supplemented as rapidly as possible by device characterization data more representative of the Jupiter radiation environment. A review of the first phase of the program led to circuit redesign and the substitution of harder components. A multifaceted screening program was instituted to ensure that the flight devices would perform as well as the comparable items in the characterization tests.

The ability of the subsystems to meet the radiation environment was accomplished by using the following priority:

(1) Direct replacement of parts from the Voyager parts lists.

(2) Circuit redesign.

(3) Radiation-hardened parts, developed through the negotiation of special processes and screening.

(4) Addition of shielding mass.

The overall approach may be illustrated with reference to bipolar transistors, many of which exhibit outliers[1] with significantly worse radiation behavior (see Section VIII-C-5). A review of the test data, the inherent radiation environment at Jupiter, and the worst-case circuit requirements led to the identification of specific radiation problems (see Figure 3-1). A study was then made of the location of the parts with respect to the radiation environment so as to evaluate spot-shielding and radiation-screening possibilities, new procurements, and schedule needs. Additional radiation experiments were performed if required. The problem was then reviewed with the subsystem personnel to see if circuit changes were possible. A final review with the project office led to the final approach, which usually took the form of selective parts screening, selective shielding, or the selection of devices with a high pre-irradiation dc gain.

Device characterization and screening (described in Section IV) were handled by the Radiation Effects Group. Hardening by device modification (described in Section VI) was attempted for a number of device types by the manufacturer. Circuit analysis and radiation shielding analysis were carried out by other personnel and are briefly discussed here to complete the picture of the total radiation effort.

[1]An "outlier" is defined as a data point that does not fall within 3σ of the mean value of that parameter at the lowest value of the independent variable.

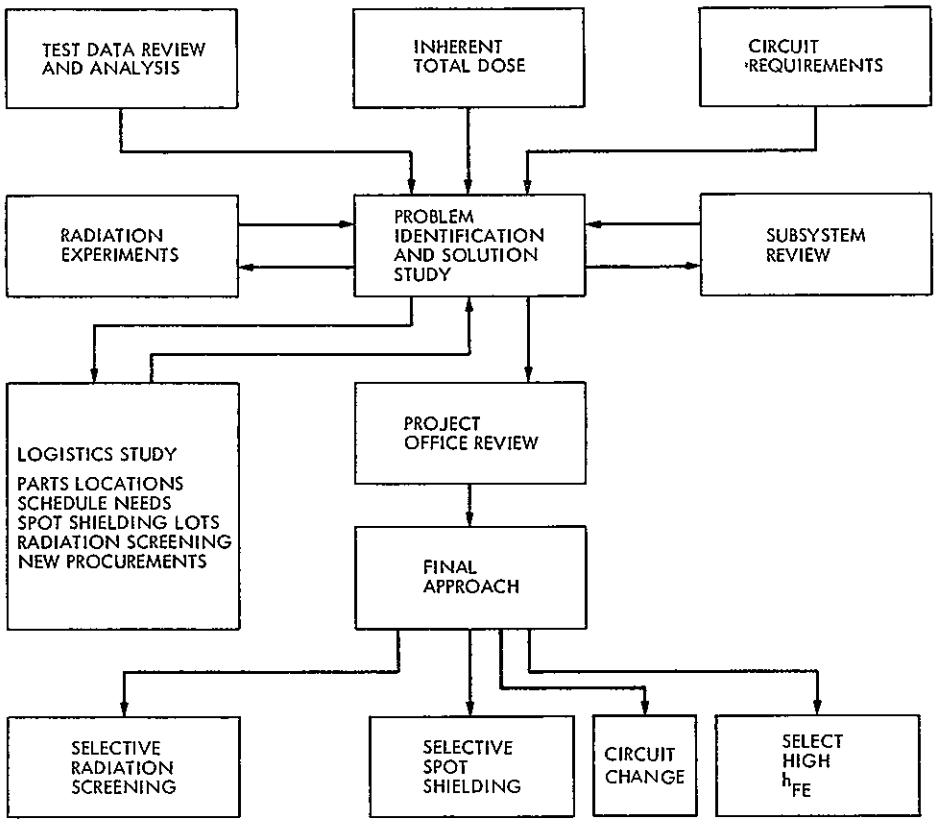

Figure 3-1. Radiation Evaluation Method

b. CIRCUIT ANALYSIS

1. Worst-Case Analysis

The radiation parts capability was determined for each application by combining the characterization test data described in Section VII with a worst-case circuit analysis. A compilation of such parts capability values is given in Reference 3-1. The parts capability is a number of krad(Si), which can be compared to the expected dose to determine the spot shielding requirements, taking into account radiation design margins.

A worst-case circuit analysis was performed for all circuits of each subsystem to assure that the electronic parts will function properly in the radiation environment. These analyses provided an efficient means for pinpointing radiation problems and establishing areas where design modifications were required.

The circuit worst-case analysis was required for all designs to demonstrate sufficient operating margin for all operating conditions of the individual circuits as a combined function of the following:

(1) Temperature design limits (typically -20°C to +85°C).

(2) Piece-part tolerance.

(3) Part aging and drift.

(4) Special piece-part factor, such as shock, vibration, or vacuum, where such conditions would contribute to variations in circuit parameter.

(5) Voltage and frequency tolerances.

(6) Radiation environment.

The worst-case analysis was performed by degrading first for temperature and life (aging) and then for radiation to obtain the final degraded value. The analysis is a worst case, in that the value for each of the variable parameters is set to limits that will drive the output to maximum or minimum and also considers ac, dc, and transient component effects on the circuit. For circuits consisting entirely of interconnected digital integrated circuits, the only consideration required for worst-case analysis are fan-out, fan-in, and power supply margins, with some considerations to propagation delays and "race" conditions. For the latter circuits, radiation analysis was not performed, because of the inherent hardness.

The analysis was conducted by utilizing:

(1) Schematic representation of the circuit.

(2) Performance specification for all piece parts.

(3) Performance criteria for the circuit.

(4) Description of all operating conditions and environmental factors, including radiation effects data for the electronic piece parts.

The analysis was constantly iterated as the design changed, to meet the margin requirements. In some cases temperature margin over the fuel range of +20°C to +85°C was sacrificed to allow for radiation degradation. In the remaining cases, the circuit, or the amount of radiation experienced by the part, did not permit this tradeoff.

Circuit analysis was a valuable tool to identify critical parts and parameters so as to assess radiation effects during radiation design reviews. The analysis was updated after all design modifications had been made and mass shielding had been added to the spacecraft. The final analysis provided the basis for establishing that the design was adequate from a radiation effects point of view.

2. Radiation Reviews

A preliminary radiation review was conducted for each engineering and science subsystem. The purpose of this review was to identify elements in the subsystem design that were particularly sensitive to radiation effects and to consider design approaches for radiation hardening the subsystems where required. The radiation reviews were attended by the design engineers, circuit analyst, parts radiation effects personnel, and representatives of the System Design Group and Spacecraft Systems Manager, who served as chairman.

The Preliminary Design Review was expanded to assure that the radiation design margin was adequately reflected in the design approach. The agenda included the results of exploratory radiation tests, the proposed packaging design approach to achieve maximum inherent shielding, circuit design rules, electronic parts sensitivity and test requirements, preliminary shielding analysis, special parts sensitivity, and potential effects on system design parameters.

The Critical Design Review (CDR) was modified to cover the radiation hardening solutions. The CDR covered the details of the design analysis, packaging approach, and detailed shielding analysis. The CDR included radiation problems previously identified and the expected radiation design margin.

A final Project-level radiation review was held in May 1976 in order to review the radiation-hardening program for the engineering subsystems and science instruments with respect to the best estimates of the radiation environment for three trajectory options. The results of the review were used to evaluate the associated mission risk and expected science return for these trajectory options in order to select the option for targeting.

C. RADIATION SHIELDING

1. Radiation Shielding Requirements

Radiation shielding was incorporated in the spacecraft bus so that the interior bus electronics would not be exposed to radiation levels exceeding those in Table 3-1.

Shielding was provided so that the radiation design margin (RDM), which is defined as the ratio of the capability to the shielded environment, was 2. Consideration was given to reducing the flux RDM for functions that do not jeopardize the mission subsequent to the electron exposure, if a significant cost or mass saving is involved.

For parts that had a capability of less than 60 krad(Si) from electrons or 1×10^{10} p/cm^2 (20 MeV equivalent), spot shielding was added unless it could be shown that the part was not exposed to the levels in Table 3-1 and that the RDM of 2 was maintained.

For other engineering subsystems and the imaging subsystem, radiation shielding (either general mass shielding applied to the subsystem or spot shielding applied to sensitive parts) was applied to provide an RDM of 2, with the exception that the minimum flux RDM for the imaging subsystem was 1. All other science instruments had a minimum RDM of 1.

2. Radiation Shield Analysis

Radiation levels were estimated for each subsystem, and if other hardening techniques were insufficient to raise allowable levels above these predicted levels, inherent or added shielding was employed to reduce the radiation environment. Because of the large shielding mass required to compensate for uncertainties in radiation environment, parts effects, and transport analyses, the goal in shielding design was to reduce radiation damage risk to shielded circuitry to an acceptable level rather than to zero.

Radiation levels at sensitive component locations were calculated using state-of-the-art radiation transport and shielding computer programs. Radiation transport calculations for isotropic electron and proton sources and spherical or slab shields included multiple scattering effects in the forward hemisphere. Fluence and dose attenuation kernels (radiation levels as a function of depth) and angular fluxes were generated for electrons, protons, and bremsstrahlung. The shielding computer program had the capability of parametrically adding shielding to specified surfaces in order to reduce the radiation to levels lower than those provided by the basic spacecraft geometry.

Table 3-1. Bus-Mounted Engineering Shielding Requirements

Environment	Flux	Displacement Fluence	Dose
Electron	RDM = 2	No requirement	30 krad(Si)
Proton	↓	5×10^9 p/cm^2 (20 MeV eq.)	No requirement
Neutron	↓	1×10^{10} n/cm^2 (1 MeV eq.)	No requirement
Gamma	↓	No requirement	No requirement

3. Radiation Shielding Support

Maximum radiation levels within all engineering subsystems were provided. Levels encountered by particular parts were computed only for those parts that did not meet the requirement of satisfactory performance at the appropriate safety margin (2 or 1 for engineering or science) and then the required shielding was determined.

D. TRANSIENT IONIZATION EFFECTS (INTERFERENCE)

We define interference as transient ionization effects that persist only while the electronics are being irradiated and whose severity is generally proportional to the dose rate. There are four types of interference in Voyager electronics:

(1) Primary photocurrents in low-current-sensitive input stages to the electronics.

(2) Electron emission from cathodes of electron-multiplier-type detectors.

(3) Ionization-induced conductivity in photosensitive materials, such as those in the Vidicon detector surface.

(4) Ionization-induced fluorescence in optical material such as detector windows and lenses (fluorescence efficiencies vary strongly with the kind of material).

Interference effects are dependent primarily on the rate of ionization energy disposition, i.e., the dose rate measured in rad(Si)/s. At the low rates of interest to Voyager, the effects are essentially proportional to dose rate. Interference effects at the relatively low peak dose rates (less than 10 rad(Si)/s at internal positions) can be important only in devices operating at extremely low currents. The effect of ionizing radiation on semiconductor devices can be represented by an equivalent current generator across reverse biased junctions (primary photocurrent) whose magnitude is up to 100 pA for low-power semiconductor devices exposed to 10 rad(Si)/s and whose magnitude is proportional to the instantaneous dose rate. Devices whose normal operating point is at currents in the μA or mA range will not be significantly affected by interferences.

Sensitive photodetectors capable of detecting single photons are sensitive to transient ionization effects. Interference effects in such devices must be measured in a separate test program reflecting actual operating conditions of the systems. A cobalt 60 source provides a suitable radiation environment for this purpose, whereas machines generating electrons also provide a source of rf noise that interferes with the measurement.

Interference effects can also occur at the cathode of electron multipliers because the quiescent currents are very low and the gain between the cathode and electronic circuitry is very high. The flux of secondary electrons emitted from a surface by passage through it of energetic electrons is about 5 to 10% of the incident electron flux.

Ionizing radiation will also affect optical materials. During excitation by ionizing radiation, a small fraction of the energy deposited may be reemitted as fluorescence. Typically, fluorescence efficiencies are much less than 1% unless the material has been carefully prepared to give high fluorescence efficiencies (e.g., nuclear particle scintillation detectors). Higher-purity optical materials (e.g., ultraviolet-grade fused silica) tend to have lower fluorescence efficiencies.

When the foregoing interferences are unacceptable, the following corrective techniques can be used:

(1) Use semiconductor devices with minimum junction area to minimize the primary photocurrents. Devices exhibiting less than 10 pA at 10 rad(Si)/s are available.

(2) The use of very pure fused silica, such as the ultraviolet-grade materials, will minimize fluorescence. In some materials the fluorescence yield is actually less than the Cerenkov radiation emitted by the fast electrons. An optical filter can sometimes be interposed between the glass and the detector to block the fluorescence wavelengths while passing the desired optical signal.

(3) There is no effective means of suppressing secondary electron emission from surfaces, other than shielding them from the incident electrons.

SECTION IV

ELECTRONIC PARTS RADIATION PROGRAM

A. PARTS RADIATION CHARACTERIZATION

1. Early Work

The earliest characterization tests on electronic components for Voyager grew out of the TOPS program and included low-level neutron, proton, and gamma tests, but were not related to the real Jupiter electron environment. The Voyager Project committee for materials and parts, formed in the beginning of 1974, commissioned some parts tests on the LINAC at Intelcom Rad Tech, La Jolla, Calif. At the same time various subsystems conducted interference tests on the Boeing Dynamitron. This was followed by a parts test on the Boeing LINAC and the cobalt 60 source at Hughes, Fullerton, monitored by JPL.

A separate Radiation Group was established at JPL in September 1974. All subsequent characterization tests were carried out in situ, using the Dynamitron at JPL and at Boeing as radiation sources. The maximum fluence was reduced to 1×10^{13} e/cm^2 in order to reduce the number of required data points. A change in the radiation model led to a further reduction to 5×10^{12} e/cm^2 after October 1975. The different experimental programs are summarized in Table 4-1.

2. Purpose and Scope

The parts radiation characterization program was designed to determine the radiation sensitivity of a part type with respect to a given application.

In the Voyager radiation environment, surface ionization effects are of prime importance, whereas bulk damage is of minor importance. For this reason, radiation tests were conducted on the following parts:

(1) Those known to be radiation-sensitive, to establish that the parts have a failure threshold that exceeds the design level of 60 krad(Si) for ionization damage.

(2) Those that do not satisfy the above requirement, to establish the amount of parameter degradation when exposed to radiation.

As a minimum, the parts characterization program placed the part type in one of the following categories contained in Reference 1-1 (see Section IV-A-8):

Table 4-1. History of Voyager Radiation Test Program

Date	Facility	Radiation Source	Type	In Situ	Max. Total Fluence/Dose	Energy, MeV	Device Types
Feb. 1974	Boeing	Dynamitron	e	Yes	2×10^{13} e/cm^2	2	Subsystem rate tests
Feb. 1974	Intelcom Rad Tech	LINAC	e	No	2×10^{13} e/cm^2	3	IC's and transistors
Feb. 1974	Intelcom Rad Tech	LINAC	e	No	3×10^{12} e/cm^2	20	IC's and transistors
May 1974	Intelcom Rad Tech	LINAC	e	No	2×10^{13} e/cm^2	3	IC's
June 1974	Boeing	LINAC	e	No	2×10^{13} e/cm^2	3	IC's and transistors
Aug. 1974	Hughes	Co^{60}	γ	No	600 krad(Si)	--	JFET's
Nov. 1974	JPL	Dynamitron	e	Yes	1×10^{13} e/cm^2	2.5	See Section V
Nov. 1974	Boeing	Dynamitron	e	Yes	1×10^{13} e/cm^2	2.0	See Section V
Oct. 1975	JPL	Dynamitron	e	Yes	5×10^{12} e/cm^2	2.5	See Section V
Oct. 1975	Boeing	Dynamitron	e	Yes	5×10^{12} e/cm^2	2.0	See Section V

(1) The device is insensitive to radiation, no special attention required.

(2) The device is insensitive to radiation except for applications requiring small parameter changes in the device. The application and magnitude of changes are specified.

(3) The device is sensitive to radiation, resulting in significant degradation of device parameters. A radiation screening of shielding program is required, if a reasonable design safety margin is lacking.

(4) The device undergoes catastrophic change and is no longer functional.

In addition, the program provided a more detailed characterization of radiation-sensitive parts in categories (3) and (4) above, along the following lines:

(1) A complete characterization of all the important dc parameters of integrated circuits.

(2) Determination of the dc gain of bipolar transistors as a function of the collector current.

(3) Determination of the leakage currents produced by suitable radiation bias conditions, which are indicative of the surface process control achieved by the production line that is being investigated.

(4) Special attention to the occurrence of "outliers," indicating an out-of-control situation.

It was beyond the scope of the program to achieve a complete quantitative characterization of all possible applications for the following reasons:

(1) The radiation properties are process-dependent and therefore vary with manufacturer, with production line, and from lot to lot.

(2) If the parts are not undergoing any form of radiation screening, "outliers" with severely degraded properties can occur (see Section VIII-C-5).

(3) In the absence of lot integrity, statistical approaches to obtain a mean and standard deviation are not meaningful, since the heterogeneous population does not represent a Gaussian distribution.

(4) The radiation properties are strongly dependent on the bias conditions during irradiation.

(5) It is not possible to carry out a large number of different sequential measurements on irradiated devices, since the time period of the measurement, the applied bias during measurement, and, particularly, the large current passing through the device during measurement cause rapid annealing.

3. Parts Selection

Parts selection required, first, that the generic category of device types be established. This was accomplished by a thorough investigation of existing literature and test results and expertise in the radiation effects field. Table 4-2 outlines the generic category of device types selected for the characterization program. Individual device types within the generic categories were selected by the cognizant engineer for each subsystem using the results of a worst-case circuit analysis of each of the 20 major subsystems. This led to the identification of the critical circuits and device types. The bias conditions during radiation exposure and the electrical parameters measured were selected according to the use of the devices in the spacecraft circuits.

The sensitivity of a given part type to radiation depends on the application. In general, radiation problems occur under the following conditions:

(1) Very low current densities.

(2) Very high voltages.

(3) Very high precision measurements.

Most of the potential problems with the Voyager electronics are due to long-term ionizing radiation effects. In semiconductor devices these are manifestations of charges trapped in insulating layers on the surfaces of the semiconductor devices. These are most important in MOS structures in which trapped charge in the gate oxide layer produces a first-order change in the apparent gate voltage. Trapped charge in surface passivation layers is also important in junction devices, where it produces an inversion layer that spreads out the effective surface area, thereby increasing recombination-generation currents. These currents are most important in bipolar transistors operated at low collector currents and in n-channel JFET devices. The susceptibility to charging depends on the quality of the oxide layer and is not usually consciously controlled in semiconductor device manufacturing.

In optical materials, long-term ionization effects appear primarily as the introduction of optical absorption in otherwise transparent spectral regions for the particular material. These are usually

Table 4-2. Radiation-Sensitive Components

Component	Effect
MOS devices	Surface ionization effects only
Linear IC's	Surface ionization and bulk damage
Analog switches	Surface ionization and bulk damage
Bipolar transistors	Surface ionization and bulk damage
JFET's	Surface ionization and bulk damage
Electro-optical devices	Ionization and bulk damage
Crystal oscillators	Ionization only
Zener diodes[a]	Bulk damage only
Other diodes and rectifiers[a]	Surface ionization effects

[a]Components sensitive to very high precision applications only.

manifestations of charge trapping at a pre-existing defect, so the rate of coloration is a strong function of the initial material.

In quartz crystals used for precision oscillators or filters, the same type of long-term ionization effects can produce significant resonant-frequency shifts. In this case, selection of the quartz crystal growth method can minimize the effect.

The magnitude of long-term ionization is a function primarily of ionizing energy deposition, i.e., the dose, as measured in rads in the material in question.

The devices of concern are:

(1) MOS devices (threshold voltage shift, enhanced leakage in CMOS pairs).

(2) Bipolar transistors (h_{FE} degradation especially at low I_C), and junction field effects transistors (JFET's) (enhanced source-drain leakage current).

(3) Analog microcircuits (offset voltage, offset current, and bias-current changes, gain degradation).

(4) Digital microcircuits (enhanced transistor leakage).

(5) Quartz resonant crystals (frequency shifts).

(6) Optical devices (coloration).

MOS devices are most likely to become nonfunctional in an ionizing radiation environment. CMOS devices present the most severe circuit problems in a moderate radiation environment, with linear devices a close second. Difficulties were also experienced with bipolar transistors at low current levels.

4. Parts Procurement

It is important to bear in mind that surface ionization effects are process-dependent. Therefore, a generic device type specifying pre-irradiation electrical characteristics may exhibit vastly different post-irradiation characteristics, depending on the fabrication line.

Ideally, all parts for a characterization program should be taken from an actual flight lot. Meaningful statistical data interpretation can be applied only to this case; i.e., the data are process-lot dependent. Procurement considerations often made this approach impractical; the characterization data were usually required long before the flight parts become available.

As a minimum requirement, parts for a characterization test were procured from the same manufacturer and bore the same part number. There are no equivalent parts regarding surface ionization effects. Preference was given to recent date codes.

Any major process modifications will invalidate the characterization results. The following are the most critical processing steps: oxidation, passivation, all forms of surface treatments, metallization, and diffusion. Subsequent heat treatments during die attachment and burn-in may modify the surface properties.

5. Test Specifications

All characterization tests were performed in accordance with the JPL test specifications shown in Appendix A. A test plan consisting of two sections was prepared by JPL. The first section, shown in Appendix B, applied to all characterization tests. It included the following information:

(1) A detailed procedure for implementing the parts radiation tests in accordance with the radiation test specification.

(2) A statement describing the manner in which the dosimetry requirements of the parts radiation test specification will be implemented.

(3) A statement of facility requirements.

The second section represents a working document, the Parts Radiation Characterization Test Requirements, not subject to approval, and including the following information:

(4) A description of the parts being tested (by the part type and number) and the lot size being tested.

(5) A statement describing the electrical operating mode of the parts during the tests, and the electrical schematic and description.

(6) A statement describing the functional tests, the method for performing the tests, and the parts parameter measurements to be made.

The characterization tests for a given device type were carried out in accordance with the Parts Radiation Test Requirements, also known as Radiation Test Requirements (RTR). A sample is shown in Appendix A. Only one basic number was assigned to each device type. This document defines the device parameters, radiation conditions, bias conditions during irradiation, and the sequence of electrical measurements to be performed.

It is important not to carry out too many sequential tests on a given device after radiation, to prevent annealing of the radiation damage. Moreover, leakage current tests are incompatible with tests requiring the passage of heavy currents. Therefore, it was often necessary to generate two or more separate tests (RTR's) using different test samples. These are indicated by capital letters after the RTR number.

The RTR's were generated from inputs provided by the cognizant engineers of the different subsystems regarding the measurement parameters and the bias conditions during radiation. The RTR's were then distributed to all cognizant engineers and to the contractors responsible for carrying out the radiation tests, to provide an opportunity for criticism and correction of errors. This resulted in the generation of one or more revisions to the RTR's.

The bias conditions specified in the RTR's during irradiation represented the worst-case conditions experienced in any of the applications of interest, i.e., the conditions leading to maximum radiation damage. As a general rule, these conditions corresponded to the maximum reverse bias across as many junctions as possible, and to minimum current flow. In the case of MOS devices, the worst bias conditions correspond to

the maximum positive voltage on the gate with respect to either source or drain. The measurement parameters depended on the application. Typical parameters for discrete devices and integrated circuits are shown in Tables 4-3 and 4-4. Measurements were carried out in order of increasing current. All high-current measurements were pulsed.

Table 4-3. Measurement Parameters for Discrete Devices

Device	Parameter
Bipolar transistors	Leakage Currents: I_{CBO}, I_{CEO}, I_{EBO}
	h_{FE} vs I_C; saturated and unsaturated
	V_{CE} (SAT)
JFET's	I_{GSS}
	I_D (off)
	R_{DS} (on)
	g_m
	V_P
Zener diodes	Zener voltage
	Temperature coefficient
Diodes and rectifiers	Leakage current
	Forward voltage
	Forward current

Table 4-4. Measurement Parameters for Integrated Circuits

Device	Parameters
Operational amplifiers	Input offset voltage
	Input offset current
	Input bias current
	Open-loop gain
	Slew rate
Voltage comparators	Input offset voltage
	Input offset current
	Input bias current
	Dynamic switching test
Voltage regulators	Line regulation
	Load regulation
	Output voltage
	Reference voltage
A/D converters	Output leakage current
	Output current
	Switching time
	Reference voltage
	Transistor parameters
Analog switches	I_S (off)
	I_D (off)
	I_D (on)
	r_{DS} (on)
	Dynamic switching test

The Radiation Test Requirements occupied a central position in the organization of the parts characterization tests as indicated in Figure 4-1. The RTR's reflect the inputs of the JPL subsystem cognizant engineers and of the circuit analysis carried out by the General Electric on-Laboratory contractors. The RTR's were then sent to the contractor responsible for the radiation test, i.e., Boeing or Hughes, Fullerton, for their evaluation and comments. It often required several iterations to reconcile the requirements of the subsystems and the circuit analysis with the test capabilities at the radiation facility. After irradiation the raw test data were processed by the Radiation Effects Group and the finished test data supplied to the subsystem cognizant engineer, the General Electric circuit analysis team, and other interested parties.

6. Radiation Test Results

The raw data obtained during the radiation test were converted to a form compatible with the Radiation Test Requirements. The latter, which give detailed information about the test plan, were appended to the radiation test results in their final form. These were then distributed to the cognizant engineers of all subsystems using the part.

The data were processed according to the following guidelines:

(1) The maximum shift was indicated for parameters changing by less than one order of magnitude after radiation.

(2) The maximum observed value was indicated for parameters that change by more than one order of magnitude, e.g., leakage currents.

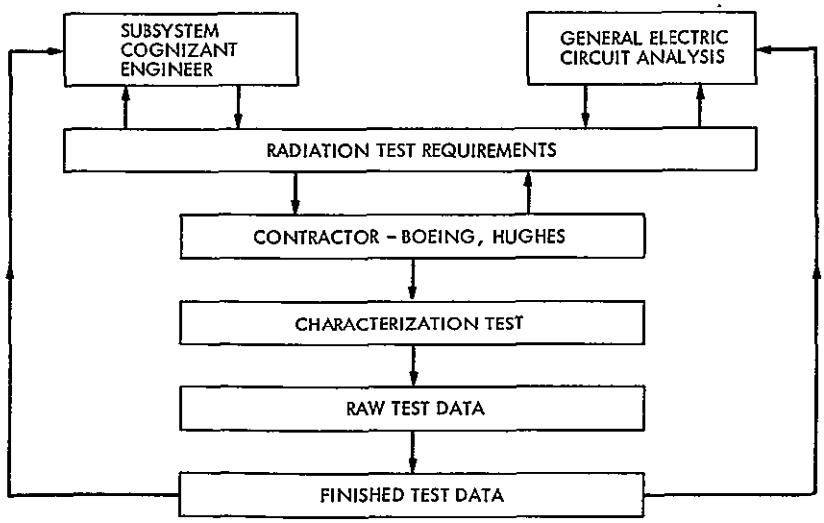

Figure 4-1. Radiation Test Sequence

(3) Changes in dc gain of bipolar transistors are best expressed as $\Delta(1/h_{FE})$ since it is the increase in base current that is responsible for the loss in gain. This parameter was plotted as a function of collector current on a log-log scale with error bars indicating the range of values.

Special attention was paid to the vendor's lot designations of the test samples whenever this information was known. The results were analyzed for "outliers" or dual populations. Both of these are indications of an out-of-control situation on the process line or else of an indiscriminate mixing of lots of different qualities, which make the utilization of the device without an adequate screening program very hazardous. It must be emphasized that the results are representative of the sample lot only and need not be representative of any future flight quality parts.

The analysis of the test results provided an important check on the validity of the experiment performed by the contractors. The evaluation of the data answered the following questions:

(1) Was the test plan faithfully carried out?

(2) Does the data contain unexplained anomalies?

(3) Are there any catastrophic failures and are the failure modes understood? Have the devices subsequently recovered?

Any anomalies were subjected to further investigations, failure analysis, and repetition of the experiment.

The final test results were utilized in the following ways:

(1) For comparison with the predictions of the General Electric worst-case analysis for different subsystems.

(2) As a data base in redesign.

(3) To determine the adequacy of the shielding.

(4) For extrapolation to other applications.

The most widely used devices have undergone a complete characterization of all significant device parameters.

7. Radiation Status Reports

Monthly Radiation Status Reports were issued for all part types in the device characterization program while the parts characterization program was in progress. The reports listed the device type RTR number, the test status, references to radiation test reports from other sources, and device types subject to radiation lot screening.

8. Radiation Design Criteria Handbook

The radiation test data for every radiation-sensitive device type was summarized in Reference 1-1. The information was presented in a form intended to be useful to the engineer for circuit design. The data include values of the mean, maximum, minimum, mean $\pm 2\sigma$, mean $\pm 3\sigma$ for every test parameter as a function of operating point, radiation bias condition, and total dose. Radiation screening requirements and accept-reject criteria were also indicated.

The following is an example of the part parameters on which data have been taken:

Transistors: $\Delta \frac{1}{h_{FE}}$, $\Delta V_{CE(SAT)}$, I_{CBO}

The $\Delta(1/h_{FE})$ data are displayed versus I_C and radiation dose, and the saturated gain is separated from the unsaturated gain.

Diodes: ΔV_f, $\Delta I_{leakage}$.

Zener diodes: ΔV_z.

Linear IC's: ΔV_{OS}, ΔI_{BIAS}, A_{VOL}.

CMOS: V_{GT}, I_{SS}, I_{LTG}. Propagation delay time.

A sample sheet is shown in Figure 4-2, with the major features indicated. An explanation of those features is given below.

(1) An outlier is here defined as a data point which does not fall within 3σ of the mean value of that parameter at the lowest value of the independent variable (i.e., lowest value of I_C or fluence, where the parameter is measured as a function of I_C or fluence respectively). Once established as an outlier in this way, it is considered an outlier for all other values of the independent variable.

(2) The data are calculated both with and without outliers whenever they exist.

(3) The standard deviation (σ) is approximated by the following expression:

$$s = \sqrt{\frac{\sum_{i=1}^{n} (x_i - \bar{x})^2}{n - 1}}$$

Where n is the number of data points, $\bar{x}$ is the mean value of the set of data points, and x_i is a measured value of the parameter. This gives an unbiased approximation of σ, including cases where the sample size (n) is small (Reference 4-1).

For transistors, in addition to the tabulated information, graphs are included giving $\Delta(1/h_{FE})$ as a function of collector current. In these graphs, only those calculated excluding the outliers are plotted. The outliers are indicated on the graphs.

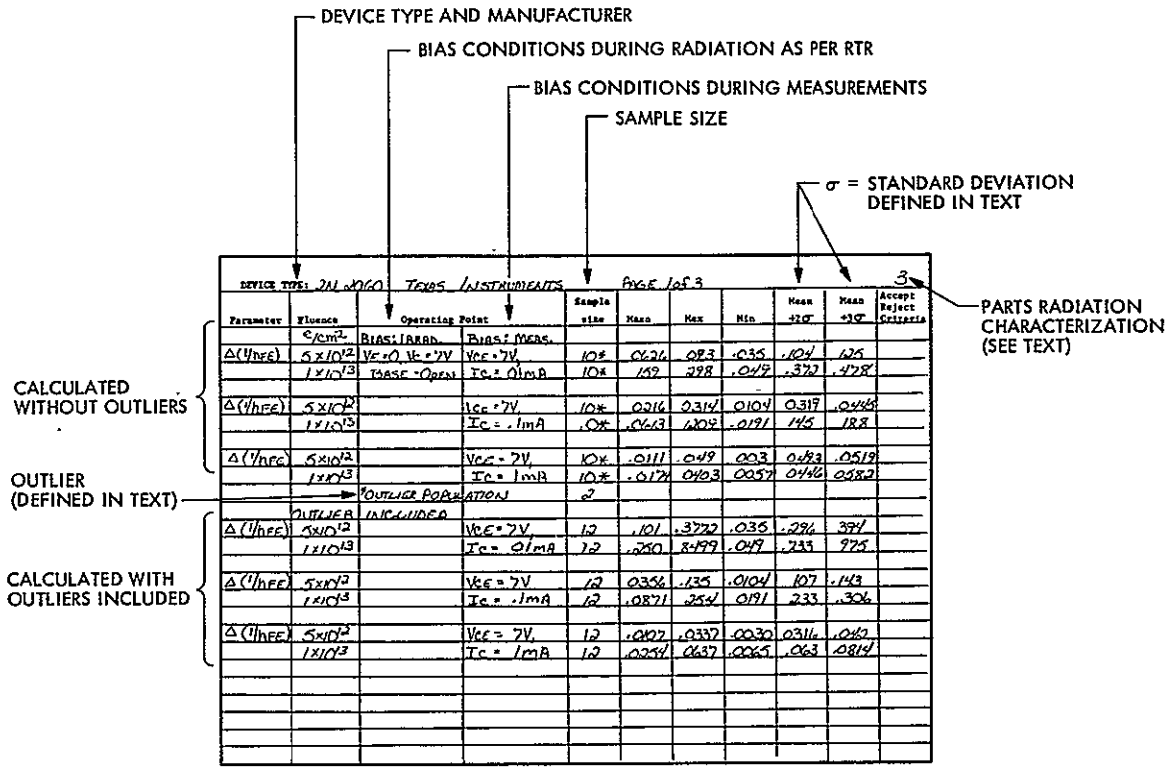

Figure 4-2. Sample Sheet

B. PARTS RADIATION SCREENING

1. Introduction

Radiation screening was applied to those device types that were sufficiently radiation-sensitive to compromise the radiation design margin. The screening was carried out on flight-quality parts to assure the necessary confidence that the parts were sufficiently radiation-hard to survive the design environment. Radiation screening was required under the following circumstances:

(1) If the parts characterization program had shown that the part was sensitive in a particular application to the radiation environment, and that an adequate design safety margin was lacking.

(2) If the part could not withstand the radiation environment without process modification, and the manufacturers had agreed to carry out such a program. The modified part must then be subjected to a screening program.

(3) If the parts characterization program had shown the presence of outliers or a dual population within the sample lot, indicating an out-of-control condition on the process line.

The screening of sensitive parts was implemented by using one or more of the following methods:

(1) Sample screening, wafer lot.

(2) Sample screening, diffusion-metallization lots.

(3) Sample screening, date code lots.

(4) 100 percent IRAN screening.

(5) Sample IRAN screening of diffusion-metallization lots.

The device categories that were subjected to these screening procedures are shown in Table 4-5.

2. Wafer Lot and Diffusion-Metallization Lot Sample Screening

In wafer lot sample screening, a few devices located in specific areas of each wafer are assembled, and the sealed packages are subjected to a radiation test. If the results are satisfactory, the remaining dice from the wafer are accepted for assembly into flight-quality devices. This method could be applied to only a limited number of device types due to the difficulties inherent in wafer traceability through the device manufacturing process. The most notable example was the modified CMOS line at RCA (see Sections VI-B, VII-F, and VIII-E). Wafer lot sampling is the most vigorous lot sampling method but it requires wafer identification.

Table 4-5. Radiation Screening Methods

Device Category	Sample Lot Type Screening			Irradiate-Anneal
	Wafer	Diffusion-Metallization	Date Code	
Bipolar transistor	Hybrid Circuits	2N2222 and 2N2905	X[a]	SDT5553
JFET, n-channel			X	2N4856, 2N5196, 2N5520 and 2N5556[b]
Operational Amplifier[c]		HA2520, HA2600, HA2620, HA2700, LM108 and LM124		LM101
Voltage follower		LM102		
Comparator[c]		LM139		LM111
Voltage regulator[c]		LM105		
A/D Converter			HI1080	
Current switch		AD550		
Analog switch		DGM11		DG129, DG133, and DG141[d]

Table 4-5. Radiation Screening Methods
(Continuation 1)

Device Category	Sample Lot Type Screening			Irradiate-Anneal
	Wafer	Diffusion-Metallization	Date Code	
CMOS	X			
RF amplifier	MIC76T			
RF mixers	MIC236 MIC336			
Quartz crystals	X			

[a]An X in a column indicates that the test was applied to the device indicated.

[b]No high-temperature annealing.

[c]The following linear IC's were considered hard to 60 krad(Si) without screening: LM103, LM106, LM710, and LM723.

[d]Diffusion-metallization lot samples only.

It proved generally easier to persuade the semiconductor manufacturer to accept diffusion-metallization lot sampling, since this sampling procedure is widely practiced as part of the scanning electron microscope quality control. This method was applied to device types where cooperation with the vendor allowed device identification with a diffusion-metallization run. This included all hardened linear devices: LM108, LM102, LM139.

All screening methods involving wafer or diffusion lot sampling and all device modification programs require the active collaboration of the manufacturer who must agree to:

(1) Furnish samples for radiation test.

(2) Maintain strict lot control on the production line.

(3) Agree to accept/reject criteria.

(4) Assemble only lots that have passed the radiation tests.

Consequently, all screening programs represent a compromise in yield, delivery time, and acceptance criteria. The latter, which could be established only after radiation data become available, required occasional modification. A list of acceptance criteria is shown in the tables in Section VIII-A-1.

The screening test was carried out using the same RTR's and test procedures as the characterization test. Additional screening radiation test requirements were sometimes needed. A sample lot of 6 to 10 devices was considered adequate. The test was carried out on a top priority basis and the lot acceptance or rejection was communicated to the manufacturer within 48 hours after the test. However, initially it took considerably longer to establish accept/reject criteria based on circuit requirements and yield considerations. The test data were published in the same manner as the characterization results.

A comparison of wafer and diffusion-metallization lot sampling in bipolar transistors was carried out by Arimura et al. (Reference 4-2). They observed a very large variability from wafer to wafer and concluded that wafers from the same diffusion run do not necessarily behave similarly in a total dose environment.

3. Date Code Lot Sample Screening

There were many device types without any lot identity other than the date code which required some kind of screening procedure. This applied to all discrete components on the spacecraft. Extensive screening was carried out on bipolar transistors and n-channel JFET's. Every available date code of all bipolar transistors was subjected to a radiation sampling test. The results were compared to previous data from earlier characterization tests and published in a preliminary Radiation Handbook (Reference 4-3), which had been made available to all cognizant engineers. All lots that performed worse than the data previously published were flagged as reject lots, so that the subsystems could either not use the devices or take some other corrective action.

N-channel JFET's sometimes exhibit leakage currents many orders of magnitude greater than devices of the same type manufactured under strict control of the silicon surface and of the oxide passivation layer. Such devices were subjected to a preliminary date code lot screening which was very effective in detecting lots with radiation-induced inversion layers. If the whole lot was shown to be defective, special shielding had to be applied, since it was too late to replace the defective lot. Lots that showed a varied response indicative of a bimodal distribution were subjected to IRAN screening.

In addition, there were some lots of radiation-sensitive integrated circuits that had been procured by subsystems before the necessity for a radiation-hardening program had become apparent. These lots were subjected to random sampling, so as to advise the designers if it was safe to incorporate the devices into the spacecraft without any special shielding measures. In the case of some operational amplifiers, the results indicated that the devices could not be used.

4. Irradiate-Anneal Screening

a. Introduction. An extensive investigation of IRAN screening of semiconductor piece parts against total dose radiation effects was carried out as part of a program to harden the Voyager spacecraft against the Jupiter radiation belts (Reference 4-4). The method consists of irradiating semiconductor devices with cobalt 60 to a suitable total dose under representative bias conditions and of separating the undesired tail of the distribution from the bulk of the parts by means of a predetermined acceptance limit. The acceptable devices are then restored to their pre-irradiation condition by annealing them at an elevated temperature.

Irradiate-anneal screening is the only known 100 percent radiation screen against outliers, i.e., devices that are significantly more sensitive to ionizing radiation than the remaining population. In general, IRAN should be supplemented by a qualification test based on a diffusion-metallization lot, in which a few samples are irradiated to a total dose in excess of the project requirements. Failure to pass this test implies lot rejection, resulting in an extension of the parts delivery by many months.

Since the lot screening method imposed intolerable time delays, it was hoped that the IRAN technique might be employed to predict the radiation behavior of each device in a quantitative manner, so that even lots of marginal radiation quality might be utilized at a somewhat lower yield. This requirement imposes far more severe constraints on the retracking of electrical parameters measured after the first irradiation than the elimination of outliers.

This method requires a high reliability parts handling and testing capability so as not to compromise the overall reliability of the devices and is therefore expensive to carry out on a large scale. Also, it is important not to overstress the devices during the annealing cycle.

b. Device Types Considered for IRAN. IRAN was considered for device types that were determined to be more radiation-sensitive than allowable by the circuit and shielding analyses. However, such screening methods work only when the devices show a significantly varied response to a radiation exposure. A list of device types that were considered for IRAN is shown in Table 4-6. The devices consist of analog switches, n-channel JFET's, and bipolar transistors. The primary cause of radiation damage induced in these devices by ionizing radiation is the formation of inversion layers due to the accumulation of positive charges in the silicon oxide insulator near the silicon-silicon oxide interface. This depends on the quality of the oxide, which is to a large extent an uncontrolled process variable.

Devices that are generally extremely sensitive to ionizing radiation, e.g., MOS devices, are poor candidates for the IRAN technique and must be shielded. An additional reason for excluding MOS devices is the difficulty of annealing out the radiation-induced interface states except at high temperatures. The important LM108 operational amplifier was excluded, because it had been possible to harden this

Table 4-6. Device Types Considered for IRAN

Device Category	Device Type
Operational amplifier	HA2520 HA2600 HA2620 HA2700 LM101
Comparator	LM111
Voltage regulator	LM105
Analog switch	DG129 DG133 DG141
JFET (n-channel)	2N4093 2N4391 2N4392 2N4393 2N4856 2N5196 2N5520 2N5556
Bipolar transistor (h_{FE} only)	SDT5553

device against ionizing radiation (see Section VI-C-2). Because all n-channel JFET's with a lightly doped base region are likely to develop sizable gate leakage currents, they were therefore considered to be candidates for IRAN. The n-channel JFET's in analog switches can cause an increase in I_S (off), the most sensitive parameter in those devices not containing MOS components. The latter were not subjected to IRAN for reasons stated above.

The only bipolar transistor subjected to IRAN procedures in the Voyager program was the SDT 5553, a device extremely sensitive to surface ionization effects at low current levels. It was considered preferable to redesign circuits using other transistors to operate with minimum dc current gain.

c. Program Constraints. The original requirement imposed on the devices was to survive a total dose of 125 krad(Si). This was later decreased to 60 krad(Si) as the result of a more precise definition of the Jovian radiation belts. A ceiling of 150°C was imposed on the annealing temperature of the devices for reliability reasons. It was

found that this temperature is inadequate for complete annealing of all surface effects. Burn-in temperatures up to 300° C have been successfully employed in high-reliability programs (Reference 4-5), but this requires device construction analysis and thermal stress analysis for each device type before procurement. Such an investigation was ruled out because of timing constraints. The devices were annealed in an inert atmosphere for 96 hours. Experiments showed that longer annealing times did not result in any additional annealing.

High-temperature annealing was considered to be unnecessary for the JFET's. In these devices, only the leakage currents are affected by the ionizing radiation; these currents are not significant in those devices that pass the IRAN acceptance criteria.

d. Experimental Investigation. The experimental investigation is discussed below.

1) Experiment. A series of experiments was conducted on each device type under consideration for IRAN. Nonflight parts had previously been exposed to 2.5-MeV electrons up to 10^{13} e/cm^2. These devices were annealed for 96 hours at 150° C approximately 2 to 3 months after the initial exposures. Most parameters annealed back to acceptable specification levels, but others did not return to their pre-irradiation values. Since high-energy electrons can induce a significant amount of displacement damage, it was decided to carry out additional experiments using a cobalt 60 source. The devices were irradiated to a total dose of either 50 or 125 krad(Si), annealed at 150°C for 96 hours, and subsequently reirradiated with 2.5-MeV electrons, making measurements at four radiation levels from 5×10^{11} to 5×10^{12} e/cm^2. Details of the work are described in Reference 4-4.

2) Linear Bipolar Devices. The parametric changes produced in each device by equal doses of the first and second irradiation were plotted, so as to indicate the ratio of the shift produced, as well as any anomalous data points. In almost all cases, reirradiation produces substantially greater shifts than the original radiation. On annealing, most parameters recover to within the manufacturer's specification limits. Exceptions to this rule are open-loop gain and the input bias current of some devices.

During the initial irradiation, most linear bipolar devices exhibit slow parametric changes up to about 35 krad, followed by a logarithmic response of the type

$$P = k \log\Phi + C \qquad (4\text{-}1)$$

After annealing and reirradiation the logarithmic response starts at about 10 krad(Si) and is of the type

$$P = k \log(\Phi - \Phi_0) + C \qquad (4\text{-}2)$$

Besides these typical responses, many anomalous reirradiation curves are also seen, particularly for the input offset current.

A thorough study was made of the factors causing anomalous behavior, since the effectiveness of an IRAN program depends on the ability to predict the response upon reirradiation. The majority of the anomalies are predictable by deviant values after the first irradiation and annealing, and the devices may be eliminated by suitable acceptance criteria that are specific to each parameter of every device type. The unpredictable results are caused by changes in sign on reirradiation, by anomalous reirradiation curve shapes, and by causes specific to a given device type and initial radiation dose level.

3) N-Channel JFET's. A number of n-channel JFET's were irradiated to 60 krad(Si) under a gate bias of 10 to 20 V. All devices showed a minimum increase of one order of magnitude due to an increase in the surface recombination velocity, with greater increases produced by inversion layers. At higher total doses I_{GSS} varies with dose as

$$I_{GSS} = (k\Phi)^a \qquad (4\text{-}3)$$

where a varies from 2 to 5. The higher values of a indicate the presence of an inversion layer.

4) Analog Switches. Three types of analog switches were irradiated at 50 to 100 krad(Si) followed by 96 hours annealing at 150°C. On reirradiation, $I_{S(off)}$ varied with the total dose as shown in Equation (4-3) over the dose range from 30 to 125 krad(Si). No serious radiation-induced inversion layers were seen in these devices resulting in a values between 1.4 and 2.

5) Bipolar Transistors. The SDT5553 was irradiated to a total dose of 5 krad(Si). The value of $\Delta(1/h_{FE})$ varied by more than 3 orders of magnitude. On reirradiation there was a sharp increase in $\Delta(1/h_{FE})$ above 5 krad(Si) due to the onset of a response of the type

$$\Delta(1/h_{FE}) = (k\Phi)^a \qquad (4\text{-}4)$$

The value of a decreased with initial radiation damage and was lowest for rejected devices.

e. Irradiate-Anneal of Flight Parts. The preliminary experiments eliminated a number of device types from the IRAN program, because there was no correlation between the first and second irradiation, or because the parameters would not anneal out. In other device types, all the devices in a given lot degraded severely during the first irradiation. Some subsystems engineers elected to increase the shielding of their electronics and forego IRAN in order to save time.

A program to irradiate-anneal flight parts was initiated on a number of integrated circuits, on one bipolar transistor, and on several JFET's. The test procedure is described in Section V-D-4. The device types tested are listed in Table 4-7 along with the acceptance criteria and the radiation screening levels developed in the experimental program.

The total number of each part type subjected to IRAN is given in Table 4-7 along with the number of rejects. It may be seen that about 1/3 of the devices failed the criteria shown in the table for some part types, while others had no failures.

As an additional safeguard, some devices for each lot were subjected to reirradiation using a series of four exposure levels from 12.5 up to 125 krad(Si). This was to ensure that the re-irradiation electrical parameter values did not exceed the limits that had been used to set the acceptance criteria listed in Table 4-7, assuming a correlation between the values on the first and second irradiation. These limits were well within the requirements of the worst-case application of Voyager subsystems.

For those parts which had to be annealed, an additional requirement was that the electrical parameters of the flight parts after annealing should return to a value within the manufacturer's specification limits. However, the input bias current I_B of the LM101 did not anneal, and I_B for the LM111 deteriorated further. The following specification for IRAN flight parts were adopted:

	Manufacturer's Limit	Post-Anneal Limit
LM101	75 nA	100 nA
LM111	100 nA	1000 nA

In general, an annealing temperature of 150°C leaves some residual radiation damage and does not guarantee the absence of annealing and reirradiation anomalies. The success of the limited irradiate-anneal program on Voyager flight parts was due to a combination of the following factors:

(1) Non-retracking problem minimized by careful selection of device types to be subjected to IRAN.

(2) Remeasuring of devices after annealing by device manufacturer.

(3) Reirradiation of sample flight parts to 125 krad(Si).

Table 4-7. Flight Parts for IRAN Program

Part Type	Number Tested	Number of Rejects	Acceptance Criteria	Screening Dose, krad(Si)
LM101A (can)	139	20	ΔV_{OS} < 0.7 mV ΔI_{OS} < 2.5 nA ΔI_B < 60 nA	125
LM101A (Flatpack)	396	83		
LM111 (can)	48	0	V_{OS} < 3 mV I_{OS} < 20 nA	50
LM111 (Flatpack)	200	14	I_B < 1 μA	
DG129[a]	18	0	$I_{S\ (off)}$ < 3 nA	50
DG133[a]	41	0	$I_{S\ (off)}$ < 3 nA	50
DG141[a]	9	0	$I_{S\ (off)}$ < 5 nA	50
2N4856	298	65	I_{GSS} < 500 pA	60
2N5196	124	17	I_{GSS} < 100 pA	60
2N5520	21	0	I_{GSS} < 100 pA	60
2N5556	96	28	I_{GSS} < 250 pA	60
SDT5553	39	4	h_{FE} >8 at I_C = 0.15 mA	5

[a]Lot Sample, IRAN only.

(4) For each critical circuit, a permissible worst-case parameter value determined by analysis. Reirradiation data indicated that this value would not be approached under the most unfavorable conditions defined as mean plus 3 times standard deviation.

(5) Some significant device degradation, e.g., I_B of LM101 and LM111, tolerated by the circuit designs.

5. Screening of Flight Parts

A special effort was made to radiation-screen and sample all the radiation flight parts for all sensitive device types, even if these devices had been subjected to some earlier screening activity. The sample screening of flight parts fell into three categories:

(1) Sampling of flight parts only. This applied to all date code lots including bipolar transistors and n-channel JFET's. It also applied to some linear devices.

(2) Wafer or diffusion-metallization lot sample screening, followed by final radiation sampling of flight parts. This method was applied to all hardened linear devices.

(3) For a fraction of the devices subjected to IRAN, reirradiation with electrons to 5×10^{12} e/cm^2.

The irradiation of completed flight parts provides the following safeguards:

(1) Comparison of the data with previous radiation data from the same lot eliminates the possibility of device mix-ups at the vendor.

(2) It indicates the existence of package effects; e.g., the HA2700 was initially tested in a can. Subsequent tests in a 10 lead flatpack showed catastrophic degradation in negative open-loop gain not seen in the cans. These effects are caused by degradation during sealing.

(3) Similar effects can also be produced in other operations involving heating in different ambients, e.g., die and lead bonding, temperature storage, and burn-in.

(4) Reirradiation tests on the LM111 revealed erroneous post-annealing measurements carried out by the semiconductor manufacturer.

SECTION V

RADIATION TESTING AND DOSIMETRY

A. INTRODUCTION

The radiation testing of Voyager piece parts was carried out using several different radiation facilities, which are described in this section, along with the procedures used. While the procedures were similar, there was some variation from one facility to another due to differences in the type of radiation equipment available, the testing personnel, and the geometry of the test.

Section II describes the Jupiter radiation environment to be simulated in these tests. The initial studies of the spacecraft radiation environments revealed a large number of different sources, including solar wind protons, neutrons, and gammas from the RTG's as well as the electrons and protons in the trapped belts at Jupiter. The Jupiter electrons were determined to be the most potentially damaging to the lightly shielded piece parts. The electron energy spectrum is discussed in Section II. There was also concern early in the program that, while the peak of ionization damage appeared to occur at 3 MeV, there would also be considerable permanent damage caused by electrons above that energy. Initial work was done with both 3-MeV and 20-MeV electrons, using a LINAC accelerator. It was found that the damage between the two energies had a predictable ratio. Subsequently there was concern that the high dose rate of the LINAC pulse would not suitably simulate the ionization effects of the steady-flux, low-dose rates at Jupiter. If the instantaneous flux rate exceeds about 10^{11} e/cm^2-s, the following additional damage effects are produced that are absent in the Jupiter steady state environment:

(1) Transient secondary photocurrents may be generated that may be large enough to damage junctions and metallic conductors in transistors and integrated circuits.

(2) The instantaneous charge deposition may produce dielectric breakdown in insulating regions like passivation layers.

Therefore, all subsequent testing was done using the Dynamitron accelerators, which have a steady rate, or using a cobalt 60 gamma source.

While proton tests were considered, it was decided that no parts tests were required for the proton fluences expected at Jupiter for Voyager. Also, no neutron tests were carried out because the neutron fluence expected from the RTG's was considered below the parts damage threshold. The RTG gammas were adequately covered by tests with electrons and cobalt 60 gammas.

All tests were done at ambient temperature and pressure. All equipment used (except equipment specifically built for the testing) was standard laboratory instrumentation, which was periodically calibrated.

B. RADIATION TEST FACILITIES

1. Dynamitron

The Dynamitron accelerators at JPL and at Boeing were used extensively during the testing program. The Dynamitron provides a steady monoenergetic beam of electrons variable in energy up to 2.5 MeV with a range of beam currents suitable for the parts testing programs, which required rates at the test devices of 10^8 to 10^{10} e/cm^2-s. All Voyager tests were performed using beam energies between 2.0 MeV and 2.5 MeV.

The parts test geometry for the two Dynamitrons is essentially the same. The electron beam is brought out of the vacuum tube into air through a 0.05mm (2-mil) titanium window, copper and aluminum scattering foils, and through 0.9 m (3 ft) of air. Each of these materials scatters the electrons slightly so that the beam has a reasonable uniformity of less than 20 percent over the array of parts being tested. The array is confined within a 25-cm (10-in.) diameter circle perpendicular to the direction of the beam. At the center of the circle is the aperture of a vacuum faraday cup which is used to control the flux and fluence of the electron beam. The beam is centered on the faraday cup with a quadrupole magnet prior to the installation of the test samples. The output from the faraday cup is a current that is fed into a current integrator. Both fluence and flux are measured. The integrator is calibrated daily with a calibrated current source. The integrator is set to shut off the electron beam automatically when the desired fluence level is received by the faraday cup. Most of the integrated circuits and transistors tested were irradiated with the Dynamitron.

2. Cobalt 60 Sources

Several cobalt 60 gamma radiation sources were used in the course of Voyager parts testing. They were located at JPL, at the Hughes Aircraft Company (HAC) and at the Naval Research Laboratory (NRL). The gamma rays are primarily 1.17 and 1.33 MeV, with a spectrum of lower energies due to scattering and absorption. Gamma radiation was used to test parts that were known to be sensitive only to ionization effects. Consequently, the type of source and the geometry of the test are of little importance. Only the total dose of ionizing radiation is important, and the fact that the measurements be done *in situ* or as soon after exposure as possible. A list of the sources used and the generic types of the tests is given in Table 5-1.

The gamma field uniformity was within $\pm$10 percent in the area where parts were exposed. Dosimetry was done with thermoluminescent dosimetry (TLD).

Table 5-1. Cobalt 60 Test Types and Sources

Test Type	Location	Type of Source
CMOS I_{SS} Screening	HAC	Pig with vertical drawer
CMOS V_T Test Patterns	HAC	Panoramic
CMOS Propagation Time	HAC	Panoramic
CMOS Characterization	NRL	Water tank
Power Transistors	JPL	Pig with window

3. Van de Graaff

A 6-MeV Van de Graaff electron accelerator, located at Notre Dame University, was used for a small number of tests on zener diodes, rectifiers, and voltage regulators. This work was performed by the General Electric Company in order to investigate the effect of higher energy electrons in producing bulk damage in devices where small amounts of such damage might be important. Tests were conducted on all parts at 3.0 MeV and on some parts at two energies, 3 and 5.5 MeV, to determine the parts' response as a function of energy.

C. TEST LEVELS AND DOSIMETRY

1. Program Test Requirements

The Voyager spacecraft must survive the radiation environments described in Section II. JPL has stipulated test levels to be used in the electron and gamma tests (see Appendix A). In the early part of the program, which consisted mainly of parts characterization tests, the values in Table 5-2 were used for electron tests.

As a result of further analysis of data from Pioneers 10 and 11, the estimates of the maximum radiation levels of Jupiter for the Voyager mission were reduced. The test levels were changed to reflect this new estimate, and another radiation level was added in order to allow information on the device response at lower radiation levels for devices that were shielded. The new levels, shown in Table 5-3, were used throughout the rest of the testing program for both parts characterization and screening of flight part lots.

Table 5-2. Radiation Flux and Fluence Levels for Early Electron Tests (3-MeV Equivalent), 1000-s Electron Exposure

Flux, e/cm^2-s	Accumulated Fluence Levels, e/cm^2
2.5×10^9	2.5×10^{12}
2.5×10^9	5.0×10^{12}
5.0×10^9	1.0×10^{13}

Table 5-3. Final Radiation Test Levels Used in Parts Testing, 1000-s Electron Exposure

Electron Flux, e/cm^2-s	Accumulated Fluence Levels, e/cm^2	Accumulated Ionizing Dose, rad(Si)
5.0×10^8	5.0×10^{11}	12,500
7.5×10^8	1.25×10^{12}	31,300
1.25×10^9	2.5×10^{12}	62,500
2.5×10^9	5.0×10^{12}	125,000

Gamma tests were also performed at the accumulated dose levels given in Table 5-3. However, the dose rates were not the same as those used in the electron tests. Test geometry and field uniformity dictated the dose rates, but the total dose values were maintained. Exposure times with gamma sources varied from about 15 to 45 min.

2. Radiation Measurements

Radiation measurements were made by two different techniques: Electrons were measured by means of a faraday cup and gammas were measured with TLD.

The faraday cup (see Figure 5-1) is designed to measure all electrons passing through an aperture. The current produced by the absorbed electrons is fed into a current integrator which is calibrated daily. The integrator indicates the rate of current flow (which is proportional to flux) and integrates the amount of current up to a preset level which has been calculated to represent the fluence level required by the test engineer. At the preset level, the accelerator beam is shut off automatically.

Most of the Dynamitron parts tests used the faraday cup as the primary standard of flux and fluence. In the early tests at Boeing, TLD calibrated with a Landsverk ion chamber was used as the standard. Subsequently, a JPL-supplied faraday cup was incorporated as part of the test setup.

Radiation field uniformity measurements were made by two methods: TLD and an ionization chamber. The TLD system was useful where high doses and rates prevented use of the ionization chamber. Also, one system could be used to check on the other when overlapping ranges allowed.

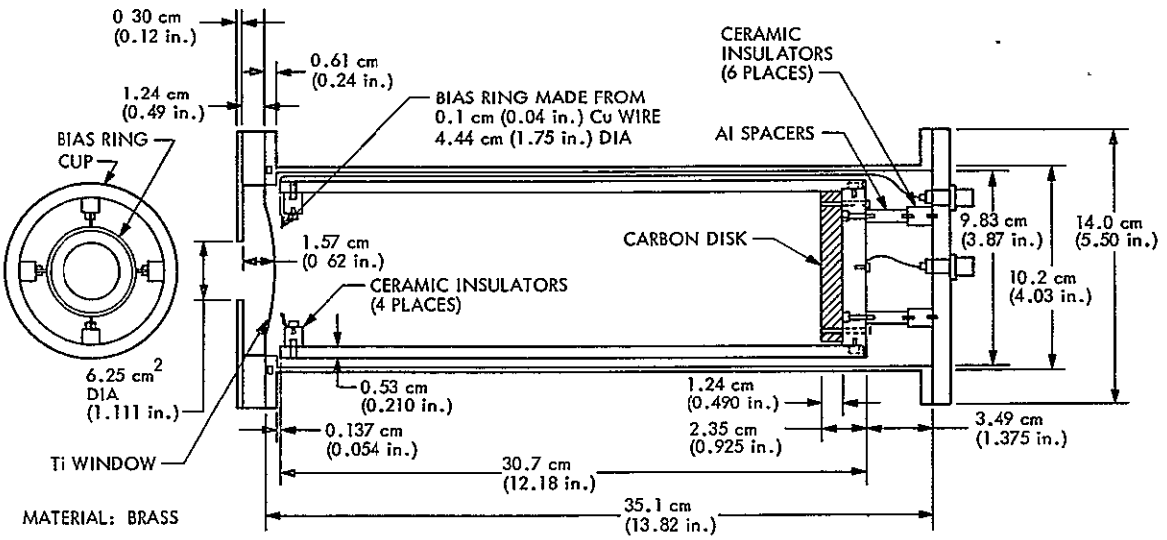

Fig. 5-1. JPL Faraday Cup

TLD dosimetry was used to calibrate the cobalt 60 sources and to determine field uniformity. The TLD system was calibrated with ion chambers (Landsverk R-meters) calibrated to ±2 percent accuracy. The accuracy of the TLD is 10 percent.

The tolerance requirements for the radiation tests are given in Appendix A. Methods used to calibrate the cobalt sources and the TLD systems are also described in Appendix A.

D. TEST SETUP AND PROCEDURES

1. General

The test setup and procedures used were guided by the specifications developed in the early part of the parts test program (Appendix A). Appendix B is a general test plan for the major portion of the characterization and flight lot sample work. Subsequently, a more detailed test procedure (Appendix C) was written specifically for use in the flight lot sample program. Some types of testing did not have a formal written procedure, but the same general test conditions and procedures were maintained, such as the type of test boards, biasing conditions, and dose as well as the flux and fluence levels. However, at different facilities there were slight variations necessary in test setup and procedure.

2. Testing With Matrix Board

The matrix board was built by Hughes personnel at the direction of JPL to be a versatile method of carrying out electrical parameter measurements on a variety of part types, with the parts remaining *in situ* at the radiation site during measurement. The matrix board, shown with power supplies, digital voltmeter, and ammeters in Figure 5-2, was an integral part of the *in situ* testing method shown in the block diagram in Figure 5-3.

Figure 5-4 shows the system setup for a test including the location of all elements in the block diagram. Figure 5-5 shows the devices under test with the faraday cup in place and the window end of the beam tube.

The purpose of the matrix board setup was to allow great versatility in testing a wide variety of device types. The bias levels during irradiation were controlled using this system. After each irradiation level was completed, the matrix board was reconnected to make the 1 to 6 electrical parameter measurements required by the RTR's, as discussed in Section IV-A-5. With this method, the Dynamitron did not have to be turned off. The beam was intercepted with a stopping block so that no electrons were impinging on the devices under test. Thus the electrical measurement could be made and the irradiation resumed with only short intervals of interruption. This prevented excessive annealing of radiation damage effects. Further details of the *in situ* testing procedure are contained in Section 11 of Appendix C.

Fig. 5-2. Matrix Board Setup for Control of Bias During Irradiation and for Electrical Parameter Measurements in situ

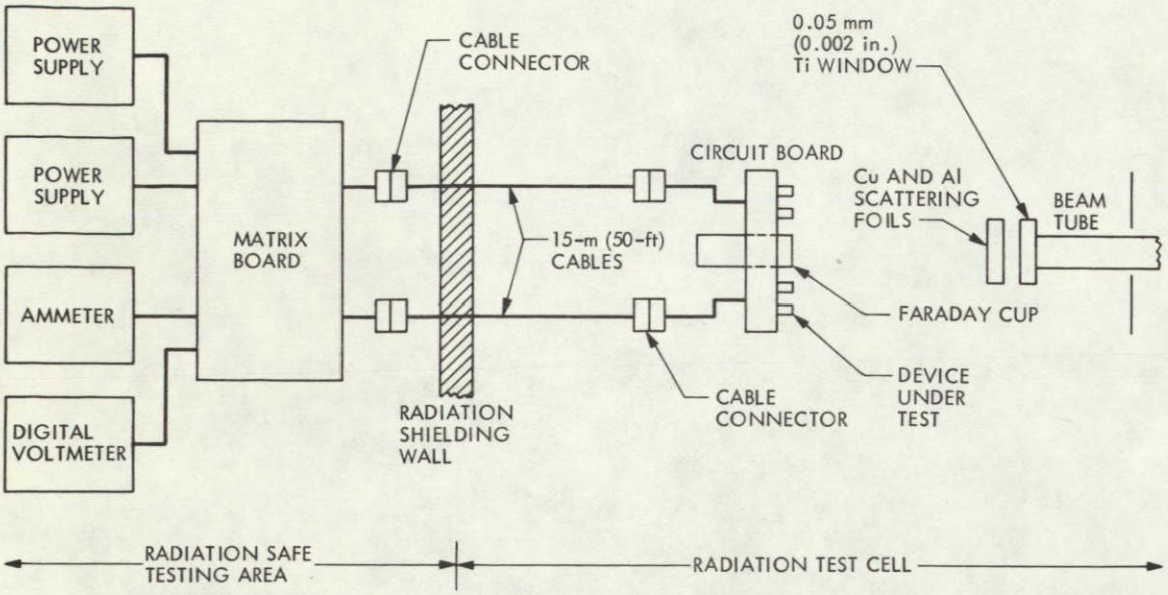

Fig. 5-3. Block Diagram of the Test Setup for <u>in situ</u> Testing With the Dynamitron

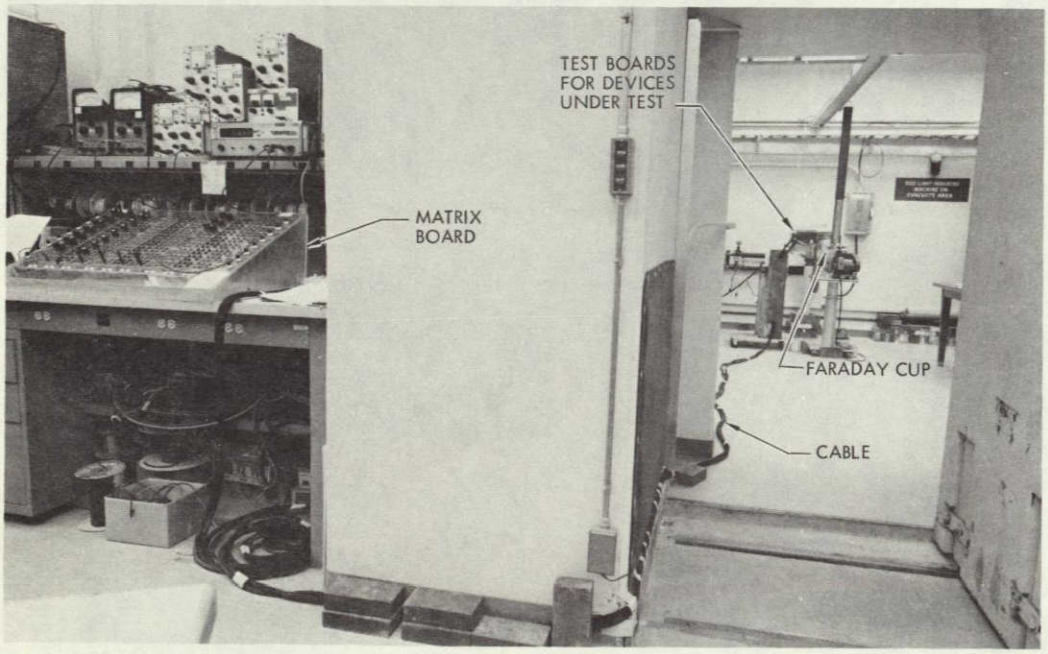

Fig. 5-4. Matrix Board, Cable, and Test Fixture Locations During Test

For the non-*in situ* tests the Dynamitron was shut down, and the test devices were removed from the site for about 15 to 20 min between each irradiation level and the next. No bias was applied to the devices during the periods between irradiations. For non-*in situ* tests, an unirradiated control device was always used as a check on the measurement instrumentation. Further details on non-*in situ* testing are given in Section 12 of Appendix C.

The characterization and screening tests done with the matrix board were on diodes, transistors, and integrated circuits. Further details are given in Sections IV-A and IV-B, and the results are discussed in Sections VII and VIII.

3. *In situ* Testing at Boeing Aircraft Company

A number of integrated circuits were tested for JPL by the Boeing Radiation Effects Laboratory personnel. A complex control system with which both biasing and electrical measurements were made remotely and *in situ* was built for the work. The physical arrangement of the test was very similar to that just described. A control or interface box for switching was located along with the measurement instrumentation in a radiation-safe location. A set of 15-m (50-ft) cables connected the measurement room to the radiation test cell where devices were irradiated by the Boeing Dynamitron.

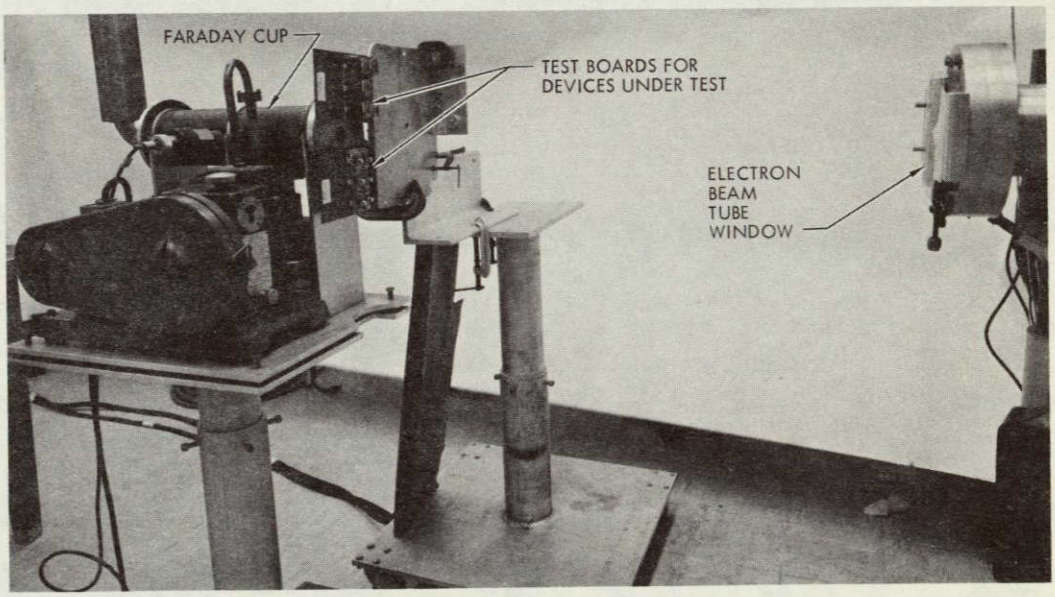

Fig. 5-5. Test Cell Setup for *in situ* Radiation Testing With the Dynamitron Electron Accelerator

In the test cell location was a test fixture which included a box of eight modules of six relays each. Within each module the six relays can be held either on or off during a test sequence, or they can be controlled by a clock. Manual switching can be used between each irradiation level and the next, to remove bias and make the required parameter measurements, or the system switching sequence can be done by an automatic circuit evaluator (ACE).

Individual circuit boards 11.5 cm (4-1/2 in.) x 13 cm (5 in.), with end plug, were made up for each device type, usually one for each test series as defined by the RTR's. The circuit board under test was plugged into a plug located on the test fixture box for irradiation. Details of the Boeing instrumentation are contained in Appendix D.

The Boeing Dynamitron was capable of producing electrons with a maximum energy of only 2 MeV. While this was less than the 2.5 MeV produced by the JPL Dynamitron, it was thought to be no serious problem since the major damage to devices was due to ionization and the ionization cross section with energy in this region is quite flat.

As in the JPL Dynamitron testing, the test devices were exposed at 0.9 m (3 ft) from the beam tube window with a beam-scattering foil on the end of the beam tube. A throughput ion chamber and a faraday cup were used to determine the flux and fluence, the ion chamber being an independent check on the beam flux stability.

The Boeing <u>in situ</u> tests were done on a limited number of the most important electrical parameters of integrated circuits. Further details on the test and results may be found in Sections IV, VII, and VIII.

4. IRAN Testing

The irradiation-anneal (IRAN) testing of flight parts was done by the Hughes Aircraft Company for JPL. A special test setup was prepared for the IRAN work, which was semi-automated so that 48 test devices could be irradiated and measured as soon after the radiation exposure as possible. Figure 5-6 is a block diagram of this system. Figure 5-7 shows the stepper switches and the test samples in the faraday cage. Figures 5-8 and 5-9 show the operating instrumentation.

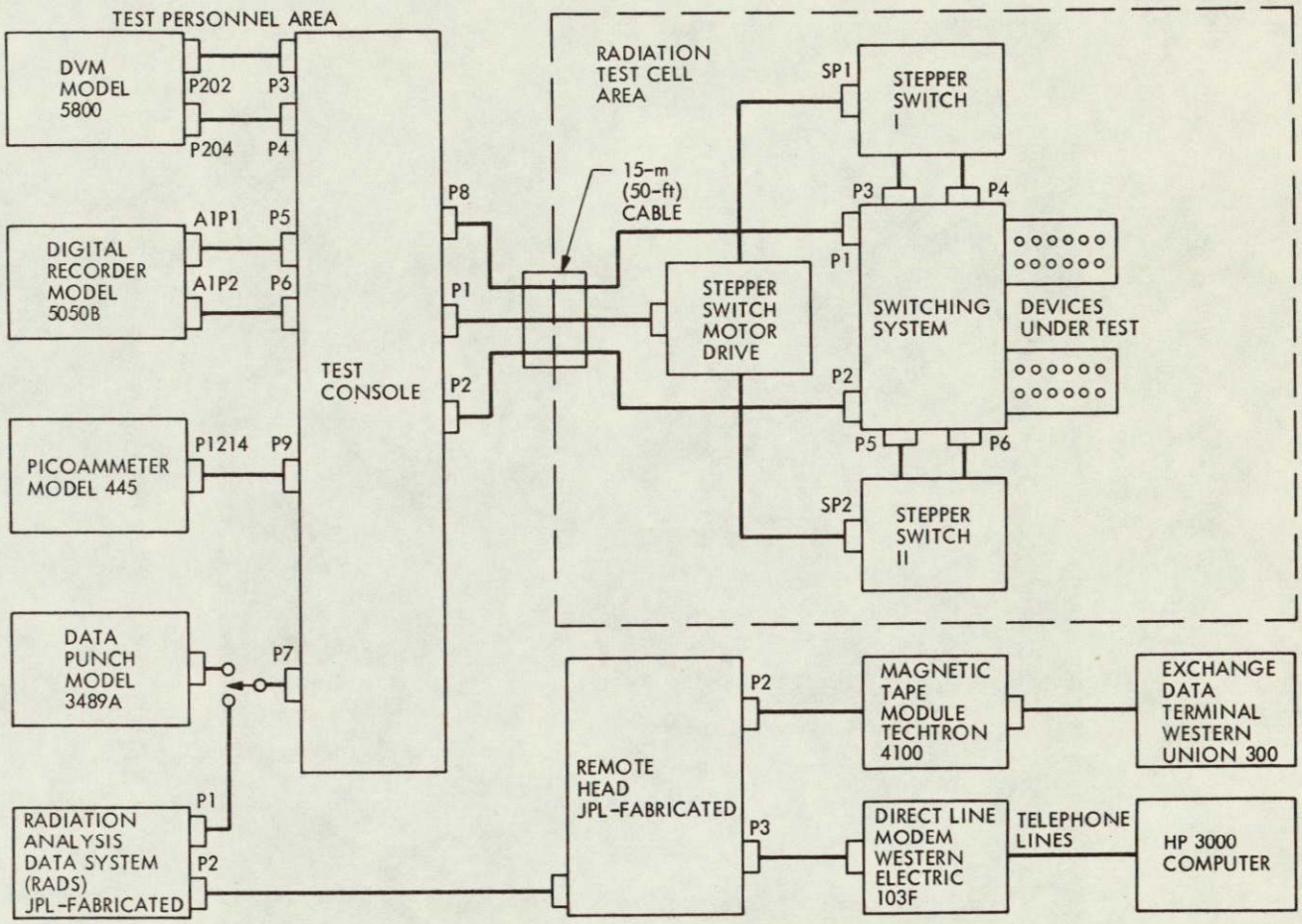

Fig. 5-6. Block Diagram of the IRAN Testing System

The functional criteria applied to the system were as follows. Electrical leakage was kept to 50 pA or less. The power supplies produced fixed voltage rather than variable voltage. A control sample was measured both before and after each series of measurements. A delay time of up to 4 seconds was required before reading a measurement value, in order to obtain reproducible readings. Measurements of voltage were made reproducible to $\pm$0.1 mV. Accuracy of the current values were within $\pm$10 percent as measured from socket to socket with a calibrated current input. A detailed procedure (Appendix E) written for the IRAN work included a step-by-step procedure for doing the IRAN testing and a section on quality assurance requirements. Quality assurance personnel were present at all times while flight parts were being handled.

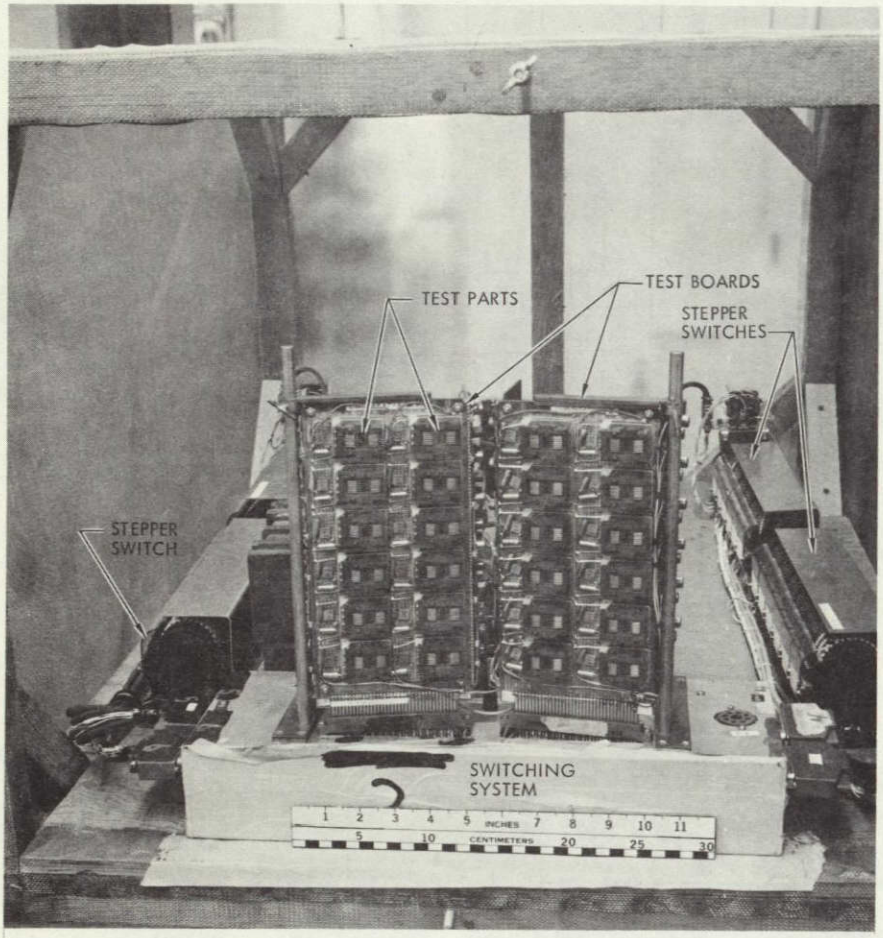

Fig. 5-7. Faraday Cage With Test Sample on Test Boards and With Stepper Switches on Either Side for Use in IRAN Screening

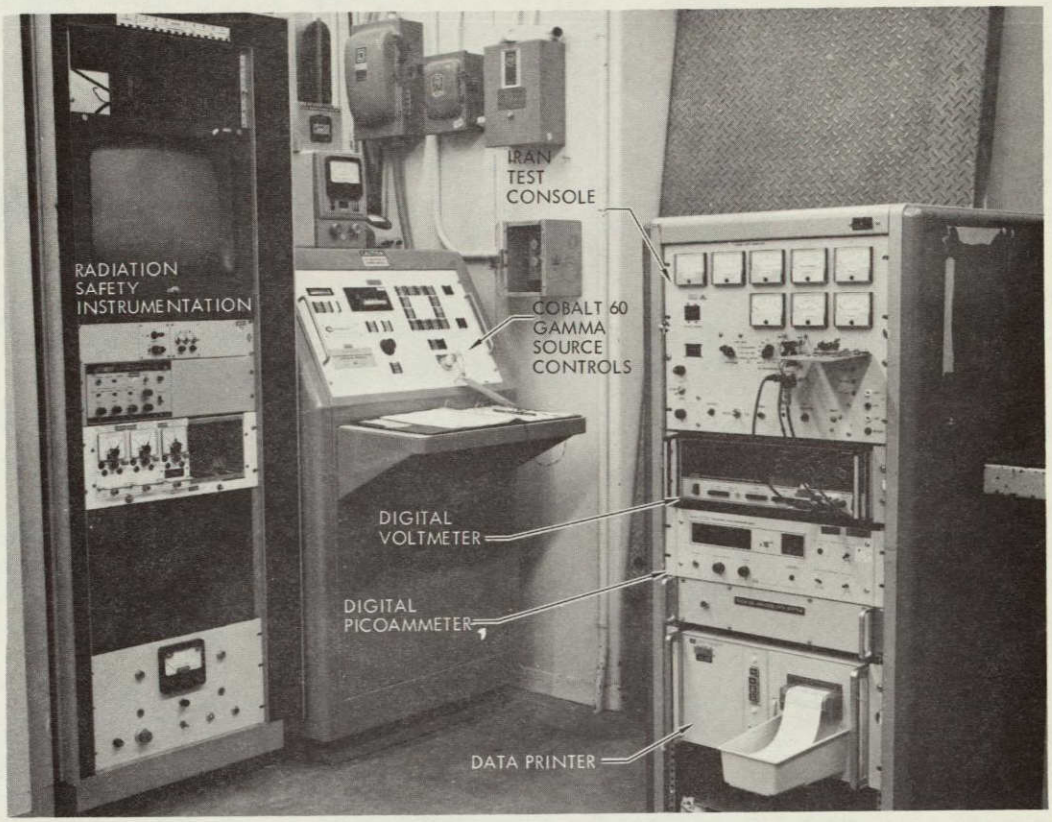

Fig. 5-8. Operating Instrumentation for the IRAN Screening Tests

The cobalt 60 source used was a 50-kilocurie panoramic irradiator, Gammabeam, Model 650, made by Atomic Energy of Canada, Ltd. The source field was calibrated with TLD, which was in turn calibrated with a ±2 percent Victoreen ion chamber. The variable-diameter source ring was kept at its minimum diameter, and the devices were irradiated at a fixed distance from the center of the source, to obtain a dose-rate of 50 rad(Si)/s. Doses used for IRAN were 50 to 125 krad(Si). Dose uniformity over the samples was better than ±10%. Figure 5-10 shows the source with an IRAN test in place.

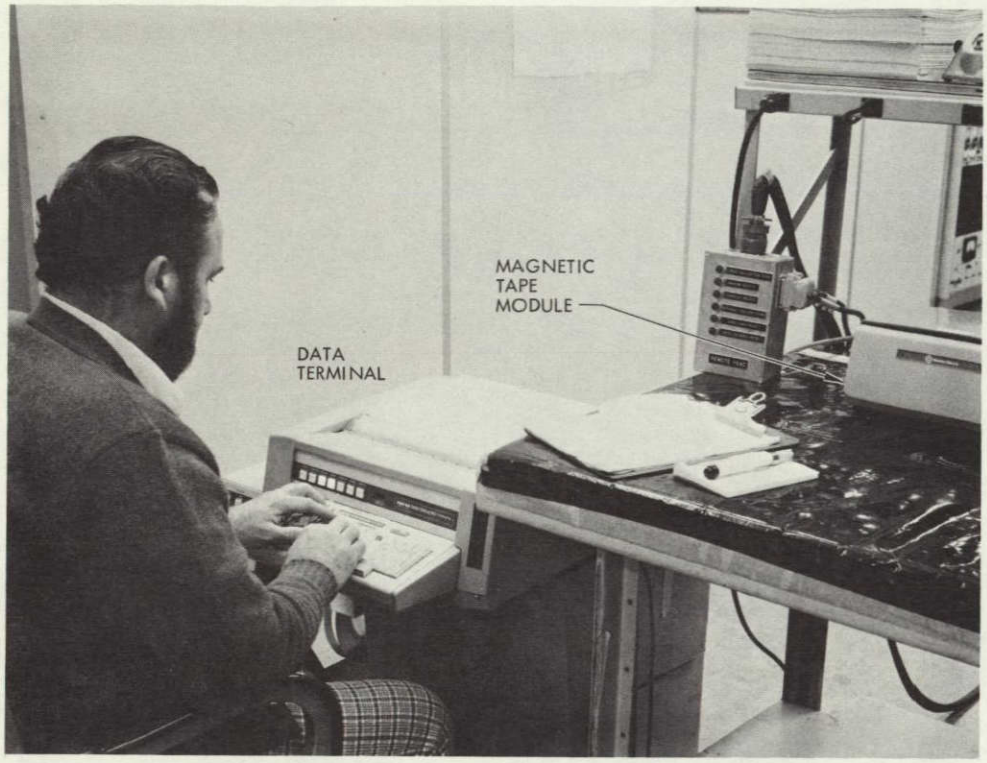

Fig. 5-9. IRAN Data Receiving and Processing Area

In the annealing oven (Figure 5-11), the temperature was maintained at 150° 5 C. Parts were routinely annealed for at least 96 hours. Nitrogen gas flow was maintained in the oven throughout the time the parts were in the ovens.

IRAN screening was carried out on a very limited number of integrated circuits and one transistor. Further details may be found in Sections IV and VIII.

5. CMOS Testing

Several types of tests were done on CMOS devices, including I_{SS} screening, V_T measurements on test patterns, propagation time measurements, and characterization measurements. All these tests were performed under JPL direction by Hughes Aircraft Company except for the characterization measurements, which required sophisticated computer analysis. These characterization tests were done at the Naval Research Laboratory.

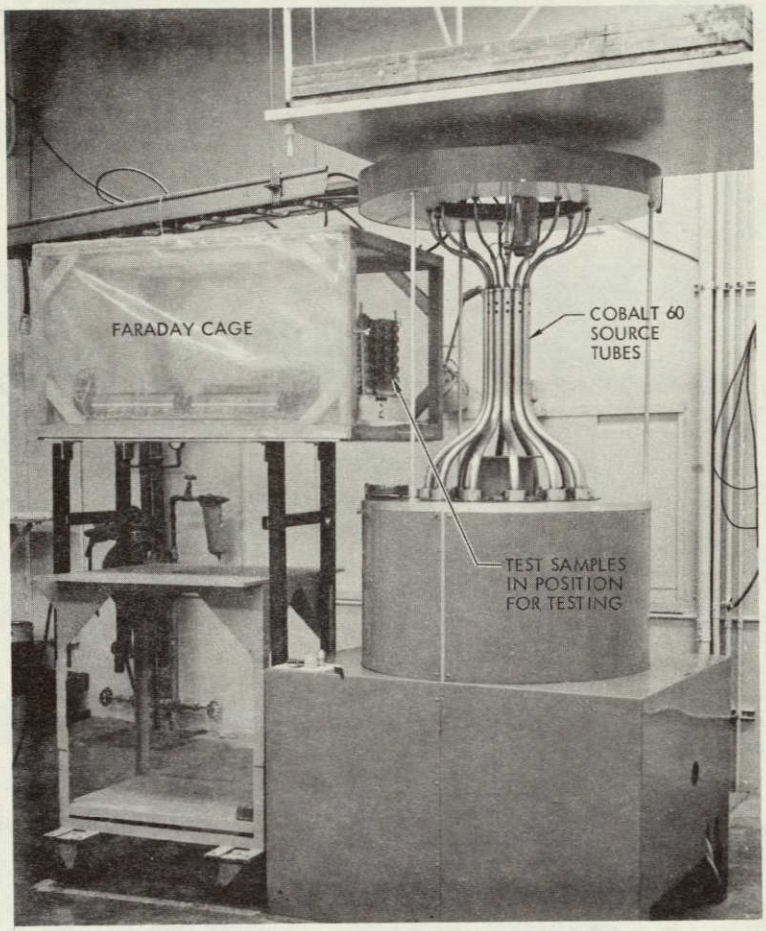

Fig. 5-10. IRAN Screening Test in Place for Irradiation

a. I_{SS} Screening. Approximately 13,000 CMOS devices were screened by measurements of I_{SS}. Throughput was somewhat limited (up to 15 devices were irradiated simultaneously) by the amount of available space in the cobalt 60 source used. Figure 5-12 shows the source used and the instrumentation. Figure 5-13 is a closeup at the irradiation chamber, showing device sockets with four samples in place. The instrumentation, built specifically for this test series, is shown in Figure 5-14. The gamma dose rate in the chamber was measured at 8510 rad(Si)/min with some small radioactivity decay over the course of the program. Adjustment in the length of exposure was made for the decay to maintain 150 kilorad(Si) as the total dose for each exposure.

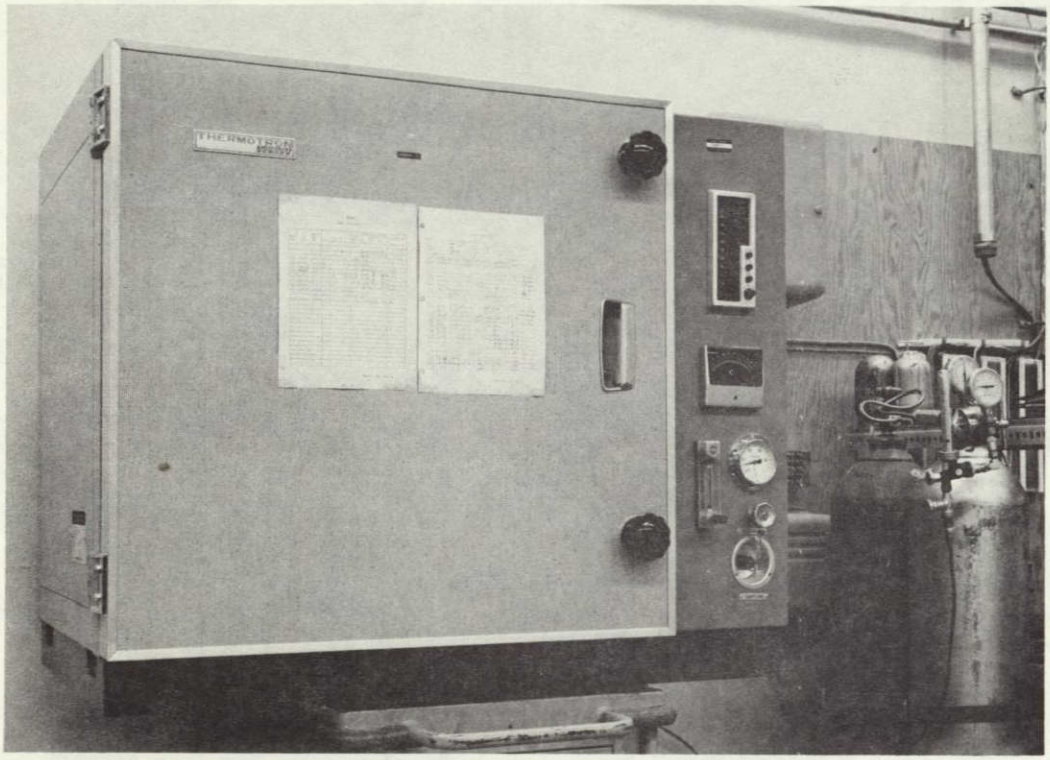

Fig. 5-11. Inert Gas Annealing Oven for the IRAN-Screened Parts

A radiation exposure was made by placing the CMOS devices in the sockets shown in Figure 5-13. Then the chamber was lowered into the radiation field for a preset time. When the chamber was raised automatically by the clock, the I_{SS} measurements were made.

b. V_T and Propagation Time Measurements. These measurements were made with different instrumentation but both used the Hughes 50-kilocurie source shown in Figure 5-10, which required 15-m (50-ft) long cables for the in situ measurements.

c. Device Characterization. The Naval Research Laboratory did the device characterization testing of CMOS devices using a cobalt 60 source shielded with water. The devices were biased during the radiation exposure. However, the bias was removed after the exposure, and the devices were taken to another building for measurements. This procedure resulted in a time delay of about 20 min which, along with the bias removal, may have resulted in some annealing of the leakage currents.

In CMOS testing the greater portion of the work was in I_{SS} screening. Each of the CMOS tests is further discussed in Sections IV, VII, and VIII.

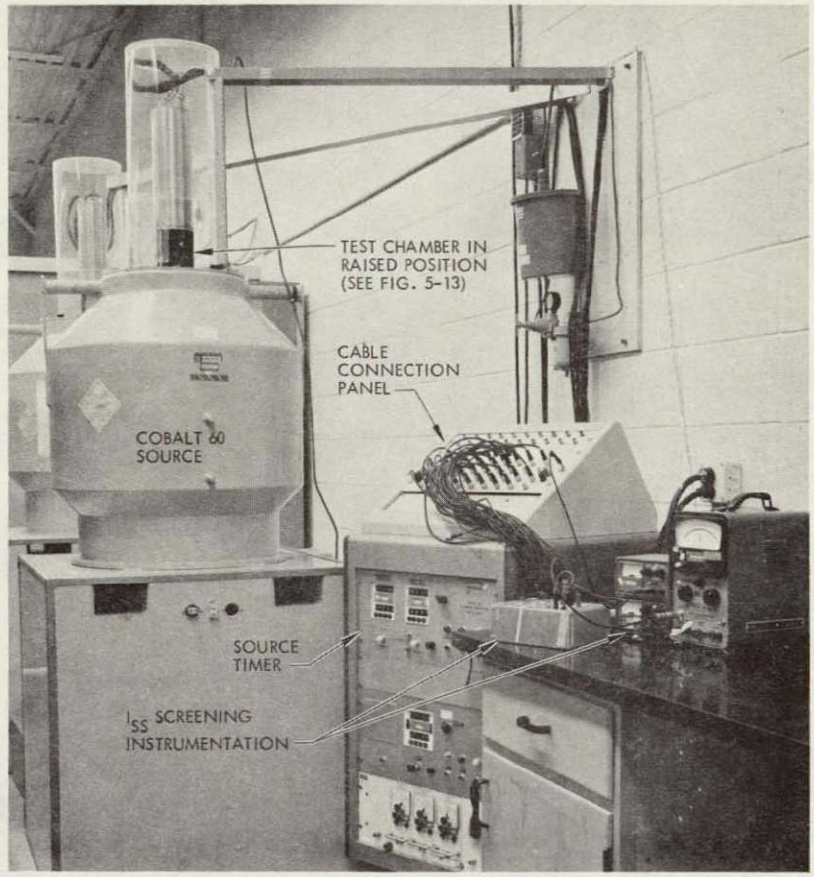

Fig. 5-12. Test setup for the I_{SS} Screening of CMOS Parts

6. Diodes and Rectifiers

The diodes and rectifiers that were required to maintain a close tolerance in output were tested using the JPL 2.5-MeV Dynamitron. In addition, on some diodes, higher energy electrons were used to determine whether displacement damage at the higher energies might be important. These higher energies were obtained by using the Van de Graaff accelerator at Notre Dame University. Both 3-MeV and 5.5-MeV electrons were used.

The tests at Notre Dame were carried out by General Electric Company personnel for JPL using a test setup much like the one used at the JPL Dynamitron described in Section D-2. The parts were biased during exposure. The electron beam was brought into the test area with an evacuated drift tube through a thin window into a gold scattering foil, then through 76 cm (30 in.) of air to the devices under test. A faraday cup was used to monitor flux and fluence. TLD was used to confirm dose at each dose point. The beam uniformity was found to be $\pm$10 percent over the test device exposure area, using an array of copper blocks as collectors. The test devices were confined to a 7-cm (2-3/4 in.) square area.

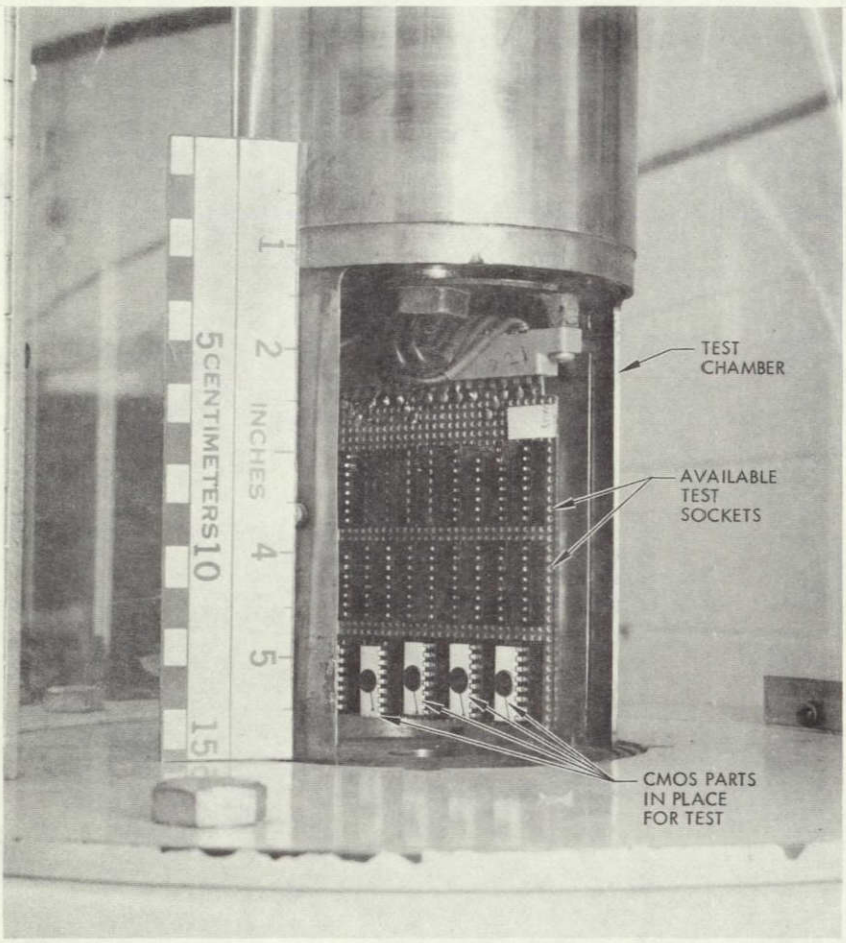

Fig. 5-13. Test Chamber in Raised Position With CMOS Parts in Place for I_{SS} Screening

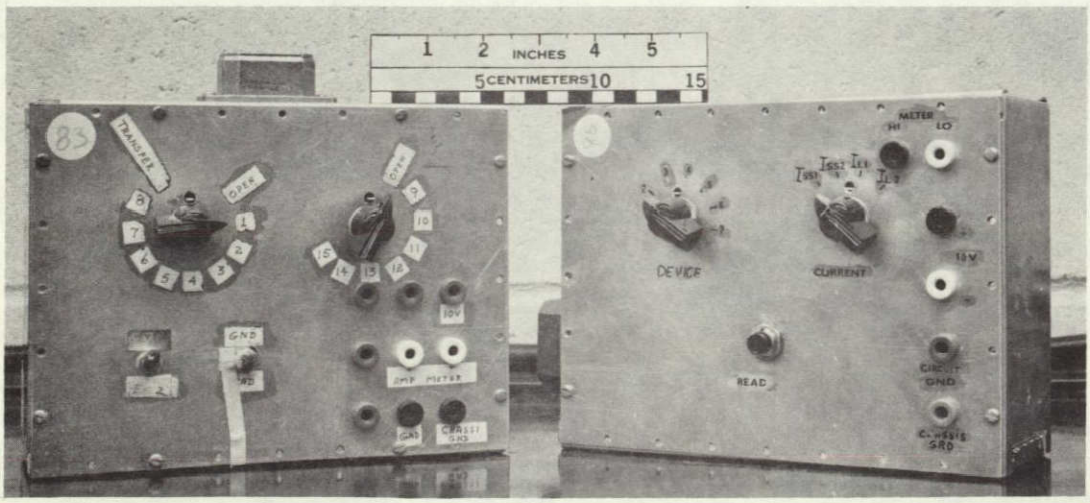

Fig. 5-14. Instrumentation for the I_{SS} Screening of CMOS Devices

The work on diodes and rectifiers amounted to a small part of the total program. Further details on these tests are given in Sections IV and VII.

7. Power Devices

A number of power devices have very thick cases and are stud-mounted devices. For such devices, electrons have difficulty in penetrating the package. Consequently, cobalt 60 was used to irradiate such devices. The work was done using the JPL dual 13-kilocurie sources. The test arrangement was the same as for other transistor testing utilizing the matrix board described earlier and the 15-m (50-ft) cable; only the source is different. In the tests, the same total doses as used in Dynamitron tests were obtained, but the dose rates were changed to accommodate reasonable exposure periods of 8 to 25 min.

Figure 5-15 shows a test board with stud-mounted devices ready for the in situ cobalt test. Figure 5-16 shows the dual 13-kilocurie source with the test fixture between the sources.

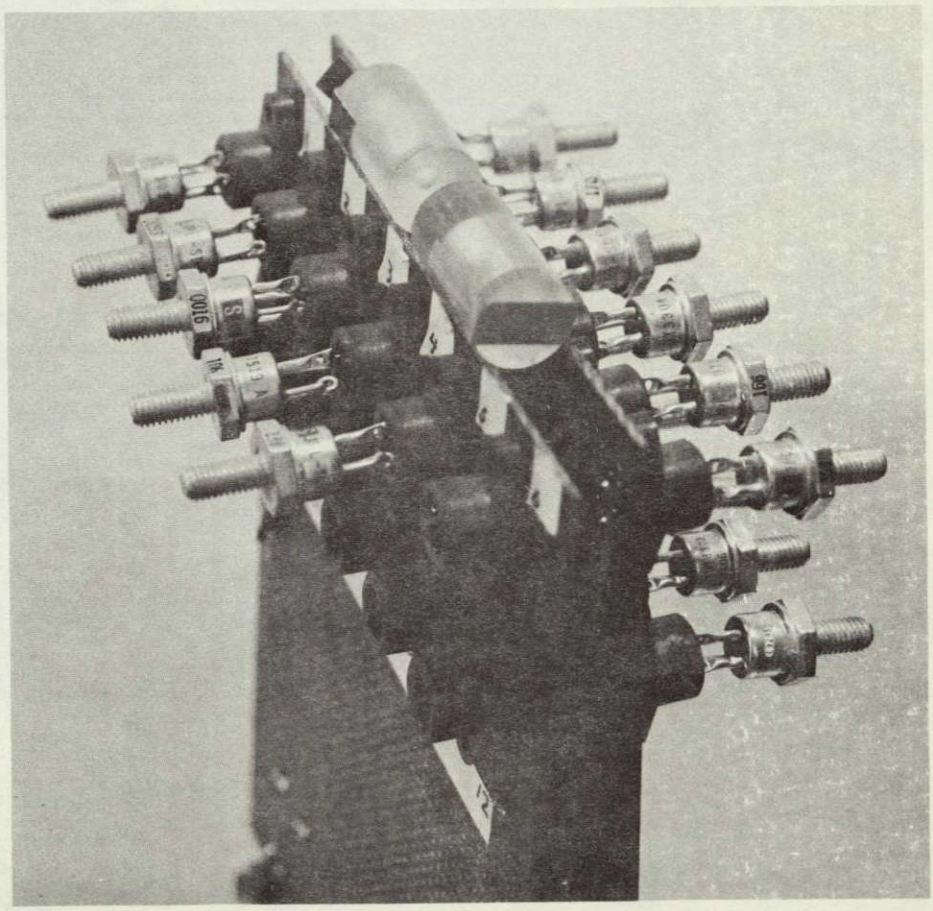

Fig. 5-15. Stud-Mounted Power Transistors Ready for Gamma Radiation Test

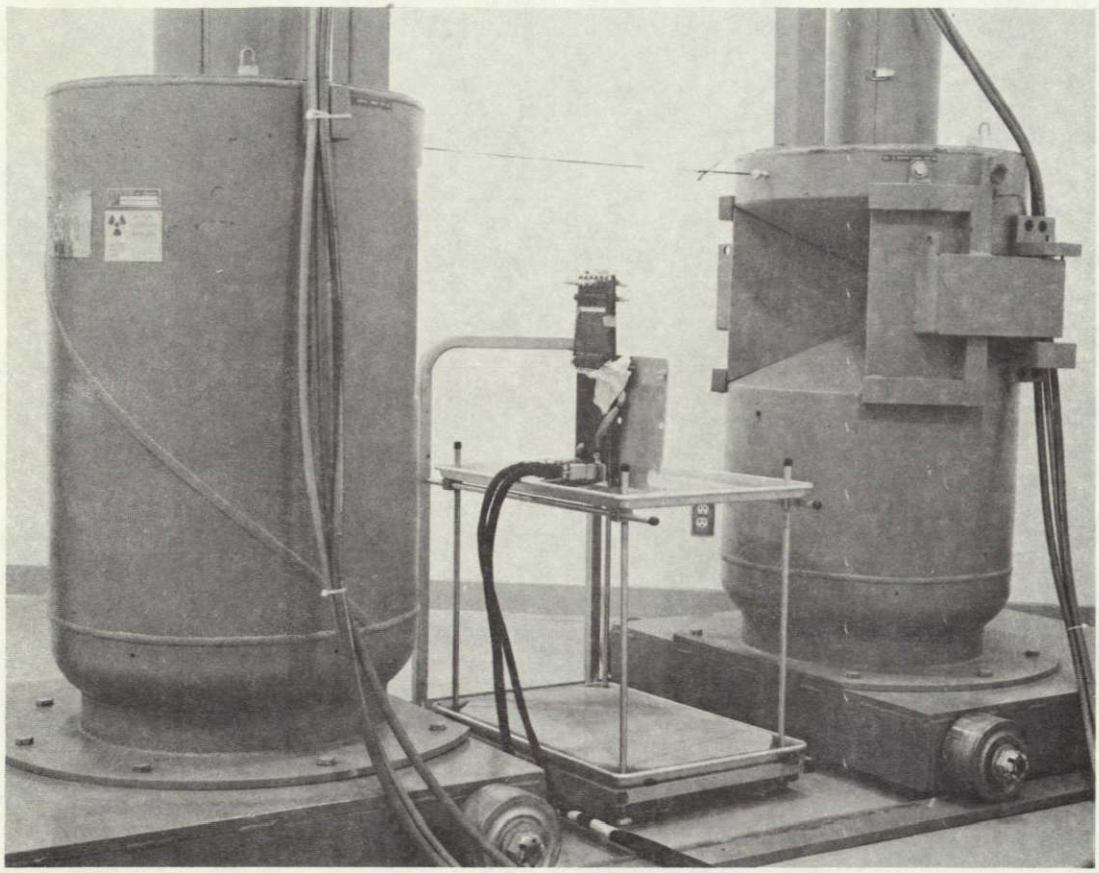

Fig. 5-16. JPL Dual 13-kilocurie Cobalt 60 Source With Power Transistors in Place for Test

SECTION VI

DEVICE HARDENING

A. INTRODUCTION

In the Voyager program, as mentioned earlier, radiation was originally not considered to be a problem. Subsequently, Pioneer Jupiter flybys indicated the presence of strong radiation belts, which led to an intensive program to harden the existing Mariner design. At this point, there was not sufficient time to undertake a device-hardening program, except in the case of the CMOS CD4000 series and of some bipolar linear devices, where hardening resulted in improved devices. The hardening programs were carried out by RCA for the CD4000 series and by National Semiconductor for the linear devices. The results of the program are described in this Section.

B. CMOS

Large quantities of CMOS devices comprising 28 different logic functions were used in the spacecraft. Devices fabricated by the standard commercial process could not withstand a fluence of 5×10^{12} e/cm^2 under normal bias conditions, due to a shift of the n-channel gate turn-on voltage toward 0 V, accompanied by an increase in the supply current. By reducing the gate oxide annealing temperature from 1100 to 950°C, it was found possible to fabricate devices that were still functional after irradiation to 5×10^{12} e/cm^2, though with somewhat degraded device characteristics (References 6-1 and 6-2). However, even these devices showed significant degradation at a dose of 150 krad(Si) as shown by Reference 6-3:

(1) Increases in the quiescent supply current by factors greater than 3000 into the microampere range, and with corresponding increases in the leakage currents between different terminals. Large-area devices or devices containing large-area transistors were particularly affected, as was the leakage current through the transmission gates of multiplexers.

Preliminary data indicate that the substitution of nitrogen for forming gas in the gate oxide annealing step has a beneficial effect on reducing the post-radiation quiescent supply current and transmission gate leakage currents of the multiplexers and on producing a more homogeneous product.

(2) Test patterns formed by n-channel MOS transistors produced a shift in the gate turn-on voltage from positive to negative values in many cases (see Figure 6-1). The true gate turn-on voltage, V_{TN}, at low currents is less than 1 V before irradiation and shifts to -0.6 V at 150 krad(Si). At higher current levels, V_{TN} stays well above zero, and does not shift significantly after irradiation. On the other hand, V_{TP} at 10 μA showed a bimodal distribution after irradiation.

(3) The devices showed an increase in the propagation delay time of up to 50 percent at 75 krad(Si) or 100 percent at 150 krad(Si). The average increases from 2 to 37 percent for different device types at 75 krad(Si) and from 6 to 62 percent at 150 krad(Si). The propagation delay is governed by a shift in the p-channel gate turn-on voltage.

A CMOS static random-access memory, very susceptible to ionizing radiation, was also used on the spacecraft. A hardening program for this component was considered to be too expensive. It was, therefore, decided to apply massive shielding, so that the impinging total dose would not exceed 10 krad(Si).

Radiation effects in MOS devices are governed by slow oxide states in the gate oxide and by fast interface states at the gate-oxide silicon interface. The interface states are important at the highest radiation levels. They cause the p-channel device threshold voltage to shift to more negative values, but cause the n-channel devices to shift to more positive values. On the other hand, the oxide states cause negative shifts in both device types. They become effective at low radiation levels and saturate at the highest radiation levels. This behavior explains the maximum change in threshold voltage in n-channel devices at intermediate radiation levels, followed by an improvement at higher fluences. In p-channel devices, both interface and oxide states produce negative shifts in threshold voltage, so that no saturation effect is seen as the total dose is increased.

The four basic CMOS failure modes in an ionizing radiation environment have been identified by Burghard and Gwyn (References 6-4 and 6-5) with their associate causes as follows:

(1) Failure to Switch - $|V_{TN}|\downarrow$ $|V_{TP}|\uparrow$

(2) Excessive Leakage - $|V_{TN}|\downarrow$

(3) Speed Reduction - $|V_{TP}|\downarrow$

(4) Noise Immunity - $|V_{TN}|\downarrow$ $|V_{TP}|\uparrow$

The arrows indicate a decrease $\downarrow$ or increase $\uparrow$ in $|V_T|$.

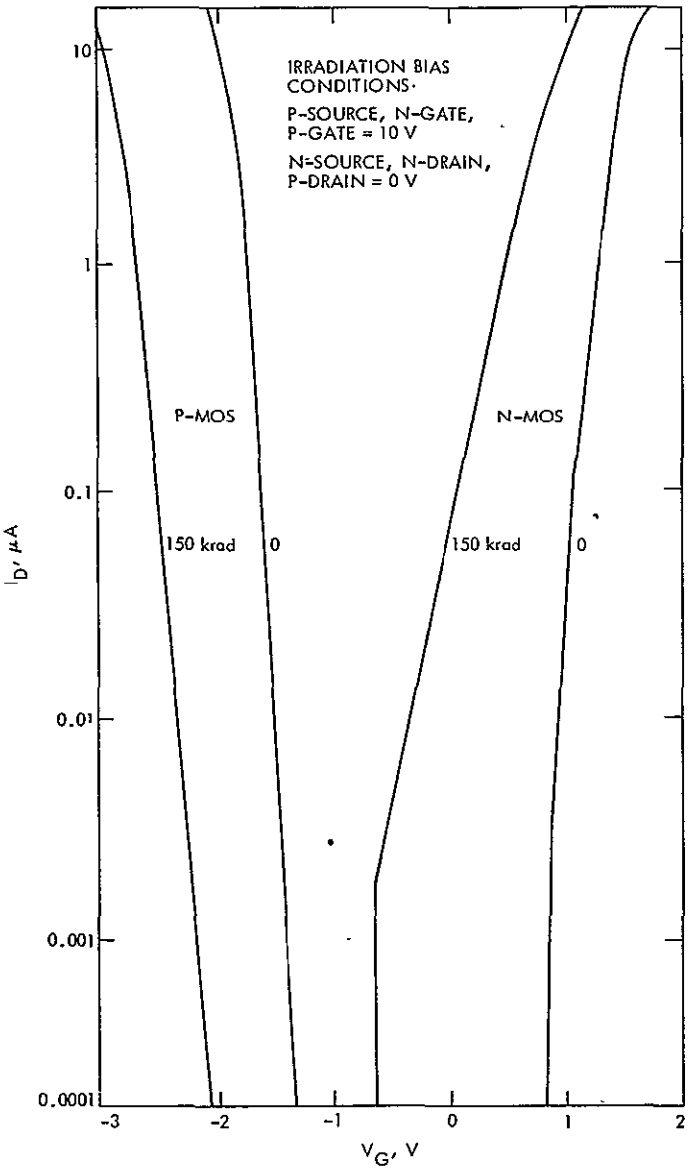

Figure 6-1. Gate Voltage vs Drain Current

C. LINEAR INTEGRATED CIRCUITS

1. Hardening Program

Sophisticated bipolar linear circuits with low power dissipation and high performance specifications are very sensitive to surface ionization damage, which can change their operating parameters by orders of magnitude beyond their specification limits (Reference 6-6). Hardening of bipolar linear circuits may be accomplished either by process changes, by changes in design, or by a combination of the two. Hardening by changes in design is more limited to a single device family and is also more costly.

The sensitivity to ionizing radiation may be significantly reduced by modifying the structure and composition of the oxide layer next

to the silicon interface, though often at the expense of reducing the manufacturer's yield of devices with the most desirable pre-irradiation electrical characteristics. The processing steps, starting with emitter diffusion and oxidation, are critical to achieve radiation hardness, i.e., the temperature and conditions of the different diffusion, oxidation, and annealing steps. In particular, the radiation resistance is believed to be deleteriously affected by subsequent dry oxidations at moderate heat and by the use of forming gas.

In late 1974 and early 1975, Voyager funded some specially processed runs at National Semiconductor in an attempt to obtain improved radiation hardness in several device types. Tables 6-1 and 6-2 show that this effort was successful in some device types, notably the LM108, but failed in others. In particular, attempts to harden the LM101 operational amplifier and the LM111 comparator were unsuccessful. Some success was also achieved in hardening the LM139 comparator; see Section VIII-A-1.

The LM108 was the prototype for the hardening effort at National Semiconductor, and LM108 kit parts were irradiated to obtain diagnostic information. The data shown in Table 6-3 indicates that the radiation generates large collector leakage currents in the unhardened lateral and vertical pnp transistors; these leakage currents are removed by the hardening process. These currents also destroy the gain of the pnp transistors. The gains of the standard and superbeta npn transistors are also improved by the hardening process.

2. LM108

Improved hardness was achieved in the LM108 and LM108A operational amplifiers, and the devices were satisfactory for Voyager applications. The modified process did, however, produce several undesirable side effects:

(1) The pre-irradiation input specifications for the LM108A could not consistently be met, and relaxation was required.

(2) Yield to electrical specifications was poor at -55°C.

(3) The devices were appreciably noisier than the standard product.

(4) The modified chip was incompatible with flatpack encapsulation, which degraded the pre-irradiation electrical characteristics as well as the radiation response.

There were a few applications where flatpacks had to be used or where the noise could not be tolerated. Heavily shielded standard devices were used in these cases. Also, a few applications requiring extreme stability through irradiation necessitated the shielding of even the hardened devices.

The noise problem is inherent in the steam oxide radiation-hardening process; it is caused by an increase in the density of fast interface states as well as by some lattice damage during the steam oxidation

process. There is considerable variation in the noise level of the hardened devices. Most devices exhibit a strong 1/f noise, and some show popcorn noise, which may be identified by a transient shift in the offset voltage.

A number of devices were irradiated with 2.5-MeV electrons at the JPL Dynamitron to study the radiation effects on the noise characteristics. The samples were chosen so as to exhibit varied pre-irradiation noise characteristics.

The irradiation results are summarized in Tables 6-4 through 6-6. The 1/f noise of the quiet parts increased by a factor 2 to 3 over the total dose range from 0 to 125 krad(Si). However, most of the increase took place at the lowest radiation level of 12.5 krad(Si) and is associated with a radiation-induced increase in the surface recombination velocity. The initially noisy devices increased by a factor of 6 at 12.5 krad(Si), but further irradiation caused a decrease in the noise level to their pre-irradiation value.

The quiet devices showed a steady increase in popcorn noise on irradiation by a factor of 2 to 3 at 125 krad(Si). The devices exhibiting strong initial popcorn noise showed an initial increase by a factor of 2 at 12.5 krad(Si). This was followed by a decrease to their pre-irradiation value.

Additional measurements were made at 400 Hz for all devices. The quiet devices showed little change on irradiation. The noisy devices decreased slightly at the 12.5 krad(Si) level, then showed little additional change during further irradiation.

3. LM139

The LM139 comparator produced at National Semiconductor failed at a fluence of 1×10^{12} e/cm^2 when biased in the <u>off</u> condition during irradiation. An attempt to harden this device was made in two stages. In the first stage, the emitter oxidation was switched to steam oxidation as in the other linear devices. In the second stage, some additional oxidation steps after the emitter oxidation were omitted.

Table 6-7 shows that the initial hardening effort was unsuccessful, whereas the final effort increased the onset of the catastrophic failure mode when the devices were irradiated in the <u>off</u> condition from 1×10^{12} to 5×12^{12}. The failure mode is caused by a latchup which causes the output voltage to move toward the positive supply voltage. The final hardened devices also showed smaller shifts in the dc parameters. The main drawback of the final hardening process was a significant worsening of the output sink current.

Table 6-1. Successful Linear Hardening Efforts

Device	Parameter	Fluence e/cm^2	Mean + 3 σ Values	
			Hardened	Unhardened
LM108	ΔV_{OS} (mV)	5×10^{12}	0.50	1050
		1×10^{13}	0.95	900
	ΔI_{OS} (nA)	5×10^{12}	0.52	6.5
		1×10^{13}	0.95	14
	ΔI_B (nA)	5×10^{12}	7.4	11.6
		1×10^{13}	14.9	43.2
	Open-loop gain (dB) at 2-mA load	5×10^{12}	84	Failed
		1×10^{13}	74.7	Failed
LM105 Voltage regulator	ΔLoad Regulation Output Voltage (mV)	5×10^{12}	3.55	26.66
		1×10^{13}	7.48	20.1
	ΔLine Regulation (mV) at 8.5 V	5×10^{12}	3.33	27.62
		1×10^{13}	8.81	18.5
	ΔLine Regulation (mV) at 40 V	5×10^{12}	13.3	25.97
		1×10^{13}	7.82	8.22
LM102 Voltage follower	ΔV_{OS} (mV)	5×10^{12}	6.36	22.7
		1×10^{13}	6.26	52.5
	ΔI_B (mV)	5×10^{12}	9.05	10.8
		1×10^{13}	18.4	41.6

Table 6-2. Unsuccessful Linear Hardening Efforts

Device	Parameter	Fluence e/cm^2	Mean + 3σ Values	
			Hardened	Unhardened
LM101 operational	ΔV_{OS} (mV)	5×10^{12}	22.1	8.5
	ΔV_{OS} (mV)	1×10^{13}	22.5	12.7
	ΔI_{OS} (nA)	5×10^{12}	13.96	158.0
	ΔI_{OS} (nA)	1×10^{13}	9.3	326.0
	ΔI_B (nA)	5×10^{12}	180.7	99.0
	ΔI_B (nA)	1×10^{13}	223.3	138.0
	Open-loop gain (dB)	5×10^{12}	105.4	90.9
	$R_L = \infty$	1×10^{13}	Failed	
	Open-loop gain (dB)	5×10^{12}	100.1	80.6
	R_L = 2.5 kΩ	1×10^{13}	Failed	
	ΔOpen-loop gain (dB)	5×10^{12}	10.0	41.3
	$R_L = \infty$	1×10^{13}	Failed	
	ΔOpen-loop gain (dB)	5×10^{12}	12.4	17.9
	R_L = 2.5 kΩ	1×10^{13}	Failed	
LM124 operational amplifier	ΔV_{OS} (mV)	5×10^{12}	4.04	11.99
	ΔV_{OS} (mV)	1×10^{13}	9.4	10.41
	ΔI_{OS} (nA)	5×10^{12}	15.494	15.5
	ΔI_{OS} (nA)	1×10^{13}	27.17	27.2
	ΔI_B (nA)	5×10^{12}	159.4	31.08
	ΔI_B (nA)	1×10^{13}	270.9	55.6

Table 6-2. Unsuccessful Linear Hardening Efforts
(Continuation 1)

Device	Parameter	Fluence e/cm^2	Mean + 3 σ Values	
			Hardened	Unhardened
LM124 operational amplifier (continued)	ΔOutput sink current (mA)	5×10^{12}	0.0126	0.0121
		1×10^{13}	0.0212	0.0198
	ΔOutput source current (mA)	5×10^{12}	0.002	0.0126
		1×10^{13}	0.0027	0.0147
	Open-loop gain (dB)	2.5×10^{12}	96.53	101.12
	2-mA load	5×10^{12}	87.41	94.03
	ΔOpen-loop gain (dB) at 2-mA load	2.5×10^{12}	5.99	6.45
		5×10^{12}	15.13	13.12
LM111 Comparator	$\Delta V_{OS(off)}$ (mV)	5×10^{12}	6.05	2.35
		1×10^{13}	11.45	5.05
	$\Delta V_{OS(on)}$ (mV)	5×10^{12}	1.74	0.851
		1×10^{13}	10.2	0.851
	$\Delta I_{OS(off)}$ (mV)	5×10^{12}	167.0	30.7
		1×10^{13}	187.7	74.1
	$\Delta I_{OS(on)}$ (mV)	5×10^{12}	18.0	118.0
		1×10^{13}	56.46	101.0
	$\Delta I_{B(off)}$ (μA)	5×10^{12}	1.3	1.91
		1×10^{13}	1.3	1.61
	$\Delta I_{B(on)}$ (μA)	5×10^{12}	1.21	2.26
		1×10^{13}	2.05	1.9

Table 6-3. LM108 Kit Parts

Parameter	Fluence, e/cm^2		Unhardened	Hardened
$\Delta(1/h_{FE})$ V_{CE} = 5 V, I_C = 50 μA	2.5×10^{12}	Vertical pnp	Failed[a]	4.7×10^{-3}
	5×10^{12}		Failed[a]	7.4×10^{-3}
	1×10^{13}		Failed[a]	1.41×10^{-2}
V_{CE} = 5 V, I_C = 50 μA	2.5×10^{12}	Lateral pnp	4.03×10^{-2}	2.33×10^{-2}
	5×10^{12}		Failed[a]	4.41×10^{-2}
	1×10^{13}		Failed[a]	8×10^{-2}
I_{CBO}	0		7.19×10^{-1} nA	1.38×10^{-1} nA
	2.5×10^{12}	Vertical pnp	11.9 μA	2.93×10^{-1} nA
	5×10^{12}		240 μA	5.82×10^{-1} nA
	1×10^{13}		135 μA	9.41×10^{-1} nA
	0		1.26×10^{-1} nA	1.25×10^{-1} nA
	2.5×10^{12}	Lateral pnp	697 nA	1.76×10^{-1} nA
	5×10^{12}		1.82 μA	3.2×10^{-1} nA
	1×10^{13}		1.87 μA	4.4×10^{-1} nA
I_{CEO}	0		56.3 nA	5.18 nA
	2.5×10^{12}	Vertical pnp	5.22 μA	2.53 nA
	5×10^{12}		35.3 μA	3.19 nA
	1×10^{13}		78.6 μA	3.0 nA

Table 6-3. LM108 Kit Parts
(Continuation 1)

Parameter		Fluence, e/cm^2		Unhardened	Hardened
I_{CEO}		0		1.23 nA	3.68×10^{-1} nA
		2.5×10^{12}	Lateral pnp	317 μA	3.89×10^{-1} nA
		5×10^{12}		906 μA	6.19×10^{-1} nA
		1×10^{13}		1270 μA	1.12 nA
$\Delta(1/h_{FE})$	V_{CB} = 0 V, I_C = 10 μA	2.5×10^{12}	Super npn beta	1.3×10^{-3}	7.5×10^{-4}
		5×10^{12}		2.7×10^{-3}	1.04×10^{-3}
		1×10^{13}		4.0×10^{-3}	1.56×10^{-3}
	V_{CE} = 5 V, I_C = 100 μA	2.5×10^{12}	Standard npn beta	9.6×10^{-3}	7.7×10^{-4}
		5×10^{12}		9.4×10^{-3}	1.81×10^{-3}
		1×10^{13}		8.9×10^{-3}	3×10^{-3}

[a]Excessive collector leakage current.

Table 6-4. 1/f Noise (Average) at 1 Hz (1-Hz Bandwidth)

Total Dose		Noise, μV, for Indicated Device					
e/cm^2	krad (Si)						
		SN 1036	SN 1037	SN 1047	SN 1049	SN 1050	SN 3119
0	0	0.5	0.7	0.4	0.4	0.5	0.9
5×10^{11}	12.5	4.0	3.0	3.0	2.5	3.0	0.5
1.25×10^{12}	30	0.5	0.5	0.5	0.5	1.5	0.6
2.5×10^{12}	62.5	0.5	0.4	0.5	0.5	1.0	0.5
5×10^{12}	125	0.4	0.5	0.4	0.8	1.3	0.8
		SN 3107	SN 3133	SN 3145	SN 3177	SN 3183	
0	0	0.5	0.12	0.15	0.14	0.17	
5×10^{11}	12.5	0.4	0.4	0.30	0.4	0.4	
1.25×10^{12}	30	0.5	0.4	0.35	0.3	0.3	
2.5×10^{12}	62.5	0.4	0.4	0.4	0.4	0.5	
5×10^{12}	125	0.6	0.5	0.5	0.5	0.60	

Table 6-5. Popcorn Noise (Peak) at 1 Hz (1-Hz Bandwidth)

Total Dose		Noise, μV, for Indicated Device					
e/cm^2	krad (Si)						
		SN 1036	SN 1037	SN 1047	SN 1049	SN 1050	SN 3119
0	0	1.3	5.6	4.3	5.6	5.1	2.3
5×10^{11}	12.5	4.5	7.5	7.0	8.0	6.5	1.7
1.25×10^{12}	30	1.3	4.9	4.0	5.7	5.0	1.1
2.5×10^{12}	62.5	1.1	4.1	4.1	5.1	5.7	1.2
5×10^{12}	125	1.4	3.8	3.7	5.7	5.7	1.2
		SN 3107	SN 3133	SN 3145	SN 3177	SN 3183	
0	0	1.7	.56	.56	.36	.51	
5×10^{11}	12.5	1.3	0.5	0.7	0.65	0.8	
1.25×10^{12}	30	1.3	0.8	0.8	0.5	0.8	
2.5×10^{12}	62.5	1.4	.75	.8	.85	1.0	
5×10^{12}	125	1.5	1.2	1.3	1.2	1.4	

Table 6-6. 400-Hz White Noise (100-Hz Bandwidth)

Total Dose		Noise, μV, for Indicated Device					
e/cm^2	krad (Si)						
		SN 1036	SN 1037	SN 1047	SN 1049	SN 1050	SN 3119
0	0	1.0	.8	.8	.7	1.3	1.1
5×10^{11}	12.5	.4	.45	.4	.4	5	.4
1.25×10^{12}	30	.4	.4	.4	.4	5.2	.4
2.5×10^{12}	62.5	.4	.4	.4	.4	5	.35
5×10^{12}	125	.37	.37	.38	.36	5	.46
		SN 3107	SN 3133	SN 3145	SN 3177	SN 3183	
0	0	.26	.26	.34	.45	5.1	
5×10^{11}	12.5	.33	.42	.37	.37	4.5	
1.25×10^{12}	30	.32	.31	.32	.32	4.4	
2.5×10^{12}	62.5	.33	.31	.33	.32	4.4	
5×10^{12}	125	.39	.32	.38	.35	4.5	

4. Inherently Hard Devices

The LM105 voltage regulator was improved somewhat by hardening (see Table 6-1), but the radiation resistance of the unhardened devices was found to be adequate for all Voyager applications. The following device types were found to be sufficiently hard, so as not to require any device modification:

Comparators: LM106, LM710
Voltage Regulators: LM103, LM104, LM723

Table 6-7. LM139 Hardening

Device	Parameter	Null Voltage, V	Fluence, e/cm^2		Mean + 3σ Initial Hardening	Mean + 3σ Final Hardening	Mean + 3σ Unhardened
LM139	ΔV_{OS} (mV)	+0.7	5×10^{11}	On during irradiation	0.975	0.307	0.48
			1×10^{12}		1.60	---	0.45
			1.25×10^{12}		---	0.4	1.58
			2.5×10^{12}		5.18	1.8	3.33
			5×10^{12}		Failed	1.8	6.28
		+1.4	5×10^{12}	On during irradiation	4.7	---	63.5
			1×10^{13}		13.33	---	Failed
		+0.7	5×10^{11}	Off during irradiation	5.68	2.18	12.24
			1×10^{12}		25.9	---	Failed
			1.25×10^{12}		---	1.59	Failed
			2.5×10^{12}		Failed	37.9	Failed
			5×10^{12}		Failed	Failed	Failed
		+1.4	5×10^{12}		Failed	---	2.25
			1×10^{13}		Failed	---	Failed

Table 6-7. LM139 Hardening
(Continuation 1)

Device	Parameter	Null Voltage, V	Fluence, e/cm^2		Mean + 3σ Initial Hardening	Mean + 3σ Final Hardening	Mean + 3σ Unhardened
LM139	ΔI_{OS} (nA)	+0.7	5×10^{11}	On during irradiation	28.31	2.4	7.01
			1×10^{12}		37.96	---	12.5
			1.25×10^{12}		---	16.98	29.0
			2.5×10^{12}		66.37	43.7	65.3
			5×10^{12}		Failed	71.3	97.2
		+1.4	5×10^{12}	On during irradiation	38.45	---	310.0
			1×10^{13}		Failed	---	Failed
		+0.7	5×10^{11}	Off during irradiation	106.99	43.4	7.78
			1×10^{12}		235.73	---	Failed
			1.25×10^{12}		---	20.2	Failed
			2.5×10^{12}		Failed	93.7	Failed
			5×10^{12}		Failed	Failed	Failed
		+1.4	5×10^{12}		Failed	---	55.5
			1×10^{13}		Failed	---	Failed

Table 6-7. LM139 Hardening
(Continuation 2)

Device	Parameter	Null Voltage, V	Fluence, e/cm^2		Mean + 3σ Initial Hardening	Mean + 3σ Final Hardening	Mean + 3σ Unhardened
LM139	Δ/B (nA)	+0.7	5 x 10^{11}	On during	106.99	149.6	96.7
			1 x 10^{12}	irradiation	235.73	---	188.9
			1.25 x 10^{12}		---	317.9	193.8
			2.5 x 10^{12}		482.48	433.0	608.3
			5 x 10^{12}		Failed	482.4	1860.0
		+1.4	5 x 10^{12}	On during	209.38	---	500.1
			1 x 10^{13}	irradiation	385.36	---	Failed
		+0.7	5 x 10^{11}	Off during	152.1	150.5	104.6
			1 x 10^{12}	irradiation	289.85	---	Failed
			1.25 x 10^{12}		---	331.9	Failed
			2.5 x 10^{12}		Failed	455.8	Failed
			5 x 10^{12}		Failed	Failed	Failed
		+1.4	5 x 10^{12}		Failed	---	512.3
			1 x 10^{13}		Failed	---	Failed

Table 6-7. LM139 Hardening
(Continuation 3)

Device	Parameter	Null Voltage, V	Fluence, e/cm^2		Mean - 3σ Initial Hardening	Mean - 3σ Final Hardening	Mean - 3σ Unhardened
LM139	Output sink current (mA)	1.5	5×10^{11}	On during irradiation	6.02	5.46	Negative
			1×10^{12}		5.14	---	1.02
			1.25×10^{12}		---	3.12	---
			2.5×10^{12}		3.96	2.11	0.04
			5×10^{12}		Failed	1.73	Negative
			5×10^{11}	Off during irradiation	6.45	5.35	Negative
			1×10^{12}		5.17	---	Failed
			1.25×10^{12}		---	3.00	---
			2.5×10^{12}		Failed	2.03	Failed
			5×10^{12}		Failed	Failed	Failed
		0.7	5×10^{11}	On during irradiation		6.99	9.98
			1.25×10^{12}			5.19	9.74
			5×10^{11}	Off during irradiation		7.60	10.05
			1.25×10^{12}			3.46	Failed

Table 6-7. LM139 Hardening
(Continuation 4)

Device	Parameter	Null Voltage, V	Fluence, e/cm^2		Mean - 3σ Initial Hardening	Mean - 3σ Final Hardening	Mean - 3σ Unhardened
LM139	Δ Output sink current (mA)	1.5	5×10^{11}	On during irradiation	-3.54	-5.50	-6.17
			1×10^{12}		-6.73	---	---
			1.25×10^{12}		---	8.13	-12.20
			2.5×10^{12}		-7.43	-9.35	-19.01
			5×10^{12}		Failed	-9.84	-24.5
			5×10^{11}	Off during irradiation	-3.72	-5.62	-6.32
			1×10^{12}		-5.66	---	Failed
			1.25×10^{12}		---	-8.23	---
			2.5×10^{12}		Failed	9.46	Failed
			5×10^{12}		Failed	Failed	Failed
		0.7	5×10^{11}	On during irradiation		-4.12	-1.93
			1.25×10^{12}			-6.39	-5.30
			5×10^{11}	Off during irradiation		-4.32	-1.99
			1.25×10^{12}			-6.29	Failed

SECTION VII

CHARACTERIZATION TEST RESULTS

The results of characterization tests conducted in the radiation program are summarized in this section under generic device type. Detailed test results are contained in Reference 1-1.

A. TEST DATA FROM OTHER SOURCES

A comprehensive analysis of existing test data was undertaken at the start of the characterization program but was eventually terminated by the Voyager Project Office due to the small benefits being derived. The critical analysis included reviewing the following:

(1) The manufacturer, device type, date, and lot codes.

(2) Bias conditions during irradiation and measurements (see Section V).

(3) Type of radiation facility, such as LINAC (potentially destructive because of high flux pulses) and cobalt 60 (no bulk damage) (see Section V).

(4) In situ testing to minimize annealing (see Section V).

(5) Annealing due to test methods (see Section V).

Analysis of these data from sources other than JPL generally revealed the following:

(1) Obsolete data.

(2) Bias conditions during irradiation not known.

(3) Measurements not in situ.

(4) LINAC, cobalt 60, and neutron test results not applicable for electron effects.

(5) Information on date codes and lot codes missing.

The bulk of the data was from

(1) Massachusetts Institute of Technology, Lincoln Laboratory --data valid but old.

(2) The Boeing literature search (Contract 952565, May 1970) and the Hughes literature search (Contract 953957).

(3) Harry Diamond Laboratories; Total Dose Data File, dated 3/4/76, and "Radiation Effects on Semiconductor Device, Summary of Data," June 1974.

(4) General Electric; "Electronic Parts Characterization for Jupiter Radiation Environments," April 1974.

(5) Jet Propulsion Laboratory; preliminary data on proton, neutron, electron and gamma ray tests.

B. BIPOLAR TRANSISTORS

Bipolar transistors degrade in an ionizing radiation environment because of an increase in the base current. There is a strong increase in the degradation at low current levels. Some transistors degrade far more than others, due to the formation of inversion layers near the surface of doped p-regions, thus causing enhanced p-n junction leakage.

In transistors, this inversion appears mostly as a decrease in h_{FE}, primarily at low collector currents, I_C. Figure 7-1 shows the effect of 5×10^{12} e/cm^2 on various transistors. The mean value of $\Delta(1/h_{FE})$ is plotted as a function of the collector current. Table 7-1 shows values for all bipolar transistors tested. The value of $\Delta(1/h_{FE})$ varies approximately as $I_C^{-1/2}$. It has, therefore, been proposed by V. A. J. Van Lint to reject devices that fall above a line $\Delta(1/h_{FE}) = 0.01\ I_C^{-1/2}$, where I_C is in mA, and to establish a design tolerance of $\Delta(1/h_{FE}) = 0.03\ I_C$ (see Figure 7-1).

It may be noted that the radiation resistance strongly depends on the processing line; e.g., the 2N2222 made by Vendor A is one of the better devices, whereas the same device fabricated by Vendor B is among the worst. Some device types show a slight dependence on operation in the saturated or unsaturated condition (Figure 7-2). Several device types show a bimodal distribution (Figure 7-3). Irradiate-anneal techniques have been employed in one instance to remove the inferior devices (see Section IV-B-4).

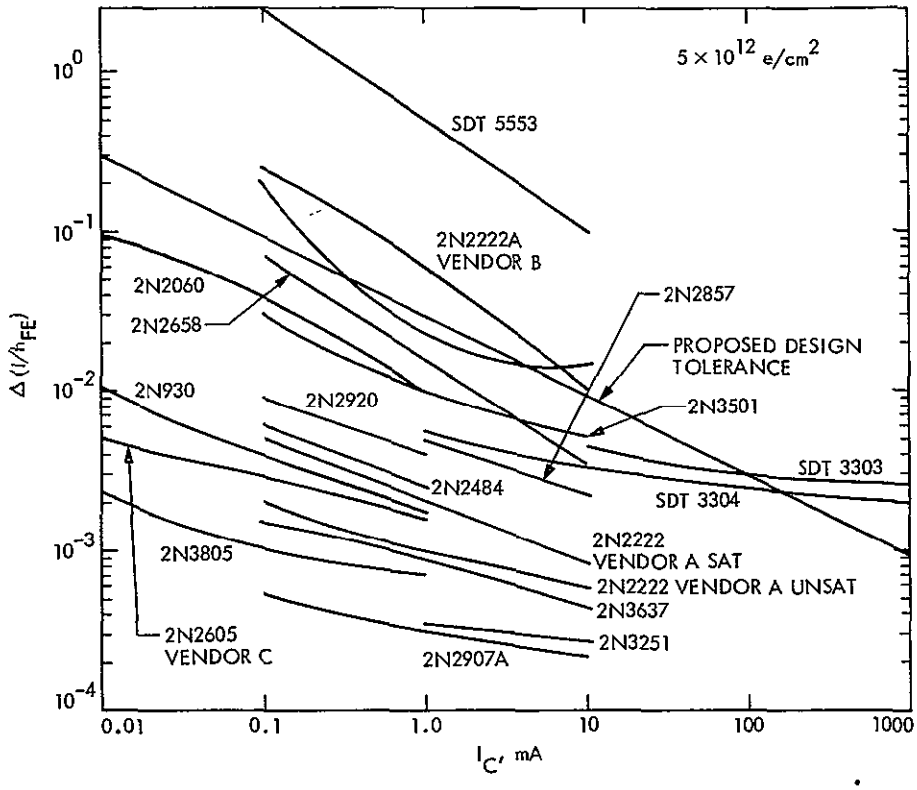

Fig. 7-1. Gain Degradation, $\Delta(1/h_{FE})$, vs Collector Current for Different Bipolar Transistors

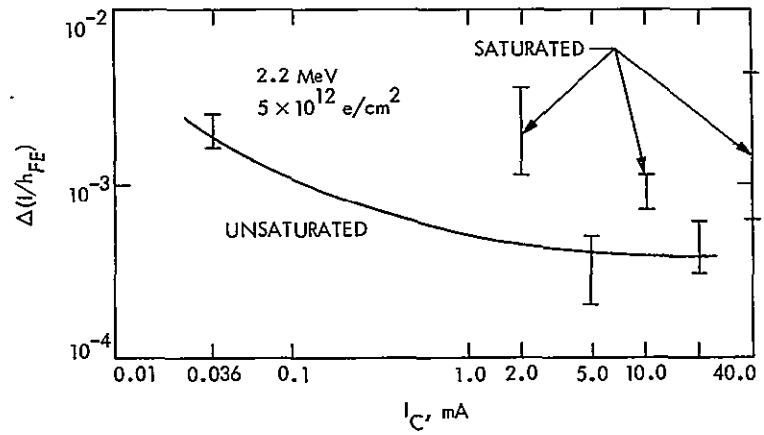

Fig. 7-2. Comparison of Gain Degradation in the Saturated and Unsaturated Mode of the 2N2907A Transistor

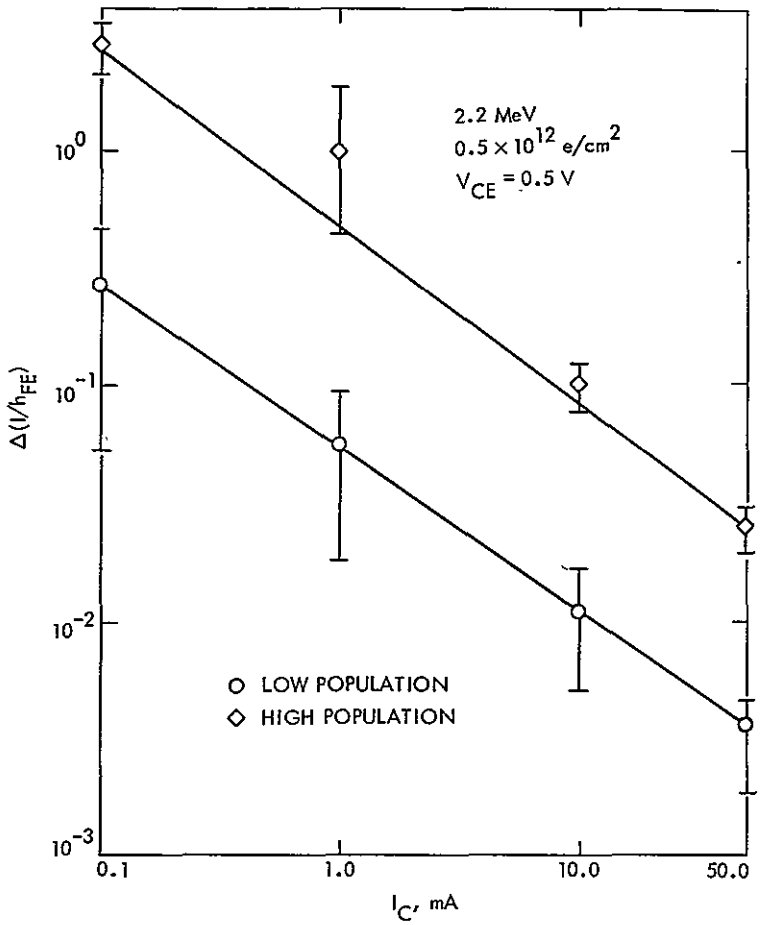

Fig. 7-3. Bimodal Distribution of a Bipolar Transistor

Table 7-1. Bipolar Transistor Types in Order of Increasing Sensitivity

Device Type	Manufacturer[a]	Sat.(S)/ Unsat.(U)	Bimodal Dist(B)/ Outliers(O)	$\Delta(1/h_{FE})$ at Indicated I_C in mA, at 5 x 10^{12} e/cm^2					
				0.01	0.1	1.0	10	100	1000
2N2907	MOT	U			5.9×10^{-4}	2.9×10^{-4}	2.2×10^{-4}		
2N3251	MOT	U				3.5×10^{-4}	2.7×10^{-4}		
2N2484	TIX	U			8.1×10^{-4}	5.4×10^{-4}			
2N2907	TIX	U			1.1×10^{-3}	4.4×10^{-4}	3.6×10^{-4}		
2N3440	RCA	U				5.5×10^{-4}			
2N3805	FAS	U		2.3×10^{-3}	1.15×10^{-3}	7.2×10^{-4}			
2N3637	MOT	U			1.3×10^{-3}	7.4×10^{-4}	1×10^{-4}		
2N2907	MOT	S					6.5×10^{-4}		
MQ2905	MOT	U,S	O			1×10^{-3}	7×10^{-4}		
2N2907	TIX	S					8×10^{-4}		
2N2605	TIX	U		3×10^{-3}	1.9×10^{-3}	1.4×10^{-3}			
2N3637	MOT	S			2.3×10^{-3}	1.4×10^{-3}			
2N2222	TIX	S[b]			2.5×10^{-3}	1.3×10^{-3}			
2N2605	CTI	U		4.9×10^{-3}	2.8×10^{-3}	1.6×10^{-3}			

Table 7-1. Bipolar Transistor Types in Order of Increasing Sensitivity (Continuation 1)

Device Type	Manufacturer[a]	Sat.(S)/ Unsat.(U)	Bimodal Dist(B)/ Outliers(O)	$\Delta(1/h_{FE})$ at Indicated I_C in mA, at 5 x 10^{12} e/cm^2					
				0.01	0.1	1.0	10	100	1000
2N3350	TIX	S	O	4.7×10^{-3}	3.4×10^{-3}	1.8×10^{-3}			
2N2920	TIX	S			6.2×10^{-3}	3.3×10^{-3}			
2N2484	CTI	U			4.8×10^{-3}	2.5×10^{-3}			
2N2975	FAS	U		1.4×10^{-2}	6.7×10^{-3}	3.1×10^{-3}			
2N2975	FAS	S		1.65×10^{-2}	7.3×10^{-3}	3.5×10^{-3}			
2N930	TIX	U	B	2×10^{-2}	8.4×10^{-3}	3×10^{-3}			
2N2222	TIX	U[c]	O		9×10^{-3}	3.4×10^{-3}	1.4×10^{-3}		
SS3137	MOT	S					1.45×10^{-3}		
2N918	MOT	U		2.4×10^{-2}	9×10^{-3}	4×10^{-3}			
2N2920	TIX	U	B		9.5×10^{-3}	4.2×10^{-3}			
2N4044	CTI	U						6.4×10^{-4}	
MQ3467	MOT	S	O			4.2×10^{-3}	1.3×10^{-3}	8.7×10^{-4}	
2N2857	MOT	U				4.7×10^{-3}	2.2×10^{-3}		
2N2222	TIX	U[b]			1.6×10^{-2}	5.4×10^{-3}	1.8×10^{-3}		

Table 7-1. Bipolar Transistor Types in Order of Increasing Sensitivity (Continuation 2)

Device Type	Manufacturer[a]	Sat.(S)/ Unsat.(U)	Bimodal Dist(B)/ Outliers(O)	$\Delta(1/h_{FE})$ at Indicated I_C in mA, at 5 x 10^{12} e/cm^2					
				0.01	0.1	1.0	10	100	1000
SDT3303	SOD	U				$4x10^{-3}$	$3.2x10^{-3}$	$2.4x10^{-3}$	$1.8x10^{-3}$
SDT3304	SOD	U				$5.5x10^{-3}$	$3.4x10^{-3}$	$2.5x10^{-3}$	$1.8x10^{-3}$
PA7443	RAY	S	O			$8.6x10^{-3}$	$2.5x10^{-3}$	$3x10^{-3}$	
KD6001	KMC	U				$1.2x10^{-2}$			
MQ2219	MOT	U	O				$2.3x10^{-3}$		
2N2222	TIX	S[c]	O		$1.7x10^{-2}$	$1.3x10^{-2}$	$2.5x10^{-3}$		
2N2060	TIX	U		$1x10^{-1}$	$3.5x10^{-2}$	$1.5x10^{-2}$			
2N3501	MOT	U			$3x10^{-2}$	$9x10^{-3}$	$5x10^{-3}$		
2N2222	TIX	S[d]			$4x10^{-2}$	$9x10^{-3}$	$4x10^{-3}$		
2N2222	TIX	U[d]		$2x10^{-1}$	$5x10^{-2}$	$1.3x10^{-2}$	$3.4x10^{-3}$		
SDT3303	SOD						$4.2x10^{-3}$	$3.2x10^{-3}$	$2.5x10^{-3}$
SA2267	RAY	S	O			$1.95x10^{-2}$	$5.5x10^{-3}$		
2N2222	MOT	U			$1.1x10^{-1}$	$2.2x10^{-2}$	$4.3x10^{-3}$		
2N3057	RAY	S			$2.2x10^{-1}$	$1.1x10^{-2}$	$3.8x10^{-3}$	$3.5x10^{-3}$	

Table 7-1. Bipolar Transistor Types in Order of Increasing Sensitivity (Continuation 3)

Device Type	Manufacturer[a]	Sat.(S)/ Unsat.(U)	Bimodal Dist(B)/ Outliers(O)	$\Delta(1/h_{FE})$ at Indicated I_C in mA, at 5 x 10^{12} e/cm^2					
				0.01	0.1	1.0	10	100	1000
2N2222	MOT	S				$3x10^{-2}$	$6.4x10^{-3}$		
3029-202-1	RAY	S					$7.8x10^{-3}$	$1.2x10^{-3}$	
SQ1079	MOT	S					$8.4x10^{-3}$	$7.6x10^{-3}$	
MQ3725	MOT	S	B,O			$2x10^{-2}$	$9x10^{-3}$	$3.5x10^{-3}$	
3029-201-1	RAY	S					$1.2x10^{-2}$	$2.7x10^{-3}$	
2N2880	SOD	U				$7.5x10^{-2}$	$1.3x10^{-2}$	$2.7x10^{-3}$	$9.5x10^{-3}$
2N2658	SOD	U				$7.6x10^{-2}$	$1.7x10^{-2}$	$3.4x10^{-3}$	
MG2219	MOT	S	O				$4x10^{-2}$	$5x10^{-3}$	
SDT5553	SOD	U	O		$1.2x10^{0}$	$2.7x10^{-1}$	$4.6x10^{-2}$		
SDT4905	SOD	U				$3.7x10^{-1}$	$3.9x10^{-2}$		
SDT5553	SOD	S	O		$2.1x10^{0}$	$5.4x10^{-1}$	$6x10^{-2}$	$3.7x10^{-3}$	

[a]See Appendix A for vendor identification codes.
[b]1974, 1975.
[c]1973.
[d]1971, 1972.

Table 7-1 may be used to estimate degradation at 5 x 10^{12} e/cm^2 at the collector currents (I_C) listed. This is calculated using the following formula:

$$h_{FE\ (post\text{-}irradiation)} = \frac{1}{\frac{1}{h_{FE\ (pre\text{-}irradiation)}} + \Delta\left(\frac{1}{h_{FE}}\right)}$$

where the degradation value is taken from Table 7-1.

For example, the TI 2N2605 has a $\Delta(1/h_{FE})$ degradation value of 0.003 (from Table 7-1) at an I_C of 0.01 mA. If, for example, the pre-irradiation h_{FE} were 100, then

$$h_{FE\ (post\text{-}irradiation)} = \frac{1}{\frac{1}{100} + .003} = 76.9$$

$$(pre\text{-}irradiation)$$

For most values of h_{FE}, Table 7-2 may be used by locating $\Delta(1/h_{FE})$ on the left side of Table 7-2 and the pre-irradiation h_{FE} across the top. The post-irradiation h_{FE} is found where the row and column intersect.

C. JFET's

The JFET's listed in Table 7-3 were all characterized by JPL in a radiation environment. From these results and consultations with Siliconix, only the lightly doped n-channel devices were screened. The p-channel and more heavily doped n-channel devices are not as prone to an inversion layer formation, which results in a large increase in the gate-source (I_{GSS}) leakage current after irradiation. In addition, the lightly doped n-channel devices are subject to enhanced leakage through the substrate. This is particularly important in JFET switches and can also contribute extra noise in sensitive input stages. Table 7-4 indicates the I_{GSS} degradation during screening tests. The leakage current is a strong function of the bias applied to the gate junction during radiation, which was chosen to conform to applications requirements. All devices showed a minimum increase of one order of magnitude due to an increase in the surface recombination velocity, with greater increases produced by inversion layers. At higher total doses, I_{GSS} varies the dose Φ as

$$I_{GSS} = (k\Phi)^a$$

where a varies from 2 to 5. The higher values of a indicate the presence of an inversion layer.

Table 7-2. Final Values of beta (based on $\Delta 1/\beta = 1/\beta = 1/\beta_0$)

β_o / $\Delta 1/\beta$	10	12	15	20	25	30	35	40	45	50	55	60	65	70	75	80	85	90	95	100	110	120	130	140	150	170	200	250	300	350	400
.0005	9.95	11.9	14.9	19.8	24.7	29.6	34.4	39.2	44.1	48.8	53.3	58.1	62.9	67.6	72.5	76.9	81.3	86.2	90.9	95.2	104	114	122	132	139	156	182	222	263	294	333
.0007	9.93	11.9	14.9	19.7	24.6	29.4	34.1	38.9	43.7	48.3	52.9	57.5	61.7	66.7	71.4	75.8	80.0	84.8	89.3	93.5	102	111	119	128	135	152	175	212	250	278	313
.001	9.90	11.9	14.8	19.6	24.4	29.2	33.8	38.5	43.1	47.6	52.1	56.6	61.0	65.4	69.9	74.1	78.1	82.6	87.0	90.9	99.0	107	115	124	130	145	167	200	233	256	286
.0015	9.85	11.8	14.7	19.4	24.1	28.7	33.2	37.7	42.2	46.5	51.8	55.0	59.2	63.4	67.6	71.4	75.2	79.4	83.3	87.0	94.3	102	109	116	122	135	154	182	208	227	250
.002	9.80	11.7	14.6	19.2	23.8	28.3	32.7	37.0	41.3	45.5	49.5	53.6	57.5	61.4	65.4	69.0	72.5	76.3	80.0	83.3	90.1	96.8	103	110	115	127	143	167	189	204	222
.0025	9.76	11.7	14.5	19.0	23.5	27.9	32.2	36.4	40.5	44.4	48.3	52.2	55.9	59.6	63.3	66.7	69.9	73.5	76.9	80.0	86.2	92.3	98.0	104	109	119	133	154	172	185	200
.003	9.71	11.6	14.3	18.9	23.3	27.5	31.7	35.7	39.7	43.5	47.2	50.8	54.4	57.9	61.4	64.5	67.6	70.9	74.1	76.9	82.6	88.2	93.5	99.0	103	112	125	143	159	170	182
.0035	9.66	11.5	14.3	18.7	23.0	27.2	31.2	35.1	38.9	42.6	46.1	49.5	52.9	56.2	59.5	62.5	65.4	68.5	71.4	74.1	79.4	84.8	89.3	94.3	98.0	106	118	133	147	156	167
.004	9.62	11.5	14.1	18.5	22.7	26.8	30.7	34.5	38.2	41.7	45.1	48.4	51.6	54.7	57.8	60.6	63.3	66.2	69.0	71.4	76.3	81.1	85.5	90.1	93.8	101	111	125	137	145	154
.005	9.52	11.3	13.9	18.2	22.2	26.1	29.9	33.3	36.8	40.0	43.1	46.2	49.0	51.9	54.6	57.1	59.5	62.1	64.5	66.7	70.9	75.0	78.7	82.6	85.7	91.7	100	111	121	127	133
.006	9.43	11.2	13.8	17.9	21.7	25.4	28.9	32.3	35.5	38.5	41.3	44.1	46.7	49.3	51.8	54.1	56.2	58.5	60.6	62.5	66.2	69.8	73.0	76.3	79.0	84.0	90.9	100	108	112	118
.007	9.35	11.1	13.6	17.5	21.3	24.8	28.1	31.3	34.3	37.0	39.7	42.3	44.6	47.0	49.3	51.3	53.2	55.2	57.1	58.8	62.1	65.2	68.0	70.9	73.2	77.5	83.3	90.9	97.1	101	105
.008	9.26	11.0	13.4	17.2	20.8	24.2	27.4	30.3	33.1	35.7	38.2	40.5	42.7	44.9	47.0	48.8	50.5	52.4	54.1	55.6	58.5	61.2	63.7	66.2	68.2	71.9	76.9	83.3	88.5	91.7	95.2
.009	9.17	10.8	13.2	16.9	20.4	23.6	26.6	29.4	32.1	34.5	36.8	39.0	41.0	42.9	44.8	46.5	48.1	49.8	51.3	52.6	55.3	57.7	60.0	62.1	63.8	67.1	71.4	76.9	81.3	84.0	87.0
.010	9.09	10.7	13.0	16.7	20.0	23.1	26.0	28.6	31.1	33.3	35.5	37.5	39.4	41.2	42.9	44.4	45.9	47.4	48.8	50.0	52.4	54.5	56.5	58.5	60.0	62.9	66.7	71.4	75.2	77.5	80.0
.011	9.01	10.6	12.9	16.4	19.6	22.6	25.3	27.7	30.1	32.3	34.3	36.1	37.4	39.5	41.1	42.6	43.4	45.3	46.5	47.6	49.7	51.2	53.5	55.3	56.5	59.2	62.5	66.7	69.9	71.9	74.1
.012	8.93	10.5	12.7	16.1	19.2	22.1	24.7	27.0	29.2	31.3	33.1	34.9	36.5	38.1	39.5	40.8	42.0	43.3	44.4	45.5	47.4	49.2	50.8	52.4	53.6	55.9	58.8	62.5	65.4	47.1	69.0
.013	8.85	10.4	12.6	15.9	18.9	21.6	24.1	26.3	28.4	30.3	32.1	33.7	35.2	36.6	38.0	39.2	40.3	42.5	42.6	43.5	45.3	47.0	48.3	49.8	50.8	52.9	55.6	58.8	61.4	62.9	64.5
.014	8.77	10.3	12.4	15.6	18.5	21.1	23.5	25.6	27.6	29.4	31.1	32.6	34.0	35.1	36.6	37.7	38.8	39.8	40.8	41.7	43.3	44.8	46.1	47.4	48.3	50.3	52.6	55.6	57.8	59.2	60.6
.015	8.70	10.1	12.2	15.4	18.2	20.7	23.0	25.0	26.9	28.6	30.1	31.6	32.9	34.1	35.3	36.4	37.3	38.3	39.2	40.0	41.5	42.9	44.1	45.3	46.2	47.9	50.0	52.6	54.6	55.9	57.1
.017	8.62	10.0	12.0	14.9	17.5	19.9	21.9	23.8	25.5	27.0	28.4	29.7	30.9	32.0	33.0	33.9	34.7	35.6	36.4	37.0	38.3	39.5	40.5	41.5	42.2	43.7	45.5	47.6	49.3	50.3	51.3
.020	8.33	9.67	11.5	14.3	16.7	18.8	20.6	22.2	23.7	25.0	26.2	27.3	28.3	29.2	30.0	30.8	31.5	32.2	32.8	33.3	34.4	35.3	36.1	36.9	37.5	38.6	40.0	41.7	42.9	43.7	44 4
.025	8.00	9.23	10.9	13.3	15.4	17.2	18.7	20.0	21.2	22.2	23.2	24.0	24.7	25.5	29.6	26.7	27.2	27.7	28.2	28.6	29.3	30.0	30.6	31.2	31.6	32.4	33.3	34.5	35.3	35.8	36.4
.030	7.69	8.82	10.3	12.5	14.3	15.8	17.1	18.2	19.2	20.0	20.8	21.4	22.0	22.6	23.1	23.5	23.9	24.3	24.7	25.0	25.6	26.1	26.5	27.0	27.3	27.9	28.6	29.4	29.9	30.4	30.8
.035	7.41	8.48	9.83	11.8	13.3	14.6	15.8	16.7	17.5	18.2	18.7	19.3	19.8	20.3	22.8	21.0	21.4	21.7	22.0	22.2	22.7	23.0	23.4	23.8	24.0	24.5	25.0	25.6	26.1	26.4	26.7
.040	7.14	8.11	9.38	11.1	12.5	13.6	14.6	15.4	16.1	16.7	17.2	17.6	18.0	18.4	18.8	19.0	19.3	19.6	19.8	20.0	20.4	20.7	21.0	21.2	21.4	21.8	22.2	22.7	23.1	23.3	23.5
.050	6.67	7.50	8.57	10.0	11.1	12.0	12.7	13.3	13.9	14.3	14.7	15.0	15.3	15.6	15.8	16.0	16.2	16.4	16.5	16.7	16.9	17.2	17.3	17.8	17.6	17.9	18.2	18.5	18.8	18.9	19.1
.060	6.25	6.98	7.89	9.09	10.0	10.7	11.3	11.8	12.2	12.5	12.8	13.0	13.3	13.5	13.6	13.8	13.9	14.1	14.2	14.3	14.5	14.6	14.8	14.9	15.0	15.2	15.4	15.6	15.8	15.9	16.0
.070	5.88	6.52	7.32	8.33	9.09	9.71	10.1	10.5	10.8	11.1	11.3	11.5	11.7	11.8	12.0	12.1	12.2	12.3	12.4	12.5	12.6	12.8	12.9	13.0	13.0	13.2	13.3	13.5	13.6	13.7	13.8
.080	5.56	6.12	6.82	7.69	8.33	8.85	9.21	9.52	9.8	10.0	10.2	10.3	10.5	10.6	10.7	10.8	10.9	11.0	11.1	11.1	11.2	11.3	11.4	11.5	11.5	11.6	11.8	11.9	12.0	12.1	12.1
.090	5.26	5.77	6.38	7.14	7.69	8.13	8.42	8.70	8.9	9.09	9.25	9.38	9.49	9.59	9.68	9.76	9.68	9.89	9.95	10.0	10.1	10.2	10.2	10.3	10.3	10.4	10.5	10.6	10.7	10.8	10:8
.100	5.00	5.45	6.00	6.67	7.14	7.52	7.81	8.00	8.2	8.33	8.46	8.57	8.67	8.75	8.83	8.89	8.95	9.00	9.05	9.09	9.17	9.23	9.29	9.34	9.28	9.44	9.52	9.62	9.68	9.72	9.76

Table 7-3. JFET Characterization Devices

Device Type	Channel Type
2N2608	p
2N3066[a]	n
2N3331	p
2N3382	p
2N3824[a]	n
2N3686[a]	n
2N4093[a]	n
2N4391[a]	n
2N4392[a]	n
2N4393[a]	n
2N4416	n
2N4856[a]	n
2N5196[a]	n[b]
2N5434	n
2N5520[a]	n[c]
2N5556[a]	n
2N5906[a]	n[c]
VCR3P	p

[a]Lightly doped n-channel devices considered to have a potential inversion layer problem.

[b]Matched.

[c]Dual.

Table 7-4. Behavior of I_{GSS} of n-channel JFET's

Device Type	Gate Bias During Irradiation, V	Current, A		a[a]
		Pre-irradiation	After 60 krad(Si) Irradiation	
2N4093	-20	10^{-10}	10^{-9}	5
2N4391	-20	10^{-10}	3×10^{-10}	2
2N4391[a]	-20	10^{-10}	9×10^{-10}	2.4
2N4392	-20	10^{-10}	10^{-9}	2.4
2N4393	-20	10^{-10}	5×10^{-9}	4
2N4856	-20	10^{-10}	4×10^{-10}	3.4
2N5196	-10	5×10^{-11}	7×10^{-11}	2.5
2N5520	-10	5×10^{-11}	7×10^{-11}	2.2
2N5556	-15	10^{-10}	3×10^{-10}	2.2

[a]Defined above (Section VII-C) in discussion of JFET's.

[b]Unscreened.

D. Linear Integrated Circuits

1. Operational Amplifiers

Low-power operational amplifiers of the type generally employed in space applications are extremely sensitive to ionizing radiation (Reference 6-4). Even at comparatively low fluences, there is a significant change in the dc parameters, causing them to exceed the specification limits. Also, some device types may exhibit failure modes at these radiation levels that render the devices inoperative.

The open-loop gain and other ac parameters degrade with ionizing radiation. The decrease in open-loop gain is strongly dependent on the output load. Under a load current of 2 mA, the decrease in open-loop gain at a fluence of 5×10^{12} e/cm^2 varies from 20 to 60 percent, depending on the device type. In defective devices with catastrophic failure modes, the decrease in open-loop gain is much greater than this. The slew rate tested under conditions defined in the manufacturer's specifications decreased slightly at 5×10^{12} e/cm^2, except in LM101 devices, where the slew rate decreased up to 50 percent.

The tables of worst-case parameter values, which are presented according to device type, list the manufacturer's specification limits (initial value) and the mean + 3σ value of the devices tested, for each stated fluence/dose; i.e., the parameters should not exceed the values listed under each mean + 3σ confidence level.

a. National LM101. This device exhibited large parameter changes with radiation exposure (see Table 7-5 for worst-case values). An inversion layer causes a large increase in the differential stage output current which makes the device unstable (Reference 6-6). Device-hardening efforts were unsuccessful, and it was necessary to subject the flight devices to IRAN screening (see Section VIII-A-2).

b. National LM108. The LM108 also had an inversion layer problem which caused a large increase in the differential stage output current, thereby making the device unstable (Reference 6-6). This is shown in Figure 7-4, together with the circuit used. This device type was successfully hardened by the manufacturer (see Section VI-C-1), and the flight devices were diffusion-metallization lot-screened (see Section VIII-A-1).

Table 7-6 lists the worst-case values. The contrast between the hardened and unhardened devices is very significant. Although the values for ΔI_B were not very different, there was an enormous difference in ΔV_{OS} and ΔI_{OS}, with the unhardened device catastrophically failing in ΔA_{OL}.

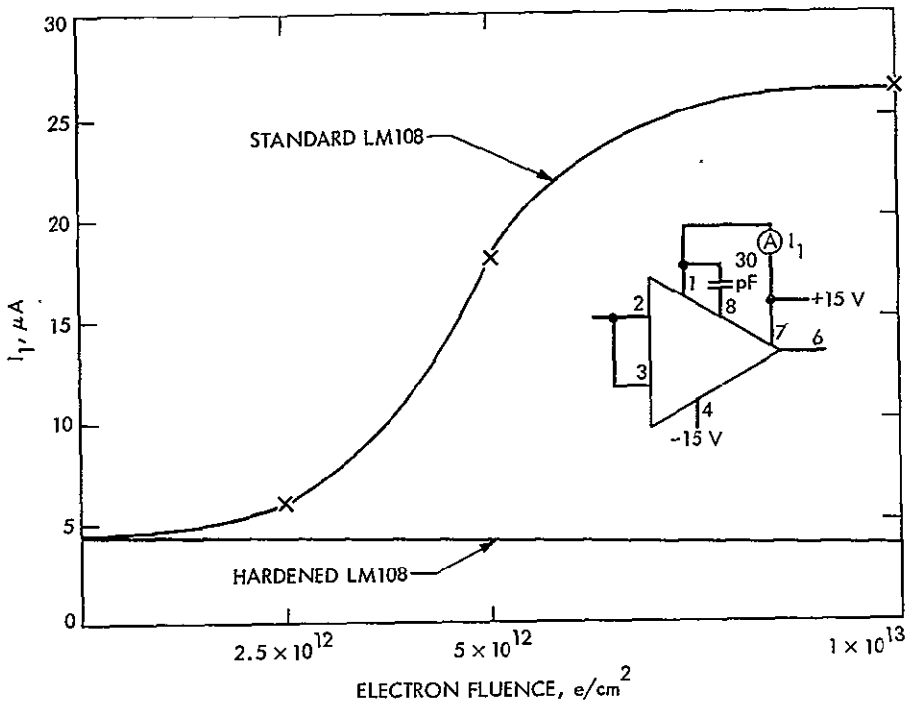

Fig. 7-4. Inversion Layer Effect in LM108 Operational Amplifiers

Table 7-5. Operational-Amplifier Worst-Case Parameter Values, National LM101

Device Type	Mfg.	Parameter	Initial Value	Post-irradiation Value[a] at Indicated Dose and Fluence			
				12.5 krad(Si) 5×10^{11} e/cm^2	30 krad(Si) 1.25×10^{12} e/cm^2	60 krad(Si) 2.5×10^{12} e/cm^2	125 krad(Si) 5×10^{12} e/cm^2
LM101AF LM101AH	NSC	V_{OS} (mV)	2	3	4	5	12
		ΔV_{OS} (mV)		1	2	3	10
		I_{OS} (nA)	10	13	14	16	25
		ΔI_{OS} (nA)		3	4	6	15
		I_B (nA)	75	135	168	212	300
		ΔI_B (nA)		35	68	112	200
LM101AF LM101AH	NSC	V_{OS} (mV)	2			2.8[b]	10.6
		ΔV_{OS} (mV)				0.8[b]	8.6
		I_{OS} (nA)	10			18.8[b]	168
		ΔI_{OS} (nA)				8.8[b]	158
		I_B (nA)	75			125[b]	151
		ΔI_B (nA)				50[b]	76

[a]Post-irradiation values indicate anticipated post-Jupiter mean $+3\sigma$.

[b]Dose = 50 krad(Si).

Table 7-6. Operational-Amplifier Worst-Case Parameter Values, National LM108

Device Type	Mfg.	Parameter	Initial Value	Post-irradiation Value[a] at Indicated Dose and Fluence			
				12.5 krad(Si) 5×10^{11} e/cm^2	30 krad(Si) 1.25×10^{12} e/cm^2	60 krad(Si) 2.5×10^{12} e/cm^2	125 krad(Si) 5×10^{12} e/cm^2
LM108 (Unhard)	NSC	V_{OS} (mV)	2.0	2.3	2.5	59	1052
		ΔV_{OS} (mV)		0.3	0.5	57	1050
		I_{OS} (nA)	0.2	0.6	1.6	6.6	6.7
		ΔI_{OS} (nA)		0.4	1.4	6.4	6.5
		I_B (nA)	2.0	3.7	6.5	13.3	13.6
		ΔI_B (nA)		1.7	4.5	11.3	11.6
		A_{OL}, (dB) 2 mA		-	-	-	Failed
LM108AH (Hard)	NSC	V_{OS} (mV)	0.9	1.0	1.1	1.35	1.65
		ΔV_{OS} (mV)		0.1	0.2	0.45	0.75
		I_{OS} (nA)	0.5	0.6	0.65	0.8	1.1
		ΔI_{OS} (nA)		0.1	0.15	0.3	0.6
		I_B (nA)	4.0	6	6	8.5	13
		ΔI_B (nA)		2	2	4.5	9

[a]Post-irradiation values indicate anticipated post-Jupiter mean $+3\sigma$.

Table 7-6. Operational-Amplifier Worst-Case Parameter Values, National LM108 (Continuation 1)

Device Type	Mfg.	Parameter	Initial Value	Post-irradiation Value[a] at Indicated Dose and Fluence			
				12.5 krad(Si) 5×10^{11} e/cm^2	30 krad(Si) 1.25×10^{12} e/cm^2	60 krad(Si) 2.5×10^{12} e/cm^2	125 krad(Si) 5×10^{12} e/cm^2
LM108AH (Hard)	NSC	A_{OL}, (dB) 2 mA		-	-	92	84
		V_{OS} (mV)	2	2.1	2.2	2.45	2.75
		ΔV_{OS} (mV)		0.1	0.2	0.45	0.75
		I_{OS} (nA)	0.5	0.6	0.65	0.8	1.1
		ΔI_{OS} (nA)		0.1	0.15	0.3	0.6
		I_B (nA)	4	6	6	8.5	13
		ΔI_B (nA)		2	2	4.5	9
		A_{OL}, (dB) 2mA		-	-	92	84

[a]Post-irradiation values indicate anticipated post-Jupiter mean +3σ.

c. National LM124. The LM124 is a quad device (four circuits on one die) and was the only operational amplifier tested for sink current. In addition, the device was biased V^+ = +15 V, V^- = 0 V and V^+ = +15 V, V^- = -15 V during testing.

The V^+ = 15 V and V^- = 0 V conditions are listed in Table 7-7 and show the Δparameters increasing from 5 to 10 times. There was no significant change in the I_{Sink} or I_{Source} current. The V^+ = +15 V and V^- = -15 V bias conditions resulted in much more severe parameter degradation than the V^+ = +15 V and V^- = 0 V conditions. Device-hardening efforts for this device were unsuccessful. The flight devices were sample-lot screened (see Section VIII-A-1).

d. Harris HA2520, HA2600, and HA2620. Table 7-8 lists the worst-case parameter values for all three devices. The HA2520 was measured using no load and a 500-ohm load. The different load conditions did not cause a significant difference in the degradation. The changes for the three devices at 5 x 10^{12} e/cm^2 were as follows:

Device	ΔV_{OS},mV	ΔI_{OS},nA	ΔI_B,nA	ΔA_{OL},dB
HA2520	8.5	50	900	-
HA2600	3.0	65	65	75
HA2620	6.0	40	85	85

The value of A_{OL} for the HA2600 degraded approximately three times as much as the HA2620, in terms of V/mV. The large signal bandwidth for the HA2620 degraded much more severely than the small-signal bandwidth, as shown in Table 7-8.

e. Harris, HA2700. Both the can and the flatpack versions of this device are discussed below.

1) HA2-2700 (Can). Although the ΔV_{OS}, ΔI_{OS}, and ΔI_B parameters degraded moderately, as shown in Table 7-9, the reduction in open-loop gain under load was severe, degrading from over 300,000 at 12.5 krad(Si) to 10,000 at 125 krad(Si).

2) HA9-2700 (Flatpack). The difference in the parameter degradation of the HA2-2700 and the HA9-2700 is of particular importance. The open-loop gain of the HA9-2700 (flatpack) degraded much more severely than the HA2-2700 can-type package (see Table 7-9 for worst-case values). In addition, five sample-lot screened irradiated Harris HA9-2700 (TO-91, 10-pin flatpack) operational amplifiers were tested for open-loop gain (A_{OL}) on the GR 1730 and on a special HA2700 A_{OL} text fixture. Four of the five parts were nonoperational because the negative output level would not swing the minimum requirement of -12.0 V, though all parts functioned normally in the positive direction. Input levels and offset adjustments were normal, but outputs would not swing per negative specification (see Table 7-10). This behavior is attributed to the method of sealing the HA9-2700 flatpack devices.

Table 7-7. Operational-Amplifier Worst-Case Parameter Values, National LM124

Device Type	Mfg.	Parameter	Initial Value	Post-irradiation Value[a] at Indicated Dose and Fluence			
				12.5 krad(Si) 5×10^{11} e/cm^2	30 krad(Si) 1.25×10^{12} e/cm^2	60 krad(Si) 2.5×10^{12} e/cm^2	125 krad(Si) 5×10^{12} e/cm^2
LM124F (Quad)	NSC	V_{OS} (mV)[b]	5	6	8	10	15
		ΔV_{OS} (mV)		1	3	5	10
		I_{OS} (nA)	30	45	60	110	150
		ΔI_{OS} (nA)		15	30	80	120
		I_B (nA)	150	210	270	350	450
		ΔI_B (nA)		60	120	200	300
		I_{Sink}[c]			No change		
		I_{Source}[c]			No change		

[a]Post-irradiation values indicate anticipated post-Jupiter mean $+3\sigma$.

[b]$V^+ = 15$ V, $V^- = 0$V.

[c]5-kilohm load.

Table 7-8. Operational-Amplifier Worst-Case Parameter Values, Harris HA2520, HA2600, and HA2620

Device Type	Mfg.	Parameter	Initial Value	Post-irradiation Value[a] at Indicated Dose and Fluence			
				12.5 krad(Si) 5×10^{11} e/cm^2	30 krad(Si) 1.25×10^{12} e/cm^2	60 krad(Si) 2.5×10^{12} e/cm^2	125 krad(Si) 5×10^{12} e/cm^2
				No Output Load			
HA9-2520 HA2-2520	HAR	V_{OS} (mV)	8	9	9.5	10.6	16.5
		ΔV_{OS} (mV)		1	1.5	2.6	8.5
		I_{OS} (nA)	25	33.7	41	66	75
		ΔI_{OS} (nA)		8.7	16	41	50
		I_B (nA)	200	315	460	650	1100
		ΔI_B (nA)		115	260	450	900
				500 Ohm Output Load			
		V_{OS} (mV)	8	9.6	11.2	13.1	16.5
		ΔV_{OS} (mV)		1.6	3.2	5.1	8.5
		I_{OS} (nA)	25	45	45	66	75
		ΔI_{OS} (nA)		20	20	41	50

[a]Post-irradiation values indicate anticipated post-Jupiter mean +3 .

Table 7-8. Operational-Amplifier Worst-Case Parameter Values, Harris HA2520, HA2600, and HA2620 (Continuation 1)

Device Type	Mfg.	Parameter	Initial Value	Post-irradiation Value[a] at Indicated Dose and Fluence			
				12.5 krad(Si) 5×10^{11} e/cm^2	30 krad(Si) 1.25×10^{12} e/cm^2	60 krad(Si) 2.5×10^{12} e/cm^2	125 krad(Si) 5×10^{12} e/cm^2
				500 Ohm Output Load			
		I_B (nA)	200	360	520	800	1100
		ΔI_B (nA)		160	320	600	900
		A_{OL}, (dB) 2mA		-	-	70	65
				No Output Load			
HA9-2600	HAR	V_{OS} (mV)	4		4.05	4.5	7.0
		ΔV_{OS} (mV)			0.05	0.5	3.0
		I_{OS} (nA)	10		18	35	75
		ΔI_{OS} (nA)			8	25	65
		I_B (nA)	10		12	24	75
		ΔI_B (nA)			2	14	65
		A_{OL}, (dB) 2 mA				90	75

[a]Post-irradiation values indicate anticipated post-Jupiter mean $+3\sigma$.

Table 7-8. Operational-Amplifier Worst-Case Parameter Values, Harris HA2520, HA2600, and HA2620 (Continuation 2)

Device Type	Mfg.	Parameter	Initial Value	Post-irradiation Value[a] at Indicated Dose and Fluence			
				12.5 krad(Si) 5×10^{11} e/cm^2	30 krad(Si) 1.25×10^{12} e/cm^2	60 krad(Si) 2.5×10^{12} e/cm^2	125 krad(Si) 5×10^{12} e/cm^2
				No Output Load			
HA9-2620 HA2-2620	HAR	V_{OS} (mV)	4			4.2[b]	10
		ΔV_{OS} (mV)				0.2[b]	6
		I_{OS} (nA)	15			27[b]	55
		ΔI_{OS} (nA)				12[b]	40
		I_B (nA)	15			23[b]	100
		ΔI_B (nA)				8[b]	85
		A_{OL}, (dB) 2 mA				85	85
		Large signal Bandwidth (kHz)				550	450
		Small Signal Bandwidth (MHz)				18	18

[a]Post-irradiation values indicate anticipated post-Jupiter mean +3σ.

[b]Dose = 50 krad(Si).

Table 7-9. Operational-Amplifier Worst-Case Parameter Values, Harris HA2700

Device Type	Mfg.	Parameter	Initial Value	Post-irradiation Value[a] at Indicated Dose and Fluence			
				12.5 krad(Si) 5×10^{11} e/cm^2	30 krad(Si) 1.25×10^{12} e/cm^2	60 krad(Si) 2.5×10^{12} e/cm^2	125 krad(Si) 5×10^{12} e/cm^2
HA2-2700 (Can)	Harris	V_{OS} (mV)	3	3.4	4	5	8
		ΔV_{OS} (mV)		0.4	1	2	5
		I_{OS} (nA)	10	11	14	16	18
		ΔI_{OS} (nA)		1	4	6	8
		I_B (nA)	20	24	30	40	45
		ΔI_B (nA)		4	10	20	25
		A_{OL}, 2 mA (dB)		110	100	90	80
HA9-2700 (Flatpack)	Harris	V_{OS} (mV)	3	4	6	12	28
		ΔV_{OS} (mV)		1	3	9.0	25
		I_{OS} (nA)	10	18	19.5	13	20
		ΔI_{OS} (nA)		8	9.5	13	20

[a]Post-irradiation values indicate anticipated post-Jupiter mean +3σ.

Table 7-9. Operational-Amplifier Worst-Case Parameter Values, Harris HA2700 (Continuation 1)

Device Type	Mfg.	Parameter	Initial Value	Post-irradiation Value[a] at Indicated Dose and Fluence			
				12.5 krad(Si) 5×10^{11} e/cm^2	30 krad(Si) 1.25×10^{12} e/cm^2	60 krad(Si) 2.5×10^{12} e/cm^2	125 krad(Si) 5×10^{12} e/cm^2
		I_B (nA)	20	32	40	45	60
		ΔI_B (nA)		12	20	25	40
		A_{OL}, 2 mA (dB)		100	90	b	b

[a]Post-irradiation values indicate anticipated post-Jupiter mean +3σ.

[b]Catastrophic reduction in output voltage swing in negative direction.

Table 7-10. Results for HA9-2700 (Flatpack) After Exposure to 5×10^{12} e/cm^2

S/N	Output Voltage Maximum Swing, V	Open-Loop Gain, dB			
		Signal on +IN (Pin 4)		Signal on -IN (Pin 3)	
		Output at 0 to +10V	Output at 1 to -10V	Output at 0 to +10V	Output at 0 to -10V
1	+.03	95	0	95	0
2	-.35	97	66	97	67
3	+.26	100	0	99	0
4	Normal	97	98	98	98
5	-3.63	96	86	96	88

f. Intersil, ICL8007AM. This device uses JFET inputs and consequently has very low initial input currents. These input currents are below normal measurement capabilities (<50 pA) and the data at 5×10^{11} and 1.25×10^{12} e/cm^2 (Table 7-11) represent the upper boundary. The degradation at 2.5×10^{12} e/cm^2 is within the equipment measurement capabilities and shows severe degradation compared to the initial manufacturer's specification values of I_{OS} = 0.2 pA and I_B = 0.5 pA maximum. At 5×10^{12} e/cm^2, these devices were catastrophic failures. It was necessary to shield these devices heavily, in addition to diffusion-metallization sample-lot screening.

2. Comparators

Comparators are sensitive to ionizing radiation, and they also proved rather difficult to measure. However the LM106 and LM710 are considered hard (see Section VI-C-4) but are included here for the sake of completness (see Table 7-12). The devices of prime interest, the LM111 and LM139, operate at extremely low current levels and are subject to frequency oscillations. The oscillations were suppressed by capacitative decoupling of all circuit elements. High-precision resistors were used to obtain accurate measurements of the input offset current. The LM111 experienced considerable increases in the dc parameters (see Table 7-13.)

Table 7-11. Operational-Amplifier Worst-Case Parameter Values, Intersil ICL8007AM

Device Type	Mfg.	Parameter	Initial Value	Post-irradiation Value[a] at Indicated Dose and Fluence			
				12.5 krad(Si) 5×10^{11} e/cm^2	30 krad(Si) 1.25×10^{12} e/cm^2	60 krad(Si) 2.5×10^{12} e/cm^2	125 krad(Si) 5×10^{12} e/cm^2
ICL8007AM	Intersil	V_{OS}(mV)	20	21.3	21.4	35	Failed
		ΔV_{OS}(mV)		1.3	1.4	15	Failed
		I_{OS}(pA)	0.2	42	42	150	Failed
		I_B(pA)	0.5	36	39	71	Failed

[a]Post-irradiation values indicate anticipated post-Jupiter mean +3σ.

Table 7-12. Comparator Worst-Case Parameter Values, LM106 and LM710

Device Type	Mfg.	Parameter	Initial Value	Post-irradiation Value[a] at Indicated Dose and Fluence: 12.5 krad(Si) 5 x 10^{11} e/cm^2	30 krad(Si) 1.25 x 10^{12} e/cm^2	60 krad(Si) 2.5 x 10^{12} e/cm^2	125 krad(Si) 5 x 10^{12} e/cm^2
LM106	NSC	V_{OS}(mV)	3				3.1
		ΔV_{OS}(mV)					0.1
		I_{OS}(μA)	3				4.7
		ΔI_{OS}(μA)					1.7
		I_B(μA)	20				22
		ΔI_B(μA)					2
LM710	NSC	V_{OS}(mV)	2.0			2.1	2.6
		ΔV_{OS}(mV)				0.1	0.6
		I_{OS}(μA)	3.0			3.9	10.5
		ΔI_{OS}(μA)				0.9	7.5
		I_B(μA)	20.0			22.0	29.9
		ΔI_B(μA)				2.0	9.9

[a]Post-irradiation values indicate anticipated post-Jupiter mean +3σ.

Table 7-13. Comparator Worst-Case Parameter Values, LM111

Device Type	Mfg.	Parameter	Initial Value	Post-irradiation Value[a] at Indicated Dose and Fluence			
				12.5 krad(Si) 5×10^{11} e/cm^2	30 krad(Si) 1.25×10^{12} e/cm^2	60 krad(Si) 2.5×10^{12} e/cm^2	125 krad(Si) 5×10^{12} e/cm^2
LM111F LM111H	NSC	V_{OS}(mV)	3	4.5	6	8	9
		$\lvert\Delta V_{OS}\rvert$(mV)		1.5	3	5	6
		I_{OS}(nA)	10	75	145	225	335
		$\lvert\Delta I_{OS}\rvert$(nA)		50	120	200	310
		I_B(nA)	100	700	1100	1250	1300
		ΔI_B(nA)		300	700	850	900
LM111	NSC	V_{OS}(mV)	3			5.5	8
		ΔV_{OS}(mV)				2.5	4
		I_{OS}(nA)	10			45	190
		ΔI_{OS}(nA)				35	180
		I_B(A)	0.1			1.1	2.1
		ΔI_B(A)				1	2

[a]Post-irradiation values indicate anticipated post-Jupiter mean +3σ.

The LM139 was the subject of a major hardening effort, described in Section VI-C. Both hardened and unhardened devices were used on the spacecraft, since the hardened devices were obtained too late in time and in insufficient numbers. The devices are extremely dependent on the bias conditions during irradiation and were therefore subjected to many different bias conditions, as shown in Table 7-14. The devices fail catastrophically at low fluences when biased in the off condition during irradiation. However, this happens only if the supply voltage is set at ±15 V. If the supply voltage is reduced to ±5 V, the devices fail only at 1×10^{13} e/cm^2. The null voltage was originally set at 1.4 V, whereas all the applications require 0.7 V. Table 7-15 shows typical worst-case values for both hardened and unhardened devices.

If the devices are cycled on and off in the radiation environment, the radiation resistance depends on the duty cycle. A 50 percent duty cycle is equivalent to the on state. A short on pulse with a long repetition frequency is equivalent to the off state. Devices irradiated passively degrade slightly more than when they are biased in the on state.

The output sink current was measured throughout most of the characterization tests with the output at 1.5 V (see Table 7-15). On repeating the measurements with the output at 0.7 V, there was a substantial improvement in the radiation resistance, as shown in Table 7-16. Moreover, the initial pre-irradiation value of the sink current was the same for both hardened and unhardened devices. This was not true of the earlier measurements at 1.5 V. All Voyager applications require 0.7 V output.

3. Voltage Regulators

Voltage regulators are relatively unaffected by ionizing radiation (Section VI-C-4). The line and load regulations of LM723 changed by less than 0.03 percent at 5×10^{12} e/cm^2. The stability of the LM105 was even better (<0.015 percent) and was improved by another factor of 2 by process changes. The LM103 regulator diode is known to be hard to 1×10^{15} e/cm^2. Table 7-17 gives the worst-case values.

4. Voltage Followers

Six National hardened semiconductor LM102F voltage followers were tested (see Section VI-C-1 for hardening details). After exposure to 5×10^{12} e/cm^2, the mean value of ΔV_{OS} = 2.48 mV and ΔI_B = 6.01 nA (see Table 7-18). These devices were samples from the only LM102 diffusion-metallization lot screened for Voyager, and the lot was accepted.

Table 7-14. LM139 Quad Comparator Radiation Test Summary

Test Date	Manufacturer	Process	Date Code code	Supply voltage, V	Null voltage, V	Bias Condition During Irradiation: Input No.	Input Condition	Outputs	No. of Devices	Failures at fluence levels[a]: 2.5×10^{11} e/cm^2	5×10^{11} e/cm^2	1×10^{12} e/cm^2	1.25×10^{12} e/cm^2	2.5×10^{12} e/cm^2	5×10^{12} e/cm^2	1×10^{13} e/cm^2
12/20/74	NSC	Standard	406	+5	+1.4	1- 1+	+50 mV Gnd	On	6	-	-	-	-	-	0	1
						2- 2+	-130 mV Gnd	Off	6	-	-	-	-	-	0	1
3/20/75	NSC	Standard	402 and 502	+15	+1.4	1- 1+	+50 mV Gnd	On	3	0	0	0	-	-	-	-
						2- 2+	-130 mV Gnd	Off	3	0	0	2	-	-	-	-
4/16/75	NSC	(LM339) Standard	403	+15	+0.7	1- 1+	+50 mV Gnd	On	6	-	0	0	-	0	1	-
						2- 2+	Gnd +50 MV	Off	6	-	0	3	-	6	6	-
11/7/75	NSC	Standard	406	+15	+0.7	1- 1+	+50 mV Gnd	On	3	-	0	-	0	0	0	-
						2- 2+	Gnd +50 Mv	Off	3	-	0	-	0	3	3	-
11/6/75	NSC	Standard	406	+15	+0.7	1- 1+	[b]	50% duty ~pulse	3	-	0	-	0	0	0	-
						2- 2+	[b]	56 µs pulse	3	-	0	-	0	3	3	-
11/6/75	NSC	Standard	406	+15 (during meas)	+0.7	1- 1+	Open	Passive[c]	3	-	0	-	0	0	0	-
						1- 1+	Open	Passive[c]	3	-	0	-	0	0	0	-
11/25/75	NSC	Hardened	Lot E2035	+15	+0.7	1- 1+	+50 mV Gnd	On	3	-	0	-	0	0	0	-
						2- 2+	Gnd +50 mV	Off	3	-	0	-	0	0	3	-

Table 7-14. LM139 Quad Comparator Radiation Test Summary
(Continuation 1)

Test Date	Manufacturer	Process	Date Code code	Supply voltage, V	Null voltage, V	Bias Condition During Irradiation: Input No.	Input Condition	Outputs	No. of Devices	Failures at fluence levels[a]: 2.5×10^{11} e/cm^2	5×10^{11} e/cm^2	1×10^{12} e/cm^2	1.25×10^{12} e/cm^2	2.5×10^{12} e/cm^2	5×10^{12} e/cm^2	1×10^{13} e/cm^2
1/23/76	NSC	Unhard Flight Parts	Lot 09079A 10145	+15	+0.7	1-	+50 mV	On	6	-	0	-	0	0	0	-
						1+	Gnd									
6/3/76	NSC	Unhard Flight Parts	Lot 09079A 10145	+15	+0.7	1-	+50 mV	On	9	-	0	0	0	-	-	-
						1+	Gnd									
						2-	Gnd	Off	9	-	0	2	6	-	-	-
						2+	+50 mV									
6/3/76	NSC	Hard Flight Parts	Lot R10213-A 7610	+15	+0.7	1-	+50 mV	On	3	-	0	-	0	0	0	-
						1+	Gnd									
						2-	Gnd	Off	3	-	0	-	0	0	3	-
						2+	+50 mV									

[a]Null amplifier saturated during dc measurements for one or more parameters.

[b]Input (1-) = 0 to 100 mV, 50% duty cycle. Input (1+) = 50 V dc.
Input (2-) = 0 to 100 mV, 56 s pulse every 3 s.
Input (2+) = 50 mV dc.

[c]No supply voltage applied during irradiation.

Table 7-15. Comparator Worst-Case Parameter Values, LM139

Device Type	Mfg.	Parameter	Initial Value	Post-irradiation Value[a] at Indicated Dose and Fluence: 12.5 krad(Si) 5 x 10^{11} e/cm^2	30 krad(Si) 1.25 x 10^{12} e/cm^2	60 krad(Si) 2.5 x 10^{12} e/cm^2	125 krad(Si) 5 x 10^{12} e/cm^2
LM139 (Unhard)	NSC	$V_{OS(on)}$(mV)	5	5.5	7.0	9.0	12.0
		$\Delta V_{OS(on)}$(mV)		0.5	2.0	4.0	7.0[b]
		$V_{OS(off)}$(mV)	5	17.5	Failed	Failed	Failed
		$\Delta V_{OS(off)}$(mV)		12.5	Failed	Failed	Failed
		$I_{OS(on)}$(nA)	25	35	55	95	375
		$\Delta I_{OS(on)}$(nA)		10	30	70	350
		$I_{OS(off)}$(nA)	25	35	Failed	Failed	Failed
		$\Delta I_{OS(off)}$(nA)		10	Failed	Failed	Failed
		$I_{BV(on)}$(nA)	100	210	400	750	2100
		$\Delta I_{B(on)}$(nA)		110	300	650	2000
		$I_{B(off)}$(nA)	100	210	Failed	Failed	Failed
		$\Delta I_{B(off)}$(nA)		110	Failed	Failed	Failed
		$\Delta I_{Sink(on)}$(mA)[c]		-7.0	-14	-22	-28

Table 7-15. Comparator Worst-Case Parameter Values, LM139
(Continuation 1)

Device Type	Mfg.	Parameter	Initial Value	Post-irradiation Value[a] at Indicated Dose and Fluence: 12.5 krad(Si) 5 x 10^{11} e/cm^2	30 krad(Si) 1.25 x 10^{12} e/cm^2	60 krad(Si) 2.5 x 10^{12} e/cm^2	125 krad(Si) 5 x 10^{12} e/cm^2
LM139 (Unhard)	NSC	ΔI_{Sink} 50% duty cycle (mA)[c]		-6.0	-14	-22	-28
		$\Delta I_{Sink(off)}$ (mA)[c]		-7.0	Failed	Failed	Failed
LM139 (Hard)		$V_{OS(on)}$ (mV)	5	5.5	5.5	7	7
		$\Delta V_{OS(on)}$ (mV)		0.5	0.5	2	2
		$V_{OS(off)}$ (mV)	5	7.2	7.2	45	Failed
		$\Delta V_{OS(off)}$ (mV)		2.2	2.2	40	Failed
		$I_{OS(on)}$ (nA)	25	27.5	45	75	100
		$\Delta I_{OS(on)}$ (nA)		2.5	20	50	75
		$I_{OS(off)}$ (nA)	25	70	70	125	Failed
		$\Delta I_{OS(off)}$ (nA)		45	45	100	Failed
		$I_{B(on)}$ (nA)	100	250	420	550	600
		$\Delta I_{B(on)}$ (nA)		150	320	450	500
		$I_{B(off)}$ (nA)	100	2500	450	600	Failed

Table 7-15. Comparator Worst-Case Parameter Values, LM139
(Continuation 2)

Device Type	Mfg.	Parameter	Initial Value	Post-irradiation Value[a] at Indicated Dose and Fluence			
				12.5 krad(Si) 5×10^{11} e/cm^2	30 krad(Si) 1.25×10^{12} e/cm^2	60 krad(Si) 2.5×10^{12} e/cm^2	125 krad(Si) 5×10^{12} e/cm^2
LM139 (Hard)		$\Delta I_{B(off)}$ (nA)		150	350	500	Failed
		$I_{Sink(on)}$ (mA)[c]		5.4	3.0	2.0	1.7
		$\Delta I_{Sink(on)}$ (mA)[c]		-5.5	-8.2	-9.4	-9.9
		$I_{Sink(off)}$ (mA)[c]		5.3	3.0	2.0	Failed
		$\Delta I_{sink(off)}$ (mA)[c]		-5.7	-8.3	-9.5	Failed

[a]Post-irradiation values indicate anticipated post-Jupiter mean +3σ.

[b]Null voltage = $0.7V_o$.

[c]V_{out} = 1.5 V.

Table 7-16. Maximum Change in Sink Current for LM139

Device Condition	Output Voltage, V	Sink Current Change, mA, for Indicated Fluence			
		5×10^{11} e/cm^2	1×10^{12} e/cm^2	1.25×10^{12} e/cm^2	2.5×10^{12} e/cm^2
Unhardened	1.5	-5.0	-10.8		
	0.7	-1.6	-4.1		
Hardened	1.5	-4.9		-7.3	-8.4
	0.7	-3.6		-5.6	-6.7

Table 7-17. Voltage Regulator Worst-Case Parameter Values, LM103, LM105, and LM723

Device Type	Mfg.	Parameter	Initial Value	Post-irradiation Value[a] at Indicated Dose and Fluence			
				12.5 krad(Si) 5×10^{11} e/cm^2	30 krad(Si) 1.25×10^{12} e/cm^2	60 krad(Si) 2.5×10^{12} e/cm^2	125 krad(Si) 5×10^{12} e/cm^2
LM103	NSC	ΔV_Z, .01ma(mV)					6.1
		ΔV_Z, 0.1mA(mV)					7.5
		ΔV_Z, 1.0mA(mV)					27
LM105	NSC	$\Delta Load_{Reg}$(mV)		7	25.5	28	140
		$\Delta Line_{Reg}$(mV)		11	26	32	112
LM723	NSC	ΔV_{out}(mV)					31
		ΔV_{Ref}(mV)					1.1
		$\Delta Line_{Reg}$(%)					0.09
		$\Delta Load_{Reg}$(%)					0.04

[a]Post-irradiation values indicate anticipated post-Jupiter mean +3σ.

Table 7-18. Voltage Follower Worst-Case Parameter Values, LM102

Device Type	Mfg.	Parameter	Initial Value	Post-Irradiation Value[a] at Indicated Dose and Fluence			
				12.5 krad(Si) 5×10^{11} e/cm^2	30 krad(Si) 1.25×10^{12} e/cm^2	60 krad(Si) 2.5×10^{12} e/cm^2	125 krad(Si) 5×10^{12} e/cm^2
LM102F (Hard)	NSC	V_{OS}(mV)	4				12
		ΔV_{OS}(mV)					8
		I_B(nA)	3				12
		ΔI_B(nA)					9

[a]Post-irradiation values indicate anticipated post-Jupiter mean +3σ.

5. Current Switches and D/A Converters

The allowable error in the current switches is usually expressed in terms of fractions of the least significant bit (LSB), with normal allowable errors being of the order of 1/2 LSB.

The ICL 8018 reached a 1/2-LSB error at 2.2 x 10^{12} e/cm^2 for a 10-bit D/A converter. The corresponding fluence for the AD550 was 0.5 x 10^{11} e/cm^2. The LSB error is due to a decrease in the LSB output current. A radiation-induced leakage path produces a loss in collector current which causes the device to be completely inoperative at 1 x 10^{13} e/cm^2 as the LSB current drops to zero. No problems were observed in current gain, logic threshold, output leakage current, or response time. Table 7-19 lists device linearity deltas; i.e., the effects of LSB current changes are subtracted out of the data. For total error for any given bit, the ΔL_{SB} must be multiplied by the bit weighting and added to the value shown in the data. Parameter ΔV_{BE} was not stable, because of servo loop biasing and collector-base leakage current problems. Parameter ΔV_{BE} and $\Delta(1/h_{FE})$ are for the test device reference transistor.

The AD550 current switches were tested in a similar manner to the ICL8018 and gave similar results (see Table 7-19). A linear model for the degradation of the output current with increasing fluence indicates that a 10-bit converter with an AD550U reference current of 0.125 mA may exhibit a 1/2-LSB error at a fluence of 6.5 x 10^{11} e/cm^2.

The current gains of the AD550U transistors begin at high values and remain high up to 5 x 10^{12} e/cm^2 and thus pose no problem in the application of these devices. The observed changes in the logic thresholds of the AD550U with radiation are within the accuracy of the measurements and thus these changes are insignificant. The radiation-induced changes in the output leakage of the AD550U are not severe enough to seriously affect the use of this device. The response time data of the AD550U shows no discernible degradation of the response time up to 5 x 10^{12} e/cm^2. An additional radiation test on three flight parts confirmed the values shown in Table 7-19.

The DAC-01, a 6-bit monolithic D/A converter, showed significant changes in bipolar zero-scale offset and in full-scale voltage on irradiation (see Table 7-19). The HI-1080 8-bit D/A converter, which is a bipolar device, was found to be relatively stable on irradiation under operating conditions. The maximum change in output voltage at 60 krad(Si) was -22 mV. The HI-1080 function is not considered impaired by a 60-krad(Si) dose.

6. Sense Amplifier

Information obtained from Motorola on their MC 1544 sense amplifier indicated that this device was hard in a weapon's radiation environment. However, there was some concern about the effect on the spontaneous switching time, which had not previously been measured. Some flight devices were irradiated to 2.5 x 10^{12} and 5 x 10^{12} e/cm^2 under representative bias conditions, and the following parameters were measured:

Table 7-19. Current Switch and D/A Converter Worst-Case Parameter Values

Device Type	Mfg.	Parameter	Initial Value	Post-irradiation Value[a] at Indicated Dose and Fluence			
				12.5 krad(Si) 5×10^{11} e/cm^2	30 krad(Si) 1.25×10^{12} e/cm^2	60 krad(Si) 2.5×10^{12} e/cm^2	125 krad(Si) 5×10^{12} e/cm^2
AD550	ADI	ΔI_{LSB}[b] (μA)		.0025	.0055	0.3	0.6
		ΔI_{BIT} (μA)		.56	.74	0.5	0.7
		ΔI_{BIT} (μA)		.20	.27	0.55	0.4
		ΔI_{BIT} (μA)		.11	.058	0.25	0.15
		ΔI_L (nA)				4	10
		ΔV_{BE} (mV)		1.1	1.8	5	5
		$\Delta(1/h_{FE})$		3×10^{-4}	3.7×10^{-4}	1.2×10^{-3}	1.8×10^{-3}
DAC-01	PMI	Bipolar Zero Scale Offset					
		$\Delta V_{OS10SF}+$ (mV)		-110	-180	-400	-530
		$\Delta V_{OS10SF}-$ (mV)		110	240	370	530
		Full-Scale Voltage					
		$\Delta V_{FS}+$ (mV)		-120	-180	-400	-530
		$\Delta V_{FS}-$ (mV)		100	170	360	510

Table 7-19. Current Switch and D/A Converter Worst-Case Parameter Values (Continuation 1)

Device Type	Mfg.	Parameter	Initial Value	Post-irradiation Value[a] at Indicated Dose and Fluence			
				12.5 krad(Si) 5×10^{11} e/cm^2	30 krad(Si) 1.25×10^{12} e/cm^2	60 krad(Si) 2.5×10^{12} e/cm^2	125 krad(Si) 5×10^{12} e/cm^2
ICL8018 ICL8019 ICL8020	Intersil	I_{LSB} (μA)				0.12	1.3
		$\Delta I_{BIT}{}^3$ (μA)				0.06	0.11
		$\Delta I_{BIT}{}^2$ (μA)				0.17	0.37
		$\Delta I_{BIT}{}^1$ (μA)				0.38	0.71
		ΔI_L (nA)				2.3	294
		ΔV_{BE} (mV)				6	8
		$\Delta(1/h_{FE})$				2×10^{-3}	2.5×10^{-3}

[a]Post-irradiation values indicate anticipated post-Jupiter mean +3σ.

spontaneous switching time, threshold voltage, propagation delay time, input bias currents, and power supply currents. Radiation produced a decrease in the spontaneous switching time, except for those devices that were initially out of specification. These showed little change. The propagation delay increased slightly at 2.5×10^{12} e/cm^2, but reverted close to its pre-irradiation level at 5×10^{12} e/cm^2. There was no significant change in any other parameter.

7. Phase-Locked Loop

The Exar Integrated Systems phase-locked-loop type XR215 was tested by the HYBIC subsystems group on the Boeing LINAC up to 2×10^{13} e/cm^2. The device showed only insignificant changes in capture range, lock range, and free-running frequency up to the highest fluence measured.

The HYBIC subsystem group also tested the Harris Type HA2800 locked loop, but the performance of this device type degraded significantly at fluence levels that exceeded 7.5×10^{11} e/cm^2. The device was deleted from Voyager usage, as the manufacturer discontinued production.

8. Voltage-Controlled Oscillator

Six devices of the Intersil Type ICL8038 voltage-controlled oscillator were irradiated 5×10^{12} e/cm^2. The mean of the output frequency decreased by 0.021 kHz with a worst-case (mean + 3σ) shift of 0.2 kHz. There was no measurable change in the output voltage.

9. RF Amplifiers

Six Motorola Type MIC 76T rf amplifiers were characterized prior to irradiation and after fluences of 5×10^{12} and 1×10^{13} e/cm^2. A test fixture was modified so that a variable control voltage was applied to the fixture instead of the two fixed voltages prior to modification. This modification allowed a complete gain curve to be monitored, covering a gain of +27 dB to -25 dB at a frequency of 20 MHz.

The radiation tests indicated no measurable gain change at positive gains and only a moderate gain change when the devices were operated at negative gains. The worst-case gain change amounted to +1.0 dB at a fluence of 1×10^{13} e/cm^2 at negative gains, which is the condition of strong rf signals at the radio input. Subsequent Dynamitron tests on flight lots with the devices biased under operating conditions during radiation gave similar results.

10. RF Mixers

Eight Motorola MIC236 and MIC336 rf mixers were irradiated at 5×10^{12} and 1×10^{13} e/cm^2 by 3-MeV electrons from the Boeing LINAC. Four each of the devices were dc biased and four were not biased during

radiation exposure. No significant difference was observed after irradiation. There were no catastrophic failures, and only slight parameter changes were noted. Similar results were obtained on subsequent tests at the JPL Dynamitron.

E. ANALOG SWITCHES

1. Analog Switches Without MOS Devices

Increased leakage in $I_{S\ (off)}$ is caused by an increase in gate leakage of JFET's under 30-V gate bias. Leakage currents up to 25 nA were observed in devices DG129 and DG133, and leakage currents up to 50 nA in DG141. The worst-case bias condition during radiation was with the inputs in the off condition. Worst-case (mean + 3σ) values are shown in Table 7-20.

The JFET's used in these hybrid devices were sample-tested separately, and the worst devices tested showed gate leakage currents up to 5 μA at 5 x 10^{12} e/cm^2 when 30 V was applied to the gate junction during irradiation. Such devices usually exhibit bimodal distributions. The leakage currents of the better devices were less than 10 nA.

2. Analog Switches Containing MOS Devices

Analog switches containing MOS devices are very sensitive to radiation, but the effects vary strongly with the bias condition during radiation and under test, and also with the manufacturer.

A dynamic test indicated that the DG181 device can latch up at about 5 x 10^{12} e/cm^2, producing $I_{S\ (off)}$ and $I_{D\ (off)}$ currents up to 1 mA. The DGM111 and the DG125 showed increases up to 5.5 kΩ in $r_{DS\ (on)}$ at 5 x 10^{12} e/cm^2, but this parameter is very dependent on bias conditions, as indicated in Table 7-20.

Table 7-20. Analog Switch Worst-Case Parameter Values

Device Type	Mfg.	Parameter	Initial Value	Post-irradiation Value[a] at Indicated Dose and Fluence: 12.5 krad(Si) 5 x 10^{11} e/cm^2	30 krad(Si) 1.25 x 10^{12} e/cm^2	60 krad(Si) 2.5 x 10^{12} e/cm^2	125 krad(Si) 5 x 10^{12} e/cm^2
				Devices without MOS			
DG129	SIL	$I_{S(off)}$(nA)	1	2	6	7.5	15[b]
DG133	SIL	$I_{S(off)}$(nA)	1	2	6	7.5	15
DG141	SIL	$I_{S(off)}$(nA)	3	5	15	30	60

[a]Post-irradiation values indicate anticipated post-Jupiter mean +3σ.

[b]25 nA for nonscreened parts.

Table 7-20. Analog Switch Worst-Case Parameter Values
(Continuation 1)

Device Type	Mfg.	Parameter	Initial Value	Post-irradiation Value[a] at Indicated Dose and Fluence			
				12.5 krad(Si) 5×10^{11} e/cm^2	30 krad(Si) 1.25×10^{12} e/cm^2	60 krad(Si) 2.5×10^{12} e/cm^2	125 krad(Si) 5×10^{12} e/cm^2
				Devices with MOS			
DG181	SIL	$I_{S(off)}$(nA)	1	1	1	7.5	Failed
		$I_{D(off)}$(nA)	1	1	1	2.0	Failed
DGM111	SIL	$I_{S(off)}$(nA)		-	-	-	30
		$I_{D(off)}$(nA)[c]		-	-	-	260
		$I_{D(off)}$(nA)[d]		0.05	0.06	0.8	5
		$r_{DS(on)}$(ohms)[c]		-	-	-	100
		$r_{DS(on)}$(ohms)[d]		120	250	250	1000

[a]Post-irradiation values indicate anticipated post-Jupiter mean +3σ.

[c]S = D = -10 V.

[d]S = GND, D = 10 V.

F. CMOS DEVICES

1. Propagation Time

A complete electrical characterization of CMOS devices was carried out for JPL at the Naval Research Laboratory using an EH4600 series computer-controlled test system at a total dose of 7.5×10^4 and 1.5×10^5 rad(Si). The parameters tested and some typical results are shown in Tables 7-21 and 7-22. It may be noted that radiation causes a significant increase in the propagation time.

Additional propagation time measurements were made at the Hughes Fullerton Facility (see the CD4000 series in Table 7-22). The propagation time after irradiation appears to be within the JPL specification limits, but the data show large increases in propagation time. These are primarily influenced by outliers whose change may be up to one order of magnitude worse than the mean.

2. Comparison of I_{SS} and t_p

Some special tests were run at Hughes to compare the effects of 150 krad(Si) on the quiescent supply current (I_{SS}) and propagation time (t_p) of some of the RCA CMOS circuit types being used in the Voyager project. The circuit types tested were CD 4019AD, CD 4025AD, CD 4027AD, CD 4029AD, CD 4051AD, CD 4052AD, and CD 4053AD. A summary of the results of these tests follows.

The effects of the radiation on I_{SS} and on t_p do not correlate. Instead, these two parameters respond independently to the radiation. In the CD 4027 data there is one device with an I_{SS} of 130 μA after radiation. Its t_p data was essentially the same as that of the other CD 4027 devices with I_{SS} measurements of 15-20 nA after radiation. Similar conditions exist in the CD 4052 and CD 4053 data. In the CD 4029 data there is an example of the opposite condition. One device has a much larger t_p shift than the other devices, but its I_{SS} readings are the same as the others. Therefore, ΔI_{SS} can be high or low when the Δt_p is constant, or vice versa.

All the test devices for each circuit type were from one wafer. The Δt_p data for the devices from the same wafer are not always consistent; i.e., Δt_p varies across the wafer. From this it is concluded that there is no effective way to wafer-sample screen for t_p.

3. Dose Rate and Annealing Effects

Srour (Reference 7-1) recently reviewed experimental observations on dose-rate dependence of the shift in V_T in MOS devices. The dependence is a function of the dose rate, the bias conditions during radiation, and the nature of the gate oxide. Srour irradiated n- and -p-channel transistors on a commercial CMOS inverter using a Cobalt 60 source at rates of 0.23 and 23 rad(Si)/s. He observed a marked rate effect.

Table 7-21. CMOS Radiation Characterization Data at 150 krad(Si)

Tests (At V_{DD} = 10 V)		4011	4029	4035	4050
1. Functional (go/no go) V_O < 5 V = "0" V_O > 5 V = "1"			All passed		
2. DC margin (go/no go) V_O < 1 V = "0" V_O > 9 V = "1"			All passed		
3. Δt_{PLH} (%) 30 pF load	Average	26.9[a]	13.8[b]	48.8[c]	10.6[d]
	Maximum	30	37	55	18
3a. Δt_{PLh} (%) 30 pF load	Average		26[e]		
	Maximum		37		
4. Δt_{PHL} (%) 30 pF load	Average	6.2[a]	28.2[b]	32.8[c]	35.6[d]
	Maximum	8.8	31	37	50
4a. Δt_{PHL} (%) 30 pF load	Average		19[e]		
	Maximum		33		
5. ΔV drop in output transistors at minimum source/sink current specified in RCA manual		N-CH<0.1 P-CH<0.1	V<0.1 V<0.1	<0.1 0.1	<0.1 <0.1
6. Range of maximum quiescent supply current Δ	from:	56X	250X	23X	25X
	to:	4700X	9800X	3300X	3400X

[a]Propagation time measurement from pin 2 to pin 3 (in to out).

[b]Propagation time measurement from pin 15 to pin 6 (C_L. to Q_1).

[c]Propagation time measurement from pin 6 to pin 1 (C_L. to Q_1).

[d]Propagation time measurement from pin 3 to pin 2 (in to out).

[e]Propagation time measurement from pin 15 to pin 7 (C_L. to carry out).

Table 7-22. Propagation Time Test Results for CMOS Devices at 150-krad(Si) Radiation

Device Type	Parameter	Load Capacitance	Specification Limit	Propagation Time, nanoseconds					
				Mean		Maximum			
				Initial	150 krad(Si)	Initial	150 krad(Si)	Δ Max	Δ Max %
CD4019	T_{PLH}	32		46.1	54.3	70	91	+27	43
		51	125	56.9	62.2	78	102	+27	39
	T_{PHL}	32		64.7	86.1	76	102	+28	45
		51	125	73.4	96.6	86	116	+30	44
CD4025	T_{PLH}	31		48.9	64.7	52	70	+18	36
		53	65	70.3	94	74	102	+30	43
	T_{PHL}	31		39.2	44	48	54	+21	68
		53	55	51	58.6	62	72	+30	42
CD4027	T_{PLH}	30		81.5	85.6	116	94	+16	26
		50	120	92.9	99	134	108	+30	47
	T_{PHL}	30		66.5	76.5	88	90	+16	26
		50	160	79.2	106	91.8	106	+19	26
CD4029	T_{PLH}	31		236	249	280	400	+120	43

Table 7-22. Propagation Time Test Results for CMOS Devices at 150-krad(Si) Radiation (Continuation 1)

Device Type	Parameter	Load Capacitance	Specification Limit	Propagation Time, nanoseconds					
				Mean		Maximum			
				Initial	150 krad(Si)	Initial	150 krad(Si)	Δ Max	Δ Max %
		51	260	260	273	330	440	+140	47
	T_{PHL}	31		221	241	280	470	+190	68
		51	260	242	262	320	520	+220	73
CD4051	T_{PLH}	30		72.0	73.4	90	90	+12	29
		51	400	74.6	75	80	92	+10	28
	T_{PHL}	30		205	207	218	245	+45	23
		51	1000	208	209	222	248	+45	23
CD4052	T_{PLH}	31		193	224	330	375	+70	23
		52	400	198	229	335	380	+70	23
	T_{PHL}	31		395	395	570	520	+55	23
		52	1000	467	464	720	650	+40	17

Annealing the devices at room temperature for 140 hours (the time it takes to perform an irradiation to 125 krad(Si) at a rate of 0.23 rad(Si)/s) following a higher ionization-rate irradiation brought the high and low dose-rate results into agreement.

Yamakawa (Reference 7-2) measured rate effects in I_{SS} of CMOS devices with a 950°C gate-oxide annealing temperature at 113 and 7.6 rad(Si)/s at a total dose of 150 krad(Si). The bias conditions were as described for the wafer screening. The two dose rates represent the screening conditions and the effect after radiation, but no rate effect could be detected. Additional experiments on the propagation time showed no annealing for several days, in agreement with the hypothesis that the propagation time is governed by interface states.

4. Conclusions

The radiation resistance of CMOS devices with a gate-oxide annealing temperature of 950°C appearsto be adequate for the Voyager project, because the devices will be exposed to a total dose of less than 125 krad(Si) and because no severe constraints have been imposed on the quiescent supply current.

Any future programs with a radiation environment in excess of that encountered by Voyager or with more stringent design requirements must use the radiation-hard dry gate-oxide process developed at RCA, Somerville, with Defense Nuclear Agency support, or the equivalent, since the 950 C annealed process cannot survive a total dose much greater than 150 krad(Si).

G. DIODES AND RECTIFIERS

1. Zener and Reference Diodes

The radiation analysis carried out by General Electric, largely from neutron data, indicated potential shifts in zener voltage sufficient to cause problems in some applications. Electron irradiation at 2.2 MeV caused relatively minor shifts in the zener voltage at fluences up to 1×10^{13} e/cm^2. Additional measurements were, therefore, carried out with 3- and 5.5-MeV electrons using the high-voltage Van de Graaff generator at Notre Dame University.

The zener voltage was determined both before and after radiation at a fixed current level by means of in situ measurements. This made it possible to determine the radiation-induced change in the zener voltage to an accuracy of ± 1 mV by relatively simple means. The experiment lasted less than 1/2 hour, and the radiation-induced thermal heating is not significant, so that thermal changes during the time of the experiment may be ignored. The absolute value of the zener voltage, which is a strong function of the zener current, has been determined to an accuracy of about ± 10 mV.

Table 7-23. Summary of Radiation Effects on Voltage in Zener Diodes

Device Type		Manufacturer	Conditions During Irradiation: V_Z, V	I_Z, mA	Maximum ΔV, mV, After 5×10^{12} e/cm^2	Electron Energy Range, MeV
			Devices with zener voltage change within measurement accuracy of ±1mV.			
1N945	TC[a] zener	MOT	11.7	7.5	-1	2.2 - 5.5
1N4569	TC Reference Diode	DIK	6.4	0.5	-2	2.2, 5.5
1N4572	TC Reference Diode	DIK	6.4	1.0	-1.9	2.2 - 5.5
1N4577	TC Reference Diode	MOT	6.4	2.0	0	2.2
1N4895A	TC zener (ultrastable)	DIK	6.35	7.5	-1	2.2, 5.5
MZ827	TC zener	MOT	6.2	7.5	-1	2.2 - 5.5
.4M4.7AZ1	Noncompensated zener	MOT	4.7	5	+2	2.2 - 5.5
.4M5.1AZ1	Noncompensated zener	MOT	5.1	5	1	2.2 - 5.5
			Devices with zener voltage change within measurement accuracy of ±1mV, but with outliers showing greater energy-independent change			
1N829	TC zener	MOT	6.2	5.5	-2 -12	2.2 - 5.5
			Devices with linear zener voltage change with energy			

7-23. Summary of Radiation Effects on Voltage in Zener Diodes (Continuation 1)

Device Type		Manufacturer	Conditions During Irradiation		Maximum ΔV, mV, After 5×10^{12} e/cm^2	Electron Energy Range, MeV
			V_Z, V	I_Z, mA		
1N935	TC Reference Diode	MOT	9.0	1.0,7.5	(see Fig. 7-5)	2.2 - 5.5
1N4907	TC Reference Diode	MOT	12.8	2	(see Fig. 7-5)	2.2 - 5.5
FCT1121	TC Reference Diode	FAS	6.8	0.1	(see Fig. 7-5)	2.2 - 5.5
			Devices with significant zener voltage change measured only at 2.2 MeV			
1N4581	TC Reference Diode	DIK	6.6	4.0	-4	2.2
1N4891	TC Reference Diode (ultrastable)	DIK	6.4	2.0	-12	2.2
				7.5	-8	
			High-surge noncompensated zeners			
UZ8770		UTR	70	0.05	+14	2.2
UZ8775		UTR	75	0.1	+220	2.2 - 5.5

[a]Temperature compensated.

The results of the measurements are summarized in Table 7-23. It may be noted that the majority of the devices tested do not change by more than the experimental error at a fluence of 5 x 10^{12} e/cm^2 for all energies up to 5.5 MeV. Three device types showed a significant linear change in zener voltage with electron energy (see Figure 7-5). One of the device types indicated a positive voltage shift, whereas the other two indicated a negative voltage shift. These changes are attributed to bulk radiation damage.

Some devices of the IN829 showed changes as great as 12 mV, whereas the remainder stayed within ±1mV. The anomalously large changes were not energy-dependent and are therefore considered to be due to a surface ionization effect.

Very few of the Unitrode U28770 and U28775 high-voltage zener diodes were available for testing, and these showed shifts from -14 to -120 mV. The 14-mV value is within experimental error. In cases where very few devices were available, devices were first irradiated to a fluence of 1 x 10^{13} e/cm^2 at 2.2 MeV and then reirradiated at a later date with 3.0 or 5.5 MeV electrons. No conclusions could be drawn from the data obtained from the second irradiation, primarily because most of the zener voltage shifts were within experimental error.

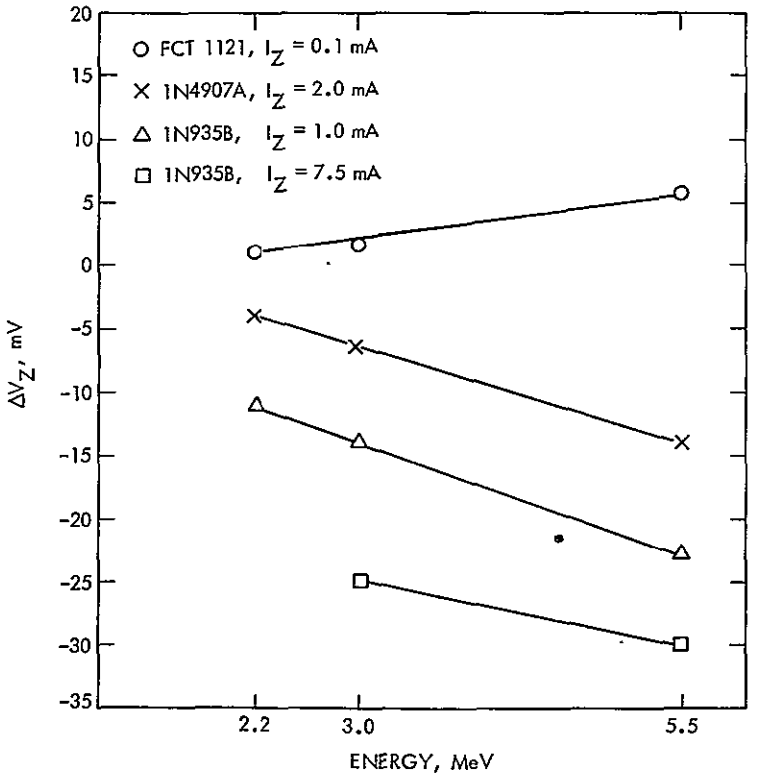

Figure 7-5. Effects of Electron Radiation Energy on Zener Voltage

An attempt was made to measure changes in the temperature coefficient of the temperature-compensated zener diodes produced by a fluence of 1×10^{13} e/cm^2 at energies of 2.2, 3.0, and 5.5 MeV. These measurements could not be carried out *in situ* and were, therefore, subject to many systematic errors. The main conclusion is that the pre-irradiation temperature coefficient of different devices of one type varies within one order of magnitude, whereas the radiation-induced changes are less than 50 percent of the initial value. The temperature coefficient from -50 to +25°C to 75°C increases with radiation. No correlation with electron energy could be detected.

2. Constant-Current Diodes

These devices are considered insensitive to radiation damage at the Voyager levels. The MOT 1N5288 and 1N5290 devices had no measurable changes at 1×10^{13} e/cm^2. The MOT 1N5297 and 1N5300 devices showed changes of less than 7 μA.

3. Diodes and Rectifiers

The following diodes and rectifiers were characterized: 1N4148, 1N5711, BC997-1, FJT 1100, MV 1404 and UTR 4320. The leakage current for these devices typically had shifts of less than 1 nA after 1×10^{13} e/cm^2. The forward voltage typically changed a few mV. Consequently, these are considered hard devices.

4. Silicon-Controlled Rectifiers

The Unitrode 2N1878 was the only device type tested. The mean for three samples of the gate voltage decreased by 0.426 V, and the gate current increased by 0.557 mA after 1×10^{13} e/cm^2.

H. PASSIVE COMPONENTS

1. Capacitors

Six each of the Component Research 0.02- and 0.05-μF, B11B Teflon capacitors were tested. The mean of the capacitance decreased 5 pF for the 0.02-μF devices and 12 pF for the 0.05-μF devices after radiation of 5×10^{12} e/cm^2.

2. Resistors

The Dale Electronics Types CDP16, CDP18, LDP16, and SDP16 metal film resistors were irradiated to 1×10^{13} e/cm^2. There was no change in the resistance within the experimental error of the equipment (±0.01 percent).

I. OPTICAL DEVICES

1. Light Sources and Light Detectors

The Texas Instruments type TIL23 and TIL24 light sources and type TIL601 and LS600 light detectors were evaluated in the JPL Dynamitron using a 2.5-MeV electron beam. Two of the tests used a 0.32-cm (1/8-in.) spacing between the source and detector in order to evaluate the spacecraft usage conditions. Three tests used a spacing of 20 cm (8 in.) in order to allow shielding and consequent evaluation of the source or detector separately. In addition, various angles were used during irradiation in order to reduce the amount of shielding caused by the lens material. All of the devices were measured in situ, within a period of 5 min, with the beam off.

a. Tests Using 0.32-cm (1/8-in.) Spacing. Test results using a 0.32-cm (1/8-in.) spacing between the light source and detector with both device types irradiated at the same time unshielded are given below.

(1) Test No. 1. Four TIL23 light sources and four LS600 light detectors were tested. The test circuit is shown in Figure 7-6.

Because of the close spacing between the TIL23 source and LS600 detector and the presence of the glass window, there was an undetermined amount of shielding of the device from the electron beam. Consequently, exposures at a number of incidence angles for the electron beam were used (i.e., 45, 90, and 135°), as shown in Figure 7-7, during the test.

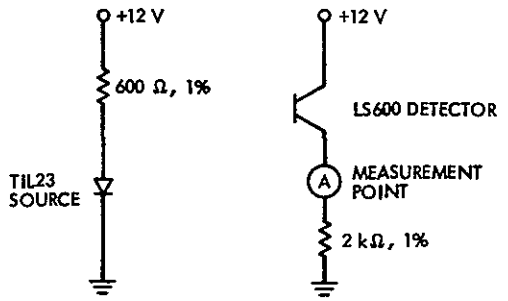

Figure 7-6. Test Circuit, Test No. 1, Light Sources and Light Detectors, 0.32-cm Spacing

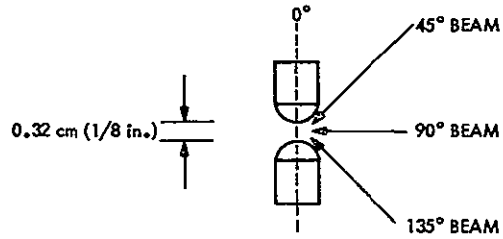

Figure 7-7. Electron Beam Incidence Angles, Test No. 1, 0.32-cm Spacing

Table 7-24. Results of Test No. 1 With 0.32-cm Spacing

Device S/N	Current Measured at Point (A), μA (Φ = Fluence, e/cm^2; ϕ = Flux, e/cm^2/s)							Beam Angle, deg
	Φ=0 ϕ=0	Φ= 1 x 10^{12} ϕ= 1 x 10^9	Δ,%	Φ= 2.5 x 10^{12} ϕ= 1.5 x 10^9	Δ,%	Φ= 5 x 10^{12} ϕ= 2.5 x 10^9	Δ,%	
12	350	213	-39	120	-66	55	-84	45
1	470	390	-17	320	-32	234	-50	135
2	282	205	-27	134	-53	75	-73	45
3	60	213	-28	0.36[a]	a	19	-68	90

[a]Data invalid; the device accidentally pulled out of position during irradiation.

(2) Test No. 2. Four LS600 light detectors and four TIL24 light sources were exposed to the electron beam at a 60° angle (see Figure 7-8). The fluence was 5 x 10^{12} and 1 x 10^{13} e/cm^2 with a flux rate of 2.5 x 10^9 e/cm^2/s. There was no significant change in the output level as measured at point (B) for any of the devices tested. Although the test devices were undoubtedly severely degraded (as indicated from previous test experience), there was still sufficient pulsed output after radiation exposure to trigger the 2N2222A transistor on, therefore maintaining a constant output at point (B). The test circuit is shown in Figure 7-9.

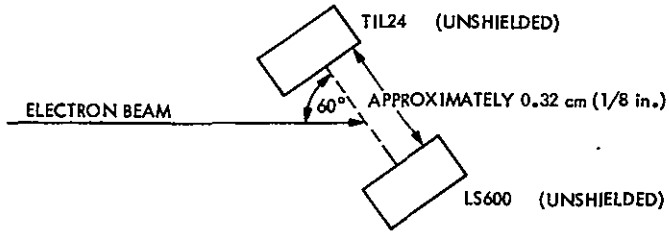

Figure 7-8. Flux Angle, Test No. 2, Light Sources and Light Detectors, 0.32-cm Spacing

The test devices in Test No. 2 were irradiated with the axis of the electron beam at 60° to the axis of the device in order to avoid the glass lid. No other components of the experiment were changed. A cosine variation in fluence with incident angle was used. The faraday cup readings of fluence were thus twice the fluence required (i.e., 10^{13} and 2 x 10^{13} e/cm^2). The effective value of the fluence on the device was obtained as of these values (i.e., 5 x 10^{12} and 10^{13} e/cm^2). This was done by using a time exposure that was twice as long, rather than by doubling the flux rate. Thus the effective flux rate at the device was one-half that in the test requirements.

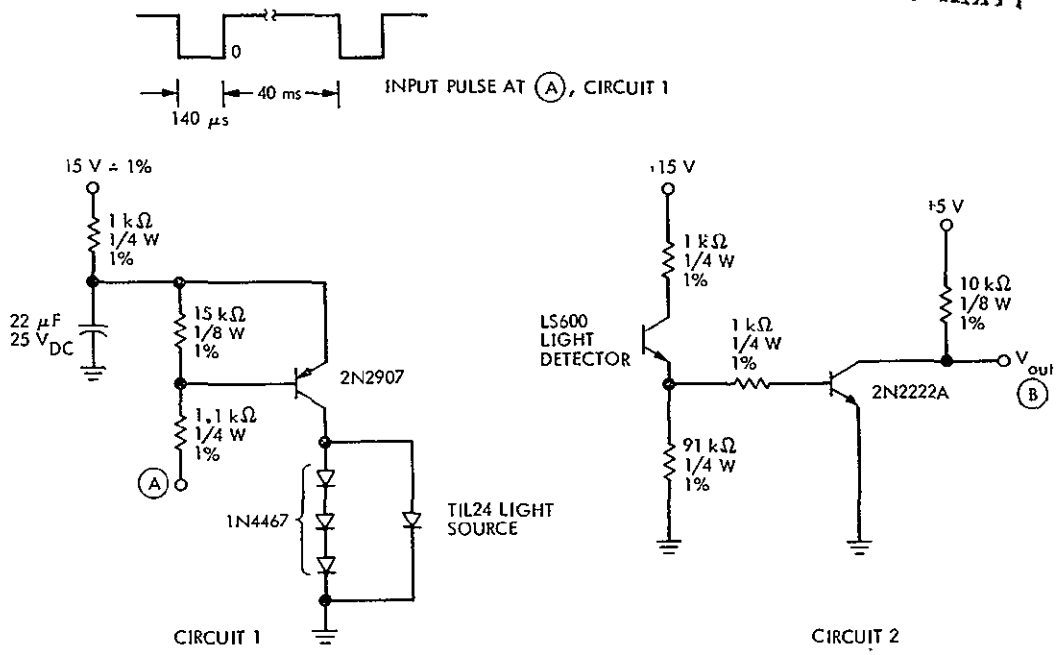

Figure 7-9. Test Circuit, Test No. 2, Light Sources and Light Detectors, 0.32-cm Spacing

b. Tests Using 20-cm (8-in.) Spacing. Test results using a 20-cm (8-in.) spacing between the light source and detector, with one of the device types shielded during irradiation, were as follows:

(1) Test No. 1. Four TIL23 light sources were exposed to the electron beam at an angle of 45°, as shown in Figure 7-10, with the detector shielded. The test circuit is shown in Figure 7-11.

Results are given in Table 7-25.

(2) Test No. 2. Four TIL601 light detectors were exposed to the electron beam at a 45° angle as shown in Figure 7-10, with the light source shielded. The test circuit is shown in Figure 7-12.

Results are given in Table 7-26.

Table 7-25. Results of Test No. 1 With 20-cm Spacing

Device S/N	TIL23 Output Voltage Measured at Point (A), nV (Φ = Fluence, e/cm^2; ϕ = Flux, e/cm^2/s)				
	Φ = 0, ϕ = 0	Φ = 5 x 10^{12}, ϕ = 3.6 x 10^9	Δ, %	Φ = 1 x 10^{13}, ϕ = 3.6 x 10^{19}	Δ, %
5	0.240	0.014	-94.2	0.004	-98.3
6	0.360	0.022	-94.0	0.006	-98.3
7	0.140	0.014	-90.0	0.005	-96.4
8	1.900	0.116	-94.0	0.038	-98.0

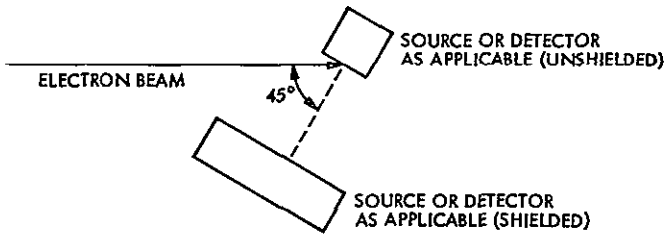

Figure 7-10. Flux Angle, Test No. 1, Light Sources and Light Detectors, 20-cm Spacing

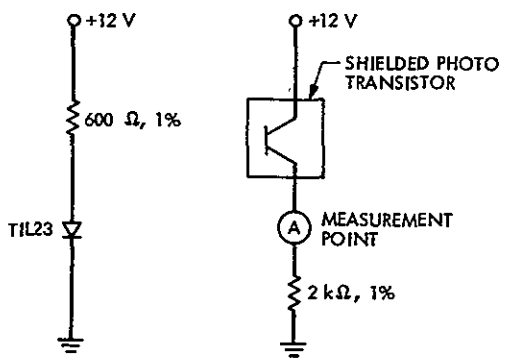

Figure 7-11. Test Circuit, Test No. 1, Light Sources and Light Detectors, 20-cm Spacing

Table 7-26. Results of Test No. 2 With 20-cm Spacing

Device S/N	TIL23 Output Voltage Measured at Point (A), nA (Φ = Fluence, e/cm^2; ϕ = Flux, e/cm^2/s)				
	Φ = 0 ϕ = 0	Φ = 5 x 10^{12} ϕ = 3.6 x 10^9	Δ, %	Φ = 1 x 10^{13} ϕ = 3.6 x 10^{19}	Δ, %
1	250.0	129.0	-48.4	38.0	-85.0
2	96.0	19.2	-80.0	8.0	-91.7
3	160.0	65.0	-59.4	19.0	-88.1
4	112.0	78.0	-30.4	53.0	-52.7

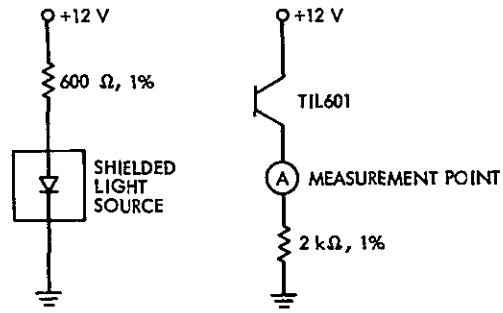

Figure 7-12. Test Circuit, Test No. 2, Light Sources and Light Detectors, 20-cm Spacing

(3) Test No. 3. Four TIL24 light sources were exposed to the electron beam at an angle of 45° as shown in Figure 7-10, with the detector shielded. The test circuit is shown in Figure 7-13. Results are given in Table 2-27.

Table 7-27. Results of Test No. 3 With 20-cm Spacing

Device S/N	TIL23 Output Voltage Measured at Point (A), mV (Φ = Fluence, e/cm^2; ϕ = Flux, e/cm^2/s)				
	Φ = 0 ϕ = 0	Φ = 5 x 10^{12} ϕ = 3.6 x 10^9	Δ, %	Φ = 1 x 10^{13} ϕ = 3.6 x 10^{19}	Δ, %
1	0.318	0.047	-85.2	0.015	-95.3
2	0.218	0.010	-95.4	0.003	-98.6
9	0.384	0.030	-92.2	0.009	-97.7
10	3.000	0.208	-93.1	0.016	-99.5

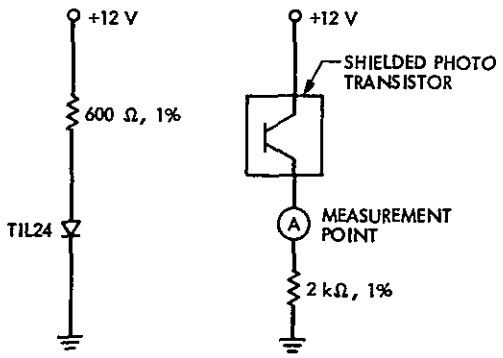

Figure 7-13. Test Circuit, Test No. 3, Light Sources and Light Detectors, 20-cm Spacing

(4) Flux Angle and Fluence. The devices tested were irradiated with the axis of the electron beam at 45° to the axis of the device as shown in the diagram in order to avoid the glass lid. A cosine variation in fluence with incident angle was used. The faraday cup readings of fluence were thus 1.4 times the fluence required (i.e., 0.707×10^{12} and 1.41×10^{13} e/cm^2). The effective value of the fluence on the device was obtained as 0.707 of these values (i.e., 5×10^{12} and 10^{13} e/cm^2). This was done by using a time exposure 1.4 times as long, rather than increasing the flux rate. Thus the effective flux rate at the devices is 0.707 times that in the test requirements.

c. Conclusions. The following conclusions can be drawn:

(1) These types of optical devices are very sensitive to radiation-induced damage.

(2) The light sources are more sensitive to radiation damage than the detectors.

(3) There is increased light scatter, due to the degraded source lens.

(4) There is more apparent degradation with 20-cm (8-in.) spacing between the source and detector than with 0.32-cm (1/8-in.) spacing because the light from the source decreases as the square of the distance from the detector, and any increase in light scatter will exhibit more effect as the distance is increased.

2. Reticon Solid State Image Sensor

A Reticon solid state image sensor was used on the Ultra-Violet Spectrometer (UVS) system. This consisted of a linear photodiode array with an associated capacitance and an MOS multiplex switch, with an MOS shift register for scanning. During operation, the gate of the MOS devices swings from 0 to -10 V for p-MOS devices that were used flight parts. Preliminary radiation experiments on the LINAC at the La Jolla facility of Intelcom Radiation Technology indicated that these devices failed at 100 krad(Si), whereas interference effects necessitated shielding the devices down to 3.4 krad(Si). Some recent improvements were made in the device structure in order to eliminate oxide surface charging effects. These should reduce the total dose susceptibility of the device still further.

J. QUARTZ RESONANT CRYSTALS

Ionization produces frequency shifts in quartz oscillator and filter crystals. The magnitudes of such shifts depend upon the source of the quartz, as shown in Figure 7-14. For all applications in which a frequency shift up to 1 part in 10^7 can be tolerated for Voyager, the use of swept synthetic quartz will ensure that the specifications are met. The use of natural quartz is not recommended unless changes

as large as 10 parts/million can be tolerated. For applications in which the radiation-induced changes must be less than 1 part in 10^7, a further screening process should be applied to carefully selected swept synthetic materials.

Three swept z-growth synthetic quartz resonators were tested to a total fluence of 1 x 10^{13} e/cm^2 on May 14, 1975. The test results are given in Table 7-28.

A total of fourteen resonators were tested to a total fluence of 2.5 x 10^{12} e/cm^2 and a nominal frequency of 24.5 MHz. The total change in frequency after irradiation ranged from 2.7 to 11.5 cycles. This change was considered insignificant.

Six resonators were tested to a total fluence of 2.5 x 10^{12} e/cm^2. The nominal frequency was 24.5 MHz. The frequency shift caused by the radiation environment ranged from 4 to 11 cycles. This change was not considered significant.

The changes after irradiation were considered insignificant.

K. DIGITAL MICROCIRCUITS

Past testing by JPL and other investigators has indicated that the Texas Instruments 54L series of integrated circuits should not be significantly degraded by the Voyager mission radiation environments. In order to verify that this still applied to current production, ten high-reliability Texas Instruments V5L30, 8-Input Positive NAND Gates (seal date 1-19-74) were irradiated at 10^{13} e/cm^2 and the results were evaluated.

In general, there were only minor shifts in the measurements after irradiation, and all devices remained well within the specification limits before and after.

The results of this test confirm that the relative radiation hardness of this type of device has not changed significantly, and the devices should not present a design problem for the Voyager program. Consequently, no additional testing of the 54L series was conducted.

Table 7-28. Irradiation Effects on Synthetic Quartz Resonators

S/N	f_S, Hz		R_S, ohms	
	Before	After	Before	After
1	24,500,060	24,500,111	19.5	19.4
3	24,499,836	24,499,826	24.2	24.3
8	24,500,129	24,500,111	23.7	23.6

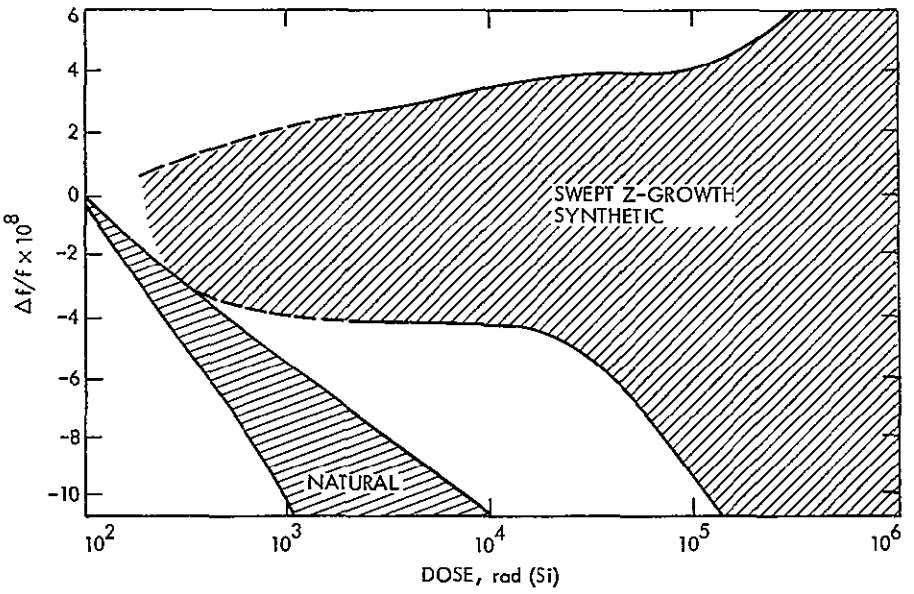

Figure 7-14. Composite Steady State Frequency Shift Data vs Dose for Quartz Crystal Resonators

SECTION VIII

SCREENING TEST RESULTS

A. LINEAR INTEGRATED CIRCUITS

1. Diffusion-Metallization Lot Screening

a. Operational Amplifiers. Typically, six devices from each diffusion-metallization lot were tested to a total dose of 125 krad(Si) (see Section V-A) for V_{OS}, I_{OS}, and I_B. Three devices were tested for open-loop gain at a 2 mA load. Table 8-1 lists the device types, acceptance limits, and number of accepted/rejected lots.

The HA2520, HA2600, and HA2620 exhibited some degradation in the dc parameters and open-loop gain. The HA2600 was not included in Table 8-1, as it was a single lot sample screened to specific circuit applications. The HA2700 (cans) showed no significant degradation at irradiation to 60 krad(Si). The poor showing of the HA2700 (flatpacks) (see Table 8-1 and Table 7-9) was attributed to the flatpack sealing methods. Similarly, the LM108 flatpacks could not be hardened, because of device degradation after sealing (see Section VI-C). LM108 Lot C1233A was an exception to the acceptance criteria shown in Table 8-1. This lot was accepted with a mean plus 3σ of $\Delta V_{OS} > 0.66$ mV, $\Delta I_{OS} > 0.89$ nA, and $\Delta I_B > 12.70$ nA, since the Infrared Interferometer Spectrometer (IRIS) and the Attitude and Articulation Control Subsystems (AACS) circuit applications could tolerate less stringent rejection criteria. The LM124 had acceptable degradation in dc parameters, provided the devices were biased at V+ = 15 V and V- = 0 V. Six HA2-2520-2 devices were tested up to a fluence of 1×10^{13} e/cm^2 in order to measure degradation in output drive capability under MDS load conditions. The test results indicated that the MDS would not require IRAN testing of the HA2-2520-2 or spot shielding.

b. Comparators. The only comparator subjected to lot screening was the LM139, in both the hardened and unhardened versions. The unhardened device was procured in a single diffusion-metallization lot whose radiation sensitivity was significantly greater than that of some other lots tested earlier (see Table 8-2). The properties of the hardened lot are shown in Table 7-15, Section VII-D.

A special determination was made of the total dose level at which the unhardened LM139 device latched-up when biased in the off condition during irradiation. At 12.5 krad(Si), all nine devices tested showed only slight changes in dc parameters. At 18.75 krad(Si), two of the devices produced offset voltage changes up to 20 mV. At 25 krad(Si), these two devices failed and another four devices showed offset voltage changes up to 40 mV. At 32.5 krad(Si), six out of nine devices failed catastrophically. These results establish 12.5 krad(Si) as the parts capability of the unhardened devices when they are biased in the off condition.

Table 8-1. Diffusion-Metallization Sample Lot Screening of Operational Amplifiers

Device Type	Mfg.	Parameter	Acceptance Criteria	Number of Lots		
				Accepted	Rejected	Total
HA2520	HAK	ΔI_{OS}	<40 nA	2	1	3
		ΔV_{OS}	<20 mV			
		ΔI_B	<1 μA			
		A_{OL}, 2 mA	2000			
HA2620	HAR	V_{OS}	<5 mV	1	0	1
		I_{OS}	<150 nA			
		I_B	<100 nA			
HA2700 (can)	HAR	V_{OS}	<10 mV	4	0	4
		ΔV_{OS}	≤5 mV			
		IOS	<30 nA			
		ΔI_{OS}	<10 nA			
		ΔI_B	<40 nA			
HA2700 (Flatpack)	HAR	ΔV_{OS}	<15 mV	1	9	10
		ΔI_{OS}	<10 nA			
		ΔI_B	<40 nA			
LM108 (Hardened)	NSC	ΔV_{OS}	<0.5 mV	21	3	
		ΔI_{OS}	<0.4 nA			
		ΔI_B	<6 nA			
		ΔA_{OL}	>45000	18[a]	6[a]	24

[a]AC parameters

Table 8-1. Diffusion-Metallization Sample Lot Screening of Operational Amplifiers (Continuation 1)

Device Type	Mfg.	Parameter	Acceptance Criteria	Number of Lots		
				Accepted	Rejected	Total
LM124	NSC	ΔV_{OS}	<25 mV	4	0	4
		ΔI_{OS}	<100 nA			
		ΔI_B	<1 μA			
		I_{Sink}, 5-kilohm load	>0.84 mA			
		I_{Source}, 5-kilohm load	>250 μA			

c. Voltage Regulator. The only voltage regulator subjected to diffusion-metallization lot screening was the LM105. Three lots, consisting of both hardened and unhardened devices, were tested. They all passed the acceptance criteria of less than 25 mV shift in load and line degradation at a fluence of 5×10^{12} e/cm^2.

d. Voltage Follower. Only one lot of hardened NSC LM102 devices was screened, and this lot was accepted. The criteria were as follows: $\Delta V_{OS} > 5$ mV and $\Delta I_B > 10$ nA.

e. RF Amplifers and Mixers. The flight lots of the MIC 76T RF amplifier and the MIC 236 and MIC 336 RF mixers were screened. All lots were found to be acceptable.

2. Irradiate-Anneal

The only two device types subjected to irradiate-annealing were the LM101 operational amplifier and the LM111 comparator. As shown in Section IV-B-4-2, there were a considerable number of rejects for the LM101, but far fewer LM111 rejects. A number of devices were shielded rather than wait for the return of the devices from the manufacturer after the IRAN cycle of operations.

Table 8-2. Diffusion-Metallization Lot Screening of the Unhardened LM139 Comparator

Device Type	Mfg.	Parameter	Initial Value	Post-irradiation Value[a] at Indicated Dose and Fluence: 12.5 krad(Si) 5 x 10^{11} e/cm^2	30 krad(Si) 1.25 x 10^{12} e/cm^2	60 krad(Si) 2.5 x 10^{12} e/cm^2	125 krad(Si) 5 x 10^{12} e/cm^2
LM139 (Unhard) Flight Lot 10145	NSC	$V_{OS(on)}$(mV)	5	5.3	5.5	5.6	6.0
		$\Delta V_{OS(on)}$(mV)		.3	0.5	0.6	1.0
		$V_{OS(off)}$(mV)	5	5.5	Failed	Failed	Failed
		$\Delta V_{OS(off)}$(mV)		0.5	Failed	Failed	Failed
		$I_{OS(on)}$(nA)	25	28	34	47	105
		$\Delta I_{OS(on)}$(nA)		3	9	22	80
		$I_{OS(off)}$(nA)	25	29	Failed	Failed	Failed
		$\Delta I_{OS(off)}$(nA)		4	Failed	Failed	Failed
		$I_{B(on)}$(nA)	100	190	230	315	525
		$\Delta I_{B(on)}$(nA)		90	130	215	425
		$I_{B(off)}$(nA)	100	160	Failed	Failed	Failed
		$\Delta I_{B(off)}$(nA)		60	Failed	Failed	Failed
		$\Delta I_{Sink(on)}$(mA)		-4	-7	-9	-11
		ΔI_{Sink}(off)(mA)		-4	Failed	Failed	Failed

[a]Post-irradiation values indicate anticipated post-Jupiter mean +3σ.

The reirradiation properties simulating the Jupiter environment are shown in Table 8-3. After annealing, there is a slight degradation of the input bias current of the LM101 and a large degradation in both input bias current and input offset current in the LM111. However, the subsystems were able to tolerate this degradation.

It was observed that there was a total lack of agreement between the dc parameter values of the LM111 measured at National Semiconductor after annealing and the same parameters measured on the JPL test boards after the parts were returned. A visit to National Semiconductor established that their test circuit saturates when testing IRAN devices, so that all the published data included in their data package is invalid.

On the basis of data from 16 flight parts in flatpacks, the properties of the IRAN parts are as follows: The input offset voltage is within the vendor's specifications, the input offset current may be as high as 25 nA, and the input bias current lies between 400 nA and 1 μA. The LM111 post-IRAN values in Table 8-3 are given as mean $+3\sigma$ worst-case values, since the devices were not correctly remeasured after annealing.

The detailed radiation behavior of the LM111 devices subject to IRAN is as follows:

(1) The first irradiation at 50 krad(Si) produces a positive shift in V_{OS} of less than 2 mV, a negative shift in I_{OS} of less than 20 nA, and a large increase in the input bias current, which increases to 300 to 500 nA.

(2) The 150°C annealing causes V_{OS} to anneal back to its starting value. I_{OS} is shifted positively by up to 30 nA, thus overshooting its starting value. The absolute post-annealing value may be as high as 25 nA. There is substantial deterioration in the input bias current during annealing, with final values in the range from 400 nA to 1 μA.

(3) Common mode rejection was measured for all dc parameters for unirradiated and for annealed devices. The supply voltage was ±15 V and the common mode voltage was varied from +10 to -10 V. Over this range the behavior was linear and was the same for unirradiated and annealed devices. No abnormalities were observed.

(4) The following shifts in dc parameters have been observed on reirradiation: V_{OS} shifts in the positive direction, but the shift is less than 4 mV at 60 krad(Si). I_{OS} shifts in the negative direction. The shift may be as much as 30 nA at 12.5 krad(Si), 65 nA at 30 krad(Si) and 120 nA at 60 krad(Si). The bias current initially decreases with radiation by up to 200 nA at 12.5 krad(Si). At about 30 krad(Si), the bias current returns to its original post-annealing value. At 60 krad(Si), some devices show an increase in bias current up to 150 nA.

Table 8-3. Simulated Jupiter Environment for LM101 and LM111

Device Type	Mfg.	Parameter	Initial Value	Post IRAN	Post-irradiation Value[a] at Indicated Dose and Fluence: 12.5 krad(Si) 5 x 10^{11} e/cm^2	30 krad(Si) 1.25 x 10^{12} e/cm^2	60 krad(Si) 2.5 x 10^{12} e/cm^2	125 krad(Si) 5 x 10^{12} e/cm^2
LM101AF, LM101AH	NSC	V_{OS}(mV)	2	2	3	4	5	12
		ΔV_{OS}(mV)			1	2	3	10
		I_{OS}(nA)	10	10	13	14	16	25
		ΔI_{OS}(nA)			3	4	6	15
		I_B(nA)	75	100	135	168	212	300
		ΔI_B(nA)			35	68	112	200
LM111F, LM111H	NSC	V_{OS}(mV)	3	3[b]	5	7	9	12
		$\lvert\Delta V_{OS}\rvert$(mV)			2	4	6	9
		I_{OS}(nA)	10	60[b]	60	100	180	300
		$\lvert\Delta I_{OS}\rvert$(nA)			60	120	200	320
		I_B(nA)	100	1800[b]	1600	2000	2300	2400
		ΔI_B(nA)			330	700	900	900

[a]Post-irradiation values indicate anticipated post-Jupiter mean +3σ.

[b]Mean +3σ.

The following device types were found not suitable for IRAN, for reasons given:

(1) HA2520, HA2600, HA2620; no correlation was found between IRAN and reirradiation behavior. The first irradiation caused significant permanent degradation in open-loop gain.

(2) HA9-2700 (flatpacks); severe degradation occurred in negative open-loop gain during the first irradiation, from which the devices did not recover on annealing.

Other devices which were investigated for IRAN but not included in the flight device IRAN program were as follows:

(1) HA2-2700 (cans); lot sample testing was found satisfactory for these.

(2) LM105 (voltage regulator); radiation damage for all devices was found to be acceptable up to 60 krad(Si).

B. ANALOG SWITCHES

1. Diffusion-Metallization Lot Screening

The DGM111 was the only analog switch for which sample lot screening was used. This device was screened for specific circuit applications. The DGM111 contains MOS transistors and is normally very sensitive to radiation. Fortunately, the subsystem was able to use the devices, since the circuit bias conditions were such that these conditions minimized the radiation degradation; i.e., drain at +10 V, source at ground, and logic supply voltage at +5 V.

2. Irradiate-Anneal

Only samples of each diffusion-metallization lot of the three analog switches, DG129, DG133 and DG141, were subjected to irradiate-annealing, and there were no rejects. On reirradiation corresponding to the post-Jupiter environment, the increase in the leakage current $I_{S(off)}$ increased somewhat, as shown in the mean $+3\sigma$ values tabulated in Table 8-4.

C. BIPOLAR TRANSISTORS

The bulk of the transistors were screened using date code lot sampling (see Section IV-B-3 for details). In addition, several lots of TIX 2N2222A and 2N2907A devices manufactured on a military line were screened by diffusion-metallization lot. A detailed discussion of the outlier problem is given in Section VIII-C-5. The SDT 5553 was subjected to irradiate-annealing procedures (Section VIII-C-6).

Table 8-4. IRAN Diffusion-Metallization Lot Sample Screening

Device Type	Mfg.	Parameter	Initial Value	Post IRAN	Post-irradiation Value[a] at Indicated Dose and Fluence: 12.5 krad(Si) 5 x 10^{11} e/cm^2	30 krad(Si) 1.25 x 10^{12} e/cm^2	60 krad(Si) 2.5 x 10^{12} e/cm^2	125 krad(Si) 5 x 10^{12} e/cm^2
DG129	SIL	$I_{S(off)}$(nA)	1	1	2	6	7.5	15
DG133	SIL	$I_{S(off)}$(nA)	1	1	2	6	7.5	15
DG141	SIl	$I_{S(off)}$(nA)	3	3	5	15	30	60

1. Date Code Lot Sampling

Extensive sampling on many device types provides a radiation history of line operation and instills confidence that outliers are absent over a prolonged period of time. Table 8-5 lists the device types screened and the pass/fail results for h_{FE} and I_{CBO}. The date code sample screening results were compared to the values listed in the Preliminary Radiation Handbook (Reference 4-3). The devices were rejected if the values exceeded those in the handbook. The New Data column in Table 8-5 indicates that there was no previous data for pass/fail criteria. Table 8-6 lists those device types that had a 100% screening failure indicated in Table 8-5, along with the subsystem usage and device disposition. Table 8-7 is a summary of the date code lot sampling results.

2. Special Low-Saturation Requirements

Special circuit applications required an h_{FE} measurement of 2N2222 devices at 0.11 V during the radiation screening test. This created a problem because the performance of this type of device at V_{CE} = 0.1 V is very unpredictable. The test results are questionable because the test instrumentation did not use separate voltage and current probes. Any small change in V_{CE} will cause a very large change in the gain at this operating point.

The performance appeared to be normal and predictable at the higher saturation voltages of 0.25 and 0.4 V. Since this part is well behaved at the higher saturation voltage and the saturation at 0.12 V is not required (except for one subsystem, which was handled separately), these parts were considered acceptable for Voyager applications.

3. TIX 2N2222A and 2N2907A Diffusion-Metallization Lot Sampling

Two lots of each device type (date codes 7533A and 7605A for the 2N2222A; 7507A and 7605A for the 2N2907A) were procured from the Texas Instruments high reliability special products group production line. These devices were then lot sample screened for radiation effects. The results are shown in Table 8-8. The rejection criteria are based on the previously published data in Reference 1-1.

4. Wafer Lot Sampling

The PWS subsystem used five different transistor types in a hybrid arrangement fabricated by Circuit Technology, Inc. Four dice from each wafer used in the hybrid circuits were mounted and sealed in a large transistor can and subjected to wafer lot screening. The data shown in Table 8-9 indicate a fairly small standard deviation (σ) in $\Delta(1/h_{FE})$, even at low current levels where surface effects predominate. Much better control of the radiation effects can be achieved by resorting to wafer lot screening. Additional flight lots were sampled at a later stage with similar results.

Table 8-5. Pass-Fail Date Code Lot Sampling Results for Bipolar Transistors

		h_{FE}				I_{CBO}			
Device Type	Mfg.	Pass	Fail	% Pass	New Data	Pass	Fail	% Pass	New Data
2N2219	TIX	3	0	100		-	-	-	-
2N2222	TIX	6	2	75		5	0	100	-
2N2484	TIX	-	-	-	3	-	-	-	3
2N2605	TIX	2	0	100		-	-	-	-
2N2658	SOL	1	1	50		1	0	100	-
2N2857	MOT	1	0	100		-	-	-	-
2N2880	SOL	3	1	75		-	-	-	-
2N2905	TIX	0	2[a]	0		-	-	-	-
2N2907	TIX	2	1	67		3	0	100	-
2N2920	TIX	2	2	50		-	-	-	-
2N2946	TIX	-	-	-	1	-	-	-	1
2N3501	MOT	0	1[a]	0		-	-	-	-
2N3637	MOT	0	2[a]	0		-	-	-	-
MQ2905	MOT	-	-	-	1	-	-	-	-
MQ2219	MOT	-	-	-	1	-	-	-	-
SDT3303	SOD	1	1	50		-	-	-	-
SDT3304	SOD	0	1[a]	0		-	-	-	-
SDT3323	SOD	1	0	100		-	-	-	-
14BB101	SOD	0	1[a]	0		-	-	-	-

[a]See Table 8-6 for further details.

Table 8-6. Device Disposition for Bipolar Transistors With 100% Failure for h_{FE}

Device Type	Mfg.	Date Code	Worst-Case Gain Requirements
2N2905	TIX	7418, 7441	Test yield is 40, which is acceptable for circuit application.
2N3501	MOT	7440	Acceptable, as there is no circuit usage below 2 mA.
2N3637	MOT	7516	Gain required is 11.1 to 13.8; predicted gain is 37 to 47.
		7520	Acceptable at 60 krad(Si).
SDI3304	SOD	7518	Acceptable at 62 krad(Si).
14BB101	SOD	7529	Gain required is 15; predicted gain is 22.
		7529	Select for high h_{FE}.

5. Outlier Problem

There is a significant problem associated with the applications of bipolar transistors on Voyager, wherein the radiation environment can cause degradations of low collector current gain h_{FE} and leakage currents I_{CBO}, which seem to occur randomly and with low incidence. These cases of severe degradation are called outliers. In fact, it is generally believed that the outliers are wafer-lot dependent and if one has diffusion lots, then radiation test sampling, with a small sample size, is sufficient to identify bad lots for rejection. The definition of an outlier, for the purposes of this report, is a device > mean + 3σ. Table 8-10 lists the device type, manufacturer, number of devices tested, and number of outliers observed. The greatest incidence of outliers (or bimodal distribution) was found on devices manufactured by Motorola and Raytheon and in 2N2222, manufactured by Texas Instruments before 1973.

Table 8-7. Summary of Date Code Lot Sampling Results for Bipolar Transistors

Device Type	Mfg.	Remarks
2N2219	TIX	Date code lots acceptable.
2N2222	TIX	
2N2484	TIX	
2N2605	TIX	
2N2658	SOD	
2N2857	MOT	
2N2880	SOD	
2N2905	TIX	h_{FE} yield of 40 acceptable for ISS.
2N2907	TIX	Date code lots acceptable.
2N2920	TIX	
2N2946	TIX	
2N3501	MOT	h_{FE} yield for I_C > 2 mA acceptable for ISS, UVS and PWR.
2N3637	MOT	h_{FE} yield of 37 to 47 acceptable for ISS; PWR acceptable at 60 krad(Si).
MQ2905	MOT	Date code lots acceptable.
MQ2219	MOT	
SDT3303	SOD	
SDT3304	SOD	h_{FE} acceptable at 62 krad(Si) for ISS.
SDT3323	SOD	Date code lots acceptable.
14BB101	SOD	h_{FE} yield acceptable for ISS; DRIRU selected high-gain devices.

Table 8-8. Diffusion-Metallization Sampling Results for 2N2222A and 2N2907A

Device Type	Date Code	h_{FE}		I_{EBO}/I_{CBO}		Remarks
		Pass	Fail	Pass	Fail	
2N2222A	7533A		X	-	-	Rejected
	7605A	X				Accepted
2N2907A	7507A		X	X		Rejected
	7605A		X	X		Rejected

Table 8-9. Results of Wafer Lot Sampling

Device Type	I_C	V_{CE},	Sample Size	$\Delta(1/h_{FE})$ at 5×10^{12} e/cm^2	
				Mean	σ
2N2369	150 μA	5	8	0.0032	0.0004
2N2484	50 μA	6	6	0.0082	0.002
	1 mA	6	6	0.0026	0.0007
2N2605	10 μA	6	8	0.0049	0.003
	1 mA	6	8	0.0016	0.0006
2N4044	50 μA	6	8	0.00084	0.0003
2N5087	50 μA	6	8	0.0021	0.0012

Table 8-10. Occurrence of Outliers in Bipolar Transistors

Device Type	Mfg.	No. Tested	No. of Outliers	Device Type	Mfg.	No. Tested	No. of Outliers
2N918	MOT	12	0	2N3497	MOT	4	0
2N930	TI	6	0	2N3499	MOT	6	0
2N2060	TI	12	0	2N3501	MOT	11	0
2N2222	MOT	17	2	2N3637	MOT	19	0
2N2222	TI	119	6	2N3742	MOT	10	0
2N2222	NSC	3	0	2N3805	FAS	12	0
2N2369	MOT	15	0	KD6001	KMC	6	0
2N2484	TI	29	0	MQ2219	MOT	20	3
2N2605	TI	14	0	MQ2905	MOT	16	1
2N2658	SOL	31	0	MQ3467	MOT	108	14
2N2857	MOT	11	0	MQ3725	MOT	124	1
2N2880	SOL	24	0	PA7443	RAY	193	6
2N2907	MOT	10	1	SA2267	RAY	187	11
2N2907	TI	61	0	SDT3303	SOL	16	0
2N2905	TI	48	0	SDT3304	SOL	11	0
2N2920	TI	24	0	SDT3323	SOL	13	0
2N2920	NSC	16	0	SDT3403	SOL	5	0
2N2946	TI	8	0	SDT4905	SOL	5	0
2N2975	FAS	26	0	SDT5553	SOL	70	0
2N3057	RAY	12	0	SDT8805	SOL	4	0
2N3251	MOT	5	0	SE7056	NSC	10	0
2N3350	TI	12	2	SS3137	MOT	6	0
2N3440	RCA	4	0	SQ1079	MOT	24	0

Table 8-10. Occurrence of Outliers in Bipolar Transistors (Continuation 1)

Device Type	Mfg.	No. Tested	No. of Outliers	Device Type	Mfg.	No. Tested	No. of Outliers
3029-201-1	RAY	36	0	96SV131	SOD	3	0
				14BB101	SOD	7	0
3029-202-1	RAY	36	0				

6. Irradiate-Anneal

The only bipolar transistor subjected to IRAN procedures was the SDT 5553, a device extremely sensitive to surface ionization effects at low current levels. This device was used only in a shielded environment (less than 5×10^{11} e/cm^2 fluence) at a collector current of 150 μA and a collector/emitter voltage of 124 V. The devices were irradiated to a total dose of 5 krad(Si), and all devices with a dc gain of less than 8 were rejected.

Four devices from the flight lots were reirradiated to a maximum fluence of 1×10^{12} e/cm^2. The results are shown in Table 8-11, which indicates mean + 3σ values.

D. JFET's

1. Date Code Screening

N-channel JFET date code lots responded to the radiation environment either by showing uniformly low leakage currents, in which case no additional testing was required; or by having uniformly high leakage currents, thereby requiring heavy shielding; or exhibiting mixed results, in which case screening was applicable (see Section IV-B-3 and Section VIII-D-2 for additional details). Table 8-12 lists the device types subjected to date code or radiation screening as well as the disposition of the lot.

Table 8-11. Post-reirradiation Values for SDT 5553

Parameter	Conditions	Fluence, e/cm^2			
		1×10^{11}	2.5×10^{11}	5×10^{11}	1×10^{12}
$\Delta(1/h_{FE})$	I_C = 0.15 mA, V_{CE} = 124 V	0.0091	0.0415	0.1220	0.335
$\Delta(1/h_{FE})$	I_C = 1 mA, V_{CE} = 18 V	0.0033	0.0148	0.0340	0.09

2. Irradiate-Anneal

A number of n-channel JFET's were irradiated to 60 krad(Si) using a cobalt 60 source. The device types selected were prone to inversion layer formation due to a lightly doped base region, resulting in large increases in the gate-source leakage current I_{GSS} after irradiation. The irradiated devices were not subjected to annealing. A few devices were reirradiated by electrons to a fluence of 5×10^{12} e/cm^2, resulting in a total accumulated dose of 185 krad(Si), in order to characterize the worst-case behavior of the devices at Jupiter.

The only JFET's subjected to IRAN were the 2N4856, 2N5196, 2N5520, and 2N5556. The flight lots of these devices showed a very varied response, so that IRAN was a necessity. A significant number of rejects was obtained, as shown in Section IV-B-4-a. The increase in leakage current on reirradiation, corresponding to the post-Jupiter environment, is indicated by the mean + 3σ values in Table 8-13.

The 2N4093, 2N4393, and 2N5906 flight lots were found to be extremely radiation sensitive, requiring shielding; i.e., no screening is possible if all the devices are bad. Lot-sample testing was found to be satisfactory for the 2N4391 and 2N4393; the sample contained no reject devices.

E. CMOS SCREENING

1. Quiescent Supply Current I_{SS}

In the wafer screening program, RCA supplied ten sample devices from each wafer. Initially, ten devices were irradiated, but this proved too time-consuming and was later reduced to five devices. Radiation was provided by a cobalt 60 source.

Table 8-12. Results of JFET Date Code and Radiation Screening

Device Type	Lot Trace No.	Date Code	Number of Devices Tested	Disposition
2N3066	-	-	14	No need for screening.
2N3686A	-	-	8	No need for screening.
2N4093	E0600 W0738	7421	11	Subsystem must shield to <25 krad(Si).
2N4093	W0738	7421	11	
2N4391	E0601 W0739	7420	11	Subsystem must shield to <25 krad(Si).
2N4391	W0739	7420	11	
2N4392	W1274[a]	7505	11	No need for screening.
2N4393	E2337B W1843	7510	11	Subsystem must shield to <25 krad(Si).
2N4416	-	7525	11	No need for screening.
2N4856	E3290	7524		100% screening at 60 krad(Si) required.[b]
2N4856	E3699	7509		
2N5196	E0787	7436	11	100% screening at 60 krad(Si) required.[b]
	W1020	7430		
2N5520	W3667[a]	7526	11	100% screening at 60 krad(Si) required.[b]
2N5556	None	7536	12	100% screening at 60 krad(Si) required.[b]
	None	7512		
2N5520	E3036 W3667	7518	-	Lot rejected.
2N5906	-	-		Subsystem must shield to <10 krad(Si).

[a]Unscreened.
[b]Devices subject to IRAN without annealing (see Section VIII-D-2).

Table 8-13. Results of JFET Reirradiation

Device Type	Mfg.	Parameter Controlled	Value						No. of Devices[a]		
			Initial	After First Irradiation	After Indicated Dose, krad(Si)						
					12.5	30	60	125	A	B	C
2N4856	SIL	I_{GSS}(nA)	0.25	0.5	1.21	2.3	4.6	16.7	298	65	9
2N5196	SIL	I_{GSS}(nA)	0.025	0.1	0.1	0.15	0.25	0.8	124	17	5
2N5520	SIL	I_{GSS}(nA)	0.025	0.1	0.19	0.26	0.45	1.1	21	0	9
2N5556	SIL	I_{GSS}(nA)	0.1	0.25	0.4	0.7	1.5	3.8	96	28	4

[a] A Screened.
B Rejected.
C Reirradiated.

The quiescent supply current I_{SS} was measured with all input terminals to ground and with all input terminals connected to 10 V. The wafer was rejected if any samples exceeded 100 times the 25°C military or JPL pre-irradiation specification limit (see Table 8-14). The rejection rate at 150 krad(Si) was less than 10% for some simple circuits (gates and flip-flops) and greater for complex and large area circuits (counters, shift registers, multiplexers, and buffers).

The test dice were not specially screened for I_{SS} before irradiation. As indicated in Figure 8-1, 75 percent of the devices (Group 1) had leakage currents below 1 nA, another 20 percent (Group 2) possessed greater leakage currents, but sufficiently low to pass the JPL specifications, whereas the remaining 5 percent (Group 3) would have been rejected in pre-irradiation screening. The post-irradiation data for Group 1 (Figure 8-2) shows a reasonable Gaussian distribution, but with the rejection limit set so as to cause a 12% rejection rate. The more than 10,000-fold increase in I_{SS} appears to be the best that can be achieved on this type with the modified annealing process, and is attributed to the shift in V_{TN} toward 0 V (see Section VI-B for a discussion of CMOS hardening).

Group 2, with marginal pre-irradiation properties, produced a post-irradiation yield of only 66 percent (see Figure 8-3a and b).

A preliminary study on the variation of I_{SS} over a given wafer after irradiation indicates a tight distribution in some wafers, while other wafers exhibit a great deal of variability. This is in agreement with the general lot variability of the product observed during radiation screening.

The distribution of I_{SS} has been analyzed for a number of different device types and for both forming gas and nitrogen annealing. The results for the CD4052 and CD4049 are shown in Figures 8-4 through 8-11. The data indicate that a number of bimodal distributions are caused by lack of process control, but that nitrogen annealing offers a substantially better product. The data that have been analyzed in this manner are summarized in Table 8-15. It is evident that the rejection limits do remove lots with lack of surface control. The rejection limits were chosen to screen out wafers with catastrophic devices or with I_{SS} higher than acceptable to the project systems designers. The yield figures of the wafer screening program are summarized in Table 8-16.

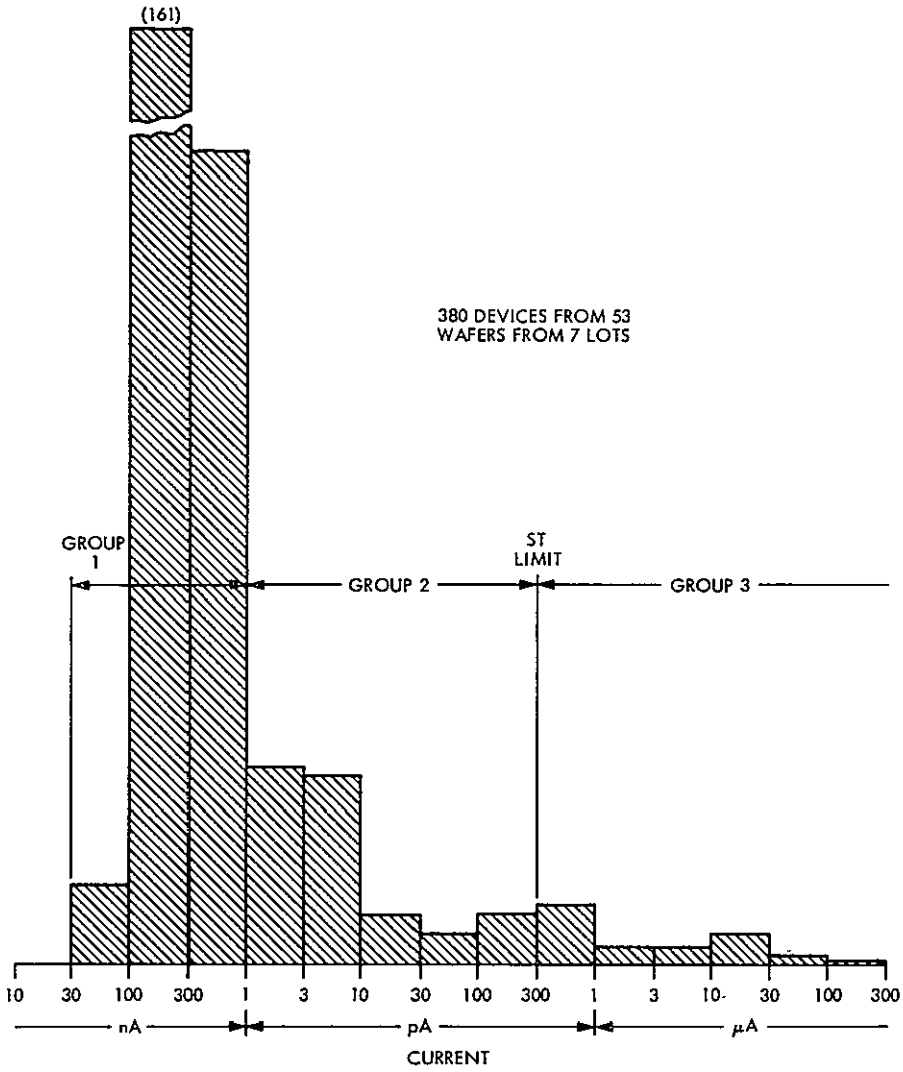

Figure 8-1. Pre-irradiation Current for RCA CD4006, Groups 1, 2, and 3

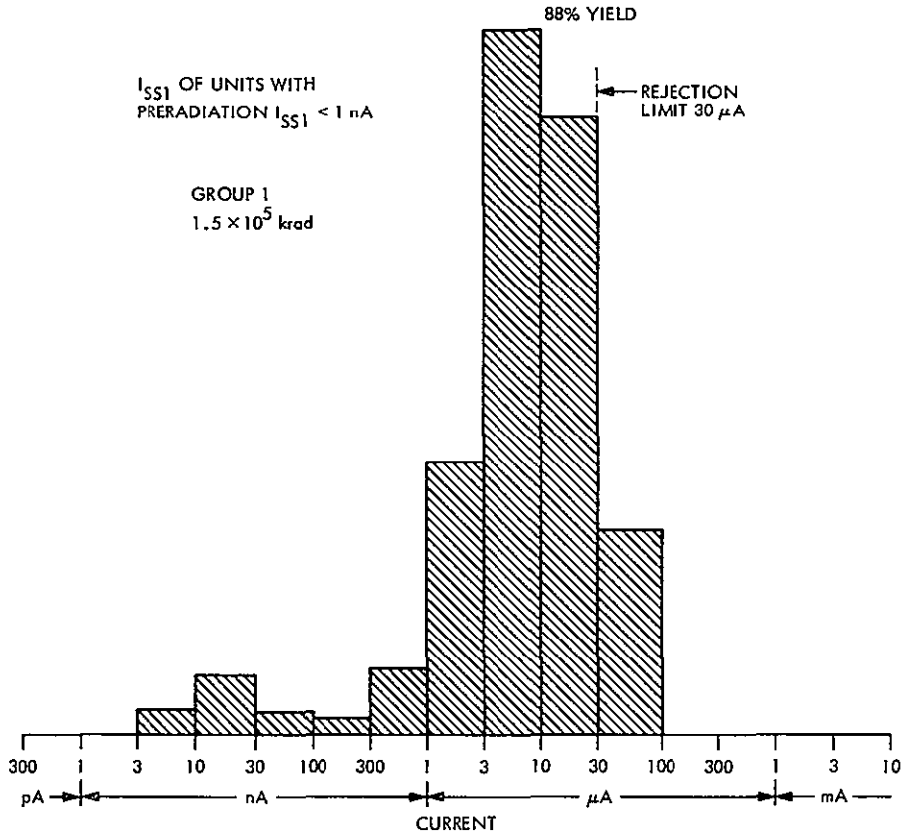

Figure 8-2. Post-irradiation Current for RCA CD4006, Group 1

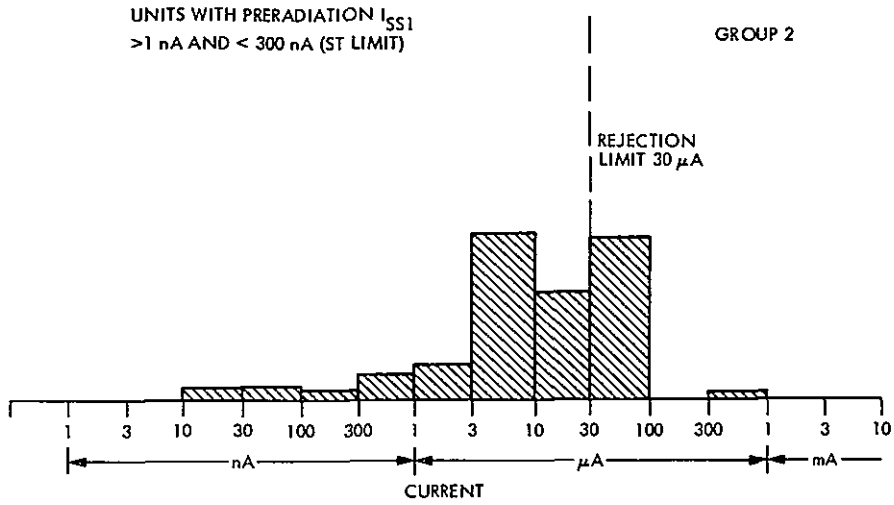

Figure 8-3a. Post-irradiation Current for RCA CD4006, Group 2

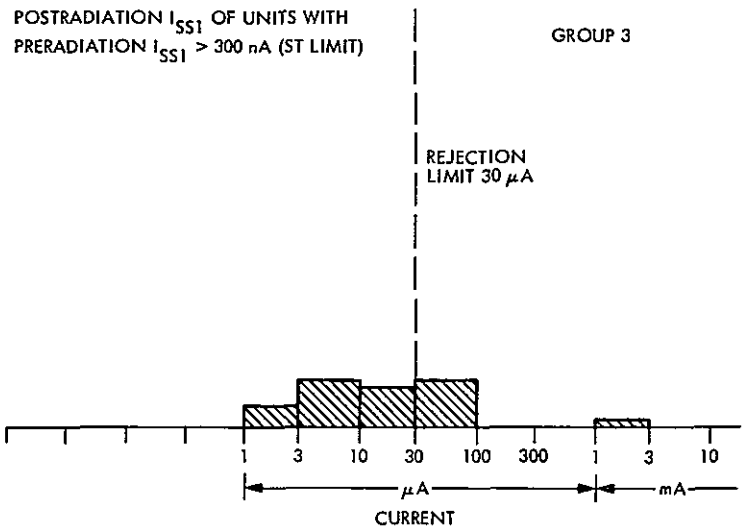

Figure 8-3b. Post-irradiation Current for RCA CD4006, Group 3

Table 8-14. Electrical Specifications and Rejection Criteria for I_{SS} Wafer Screening

Device Type	Electrical Specification Maximum Limit at 25°C		Device Type	Electrical Specification Maximum Limit at 25°C	
	Pre-irradiation nA	Post-irradiation µA		Pre-irradiation nA	Post-irradiation µA
CD4001	25	2.5	CD4027	250	7.5
CD4002	25	2.5	CD4028	500	7.5
CD4006	25	30	CD4029	500	50
CD4011	25	2.5	CD4030	50	5.0
CD4012	25	2.5	CD4031	2000	100
CD4013	250	7.5	CD4035	500	50
CD4014	500	50	CD4040	1000	50
CD4015	500	50	CD4042	2000	25
CD4016	75	7.5	CD4043	2000	25
CD4017	500	50	CD4049	75	7.5
CD4019	75	7.5	CD4050	75	7.5
CD4021	500	50	CD4051	500	50
CD4023	25	2.5	CD4052	500	50
CD4025	25	2.5	CD4053	500	50

Table 8-15. Analysis of I_{SS} data

Device Type	Function	Annealing Gas	Distribution	Peak of Prime Devices	Other Peaks, μA	Rejection Limit, μA
CD4006	18-stage shift register	Forming gas	Gaussian	10 μA		30
CD4019	Quad AND-OR gate	Forming gas	Gaussian	5 nA		7.5
		Nitrogen	Gaussian	20 nA		7.5
CD4027	Dual flip-flop	Forming gas	Gaussian	20 nA		7.5
CD4029	Up/down counter	Forming gas	Bimodal	50 nA	20	50
		Nitrogen	Bimodal	5 nA 50 nA	2	50
CD4049	Hex-buffer	Forming gas	Bimodal	50 nA	2	7.5
		Nitrogen	Quasi-Gaussian	20 nA	2	7.5
CD4052	Multiplexer	Forming gas	Bimodal	3 nA	2 30	50
		Nitrogen	Gaussian	500 nA		50

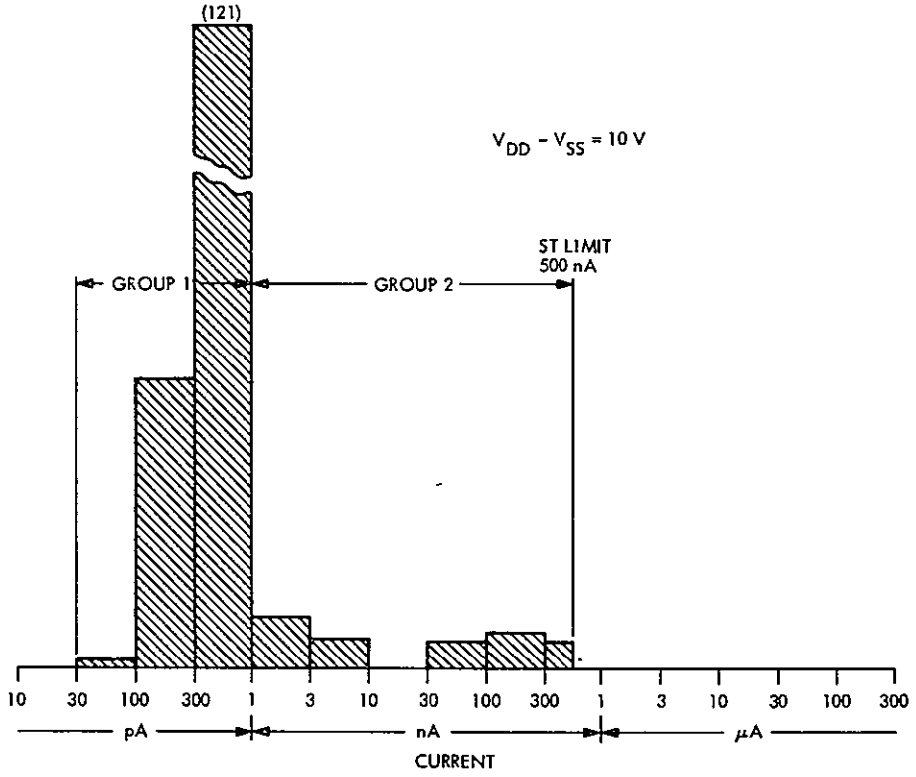

Figure 8-4. Pre-irradiation Current for RCA CD4052A Multiplexers With 950°C Gate Oxide Anneal in Forming Gas

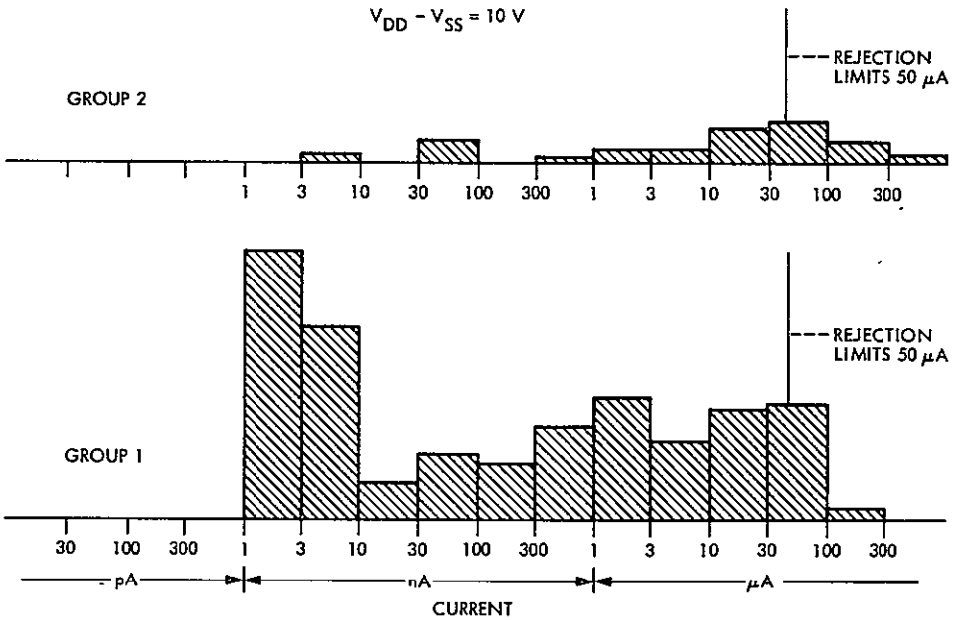

Figure 8-5. Post-irradiation Current for RCA CD4052A Multiplexers With 950°C Gate Oxide Anneal in Forming Gas

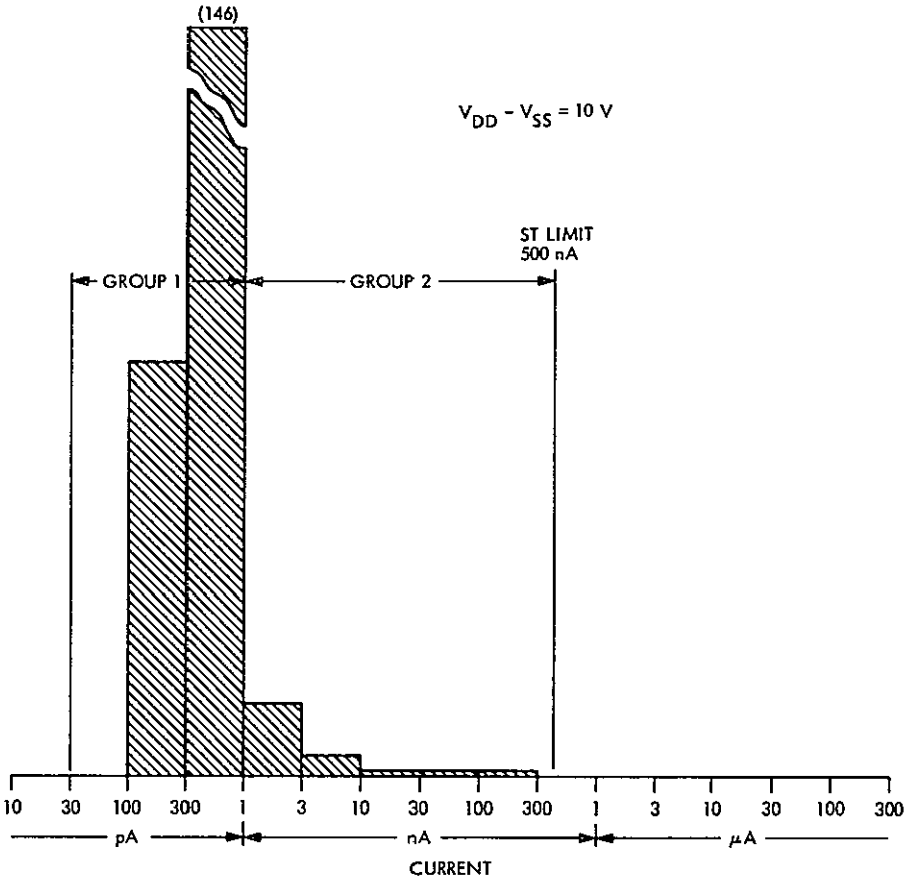

Figure 8-6. Pre-irradiation Current for RCA CD4052A Multiplexers With 950°C Gate Oxide Anneal in Nitrogen

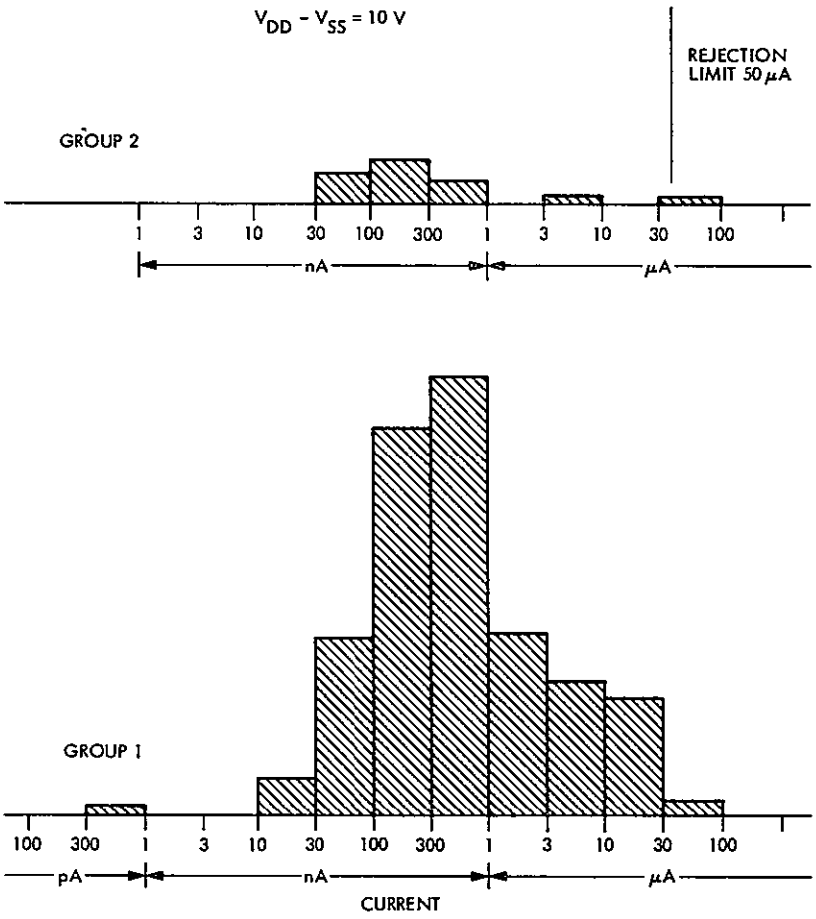

Figure 8-7. Post-irradiation Current for RCA CD4052A Multiplexers With 950°C Gate Oxide Anneal in Nitrogen

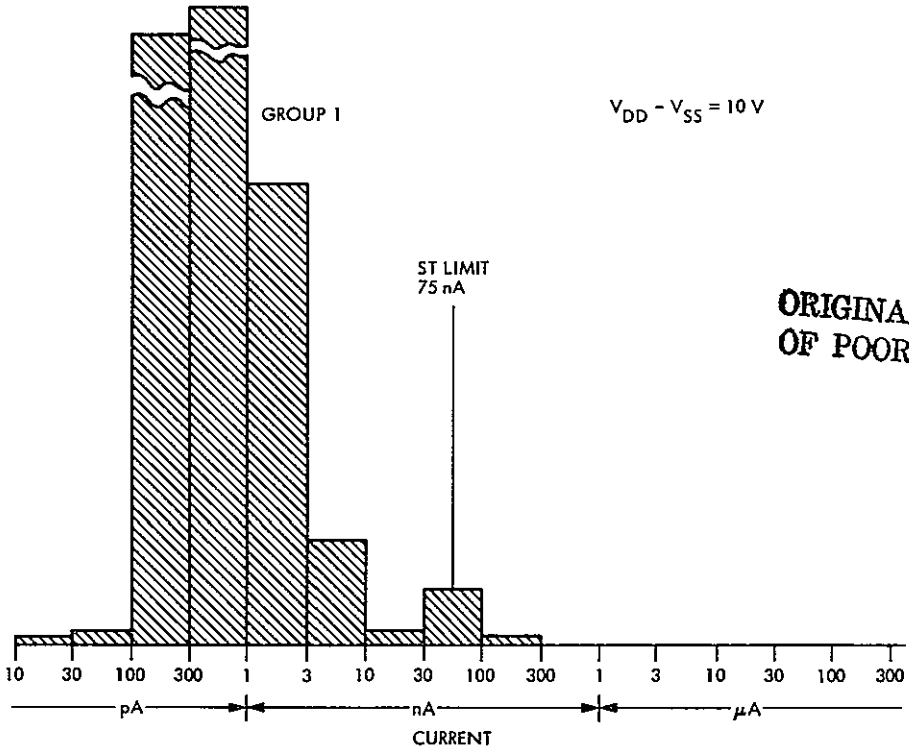

Figure 8-8. Pre-irradiation Current for RCA CD4049 With 950°C Gate Oxide Anneal in Forming Gas

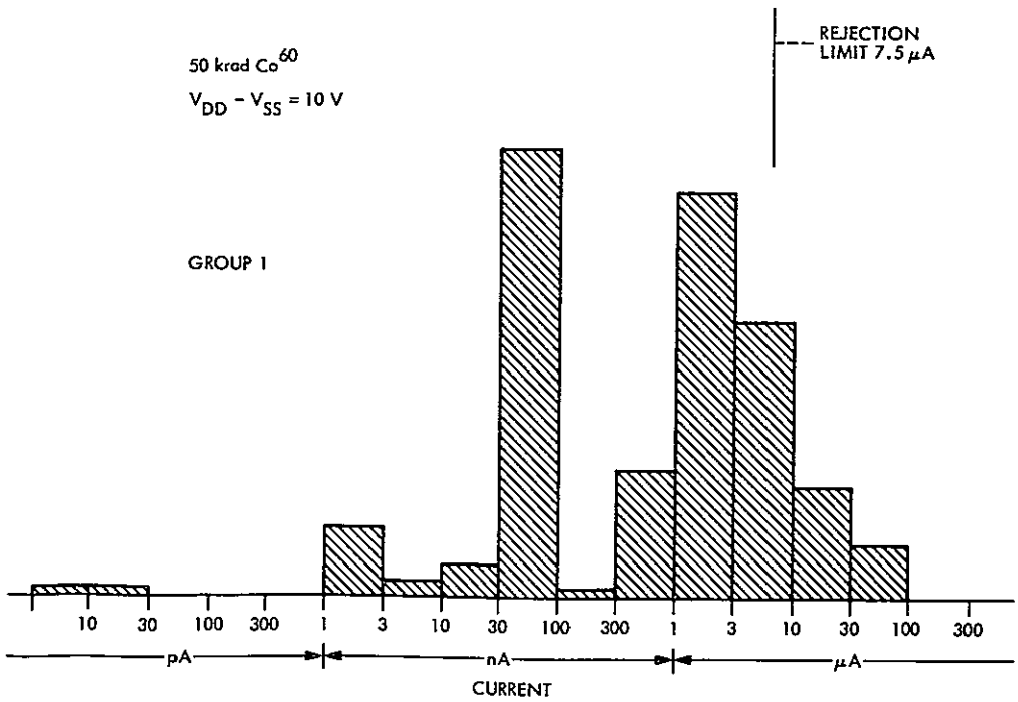

Figure 8-9. Post-irradiation Current for RCA CD4049 With 950°C Gate Oxide Anneal in Forming Gas

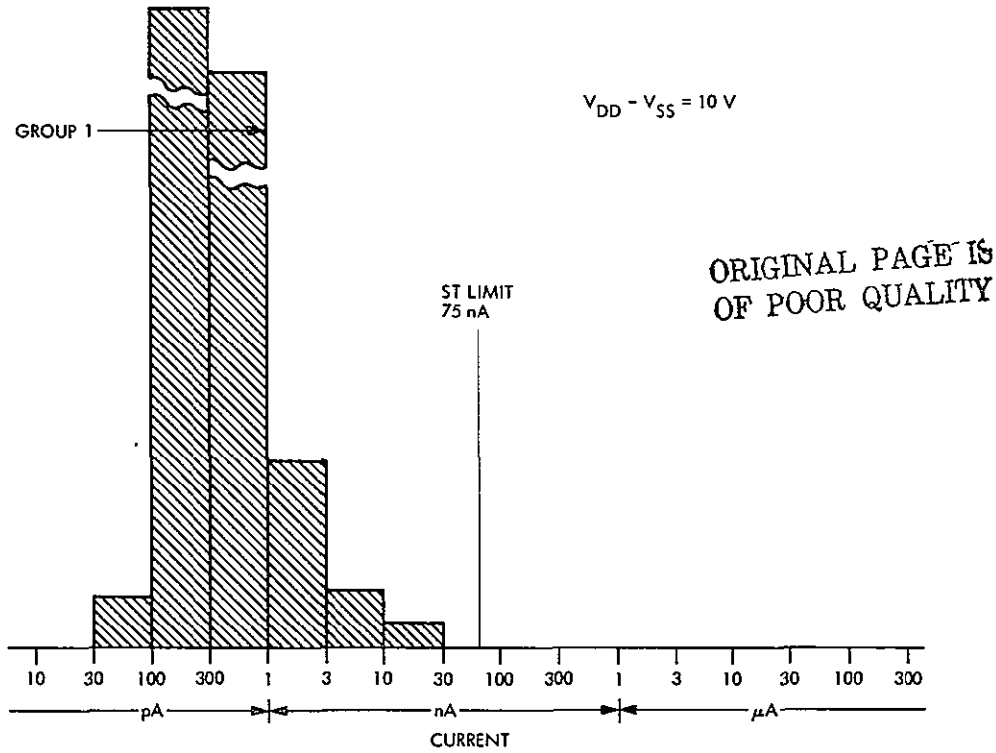

Figure 8-10. Pre-irradiation Current for RCA CD4049 With 950°C Gate Oxide Anneal in Nitrogen

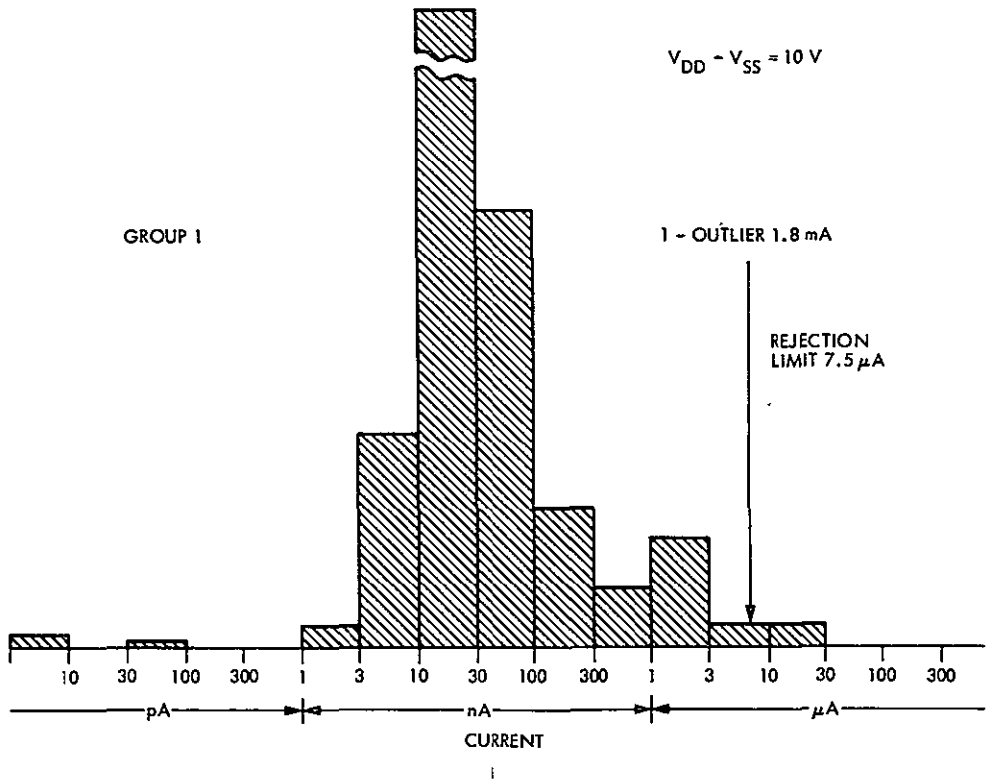

Figure 8-11. Post-irradiation Current for RCA CD4049 With 950°C Gate Oxide Anneal in Nitrogen

The wafer screening of I_{SS} is expensive but necessary in view of the lack of safety margin shown in the distribution, the presence of outliers, and the bimodal distributions. For future programs, radiation screening of n-channel and p-channel test transistors associated with each wafer should be considered, since the absolute values of post-irradiation V_{Tn} and V_{Tp} are more fundamental parameters directly related to oxide and interface states. At present V_{Tp} is not screened, and this produces a barely tolerable variation in the propagation time. In future programs, other process controls involving capacitor measurements should be considered in direct collaboration with the manufacturer. Such controls have been described in a paper by Gregory (Reference 8-1).

2. Transmission Gate Leakage I_L

The multiplexers CD4051, CD4052, and CD4053 were subjected to an additional screening. The off leakage current through all transmission gates in parallel was required to be less than 100 nA, measured with all switch inputs at 10 V and the outputs at ground (I_{L_2}), and less than 100 mA for the CD 4052 and CD 4053, with all switch outputs at 10 V and the inputs at ground (I_{L_2}). This resulted in a yield of about 50% for these device types. The leakage current limit for the CD4051 was originally set at 3 μA, but improvements after switching to nitrogen annealing enabled the limit to be reduced to 100 nA.

Figures 8-12 and 8-13 show the distribution of the I_{L_2} leakage current before and after irradiation respectively, for devices annealed in forming gas. It may be seen that prime pre-irradiation devices show a bimodal distribution after irradiation, resulting in a high yield loss. This problem was solved by switching to nitrogen annealing. The pre-irradiation distribution (Figure 8-14) was the same as before, but the post-irradiation data (Figure 8-15) showed a more Gaussian distribution, though with a few outliers beyond 1 μA. The I_{SS} data for the same devices, shown in Figures 8-4 through 8-7, exhibit a very similar behavior.

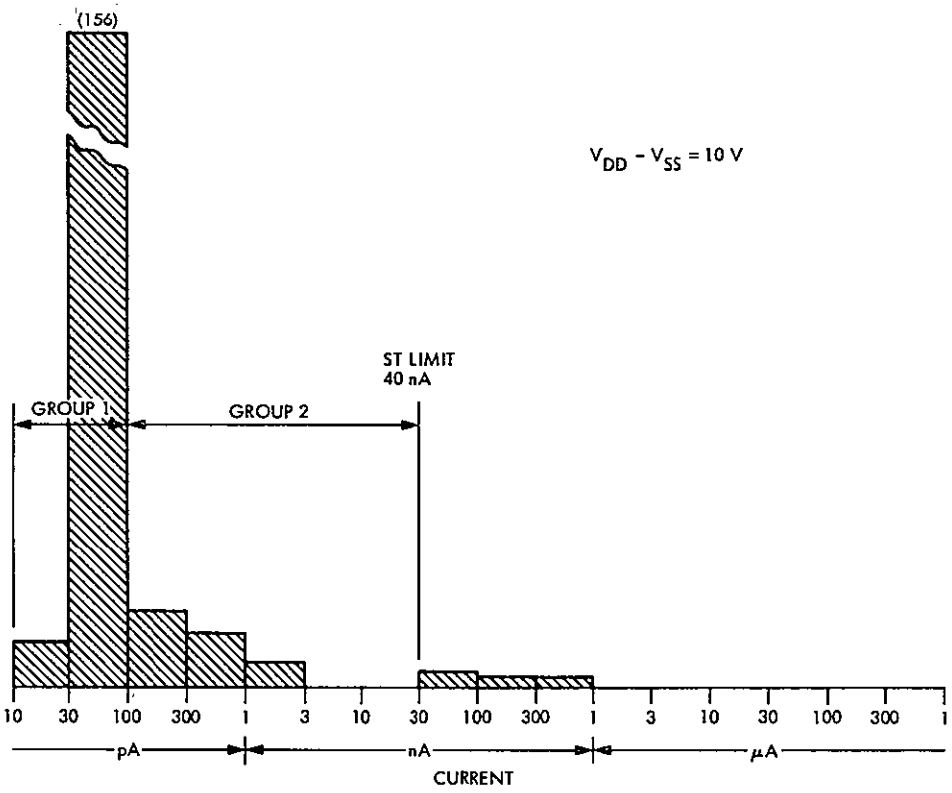

Figure 8-12. Pre-irradiation Switch Leakage Current for RCA CD4052A Multiplexers with 950°C Gate Oxide Anneal in Forming Gas

Table 8-16. Screening Data at 150 krad(Si)

Device Type	Forming Gas Anneal No. of Wafers Tested	Forming Gas Anneal No. of Wafers Passed	Forming Gas Anneal % Passed	Nitrogen Anneal No. of Wafers Tested	Nitrogen Anneal No. of Wafers Passed	Nitrogen Anneal % Passed	Total Devices Tested
CD4001	24	20	83	79	20	25	528
CD4002	11	9	82	-	-	-	68
CD4006	123	66	54	99	96	97	1155
CD4011	41	37	90	-	-	-	217
CD4012	10	9	90	35	33	94	237
CD4013	12	12	100	16	16	100	147
CD4014	16	14	87.5	22	22	100	208
CD4015	22	21	95	16	16	100	206
CD4016	16	15	94	15	14	93	165
CD4017	-	-	-	4	4	100	30
CD4019	22	22	100	59	47	80	419
CD4021	85	77	91	66	54	82	785
CD4023	7	6	86	21	21	100	149
CD4025	14	12	86	-	-	-	87
CD4027	113	101	89	29	28	97	744

Table 8-16. Screening Data at 150 krad(Si)
(Continuation 1)

Device Type	Forming Gas Anneal No. of Wafers Tested	Forming Gas Anneal No. of Wafers Passed	Forming Gas Anneal % Passed	Nitrogen Anneal No. of Wafers Tested	Nitrogen Anneal No. of Wafers Passed	Nitrogen Anneal % Passed	Total Devices Tested
CD4028	24	24	100	16	16	100	215
CD4029	147	125	85	175	133	76	1646
CD4030	12	0	0	16	16	100	147
CD4031	146	115	79	-	-	-	773
CD4035	63	57	90	29	14	48	489
CD4040	28	19	68	116	101	87	435
CD4042	-	-	-	25	18	72	129
CD4043	-	-	-	18	16	89	100
CD4047	-	-	-	34	32	94	180
CD4049	133	88	66	158	96	61	1519
CD4050	66	51	77	-	-	-	356
CD4051	120	62	52	74	72	97	1011
CD4052	44	10	23	159	129	81	1035
CD4053	60	42	70	88	52	59	760
TOTAL	1359	1014	75%	1369	1066	77%	13,940

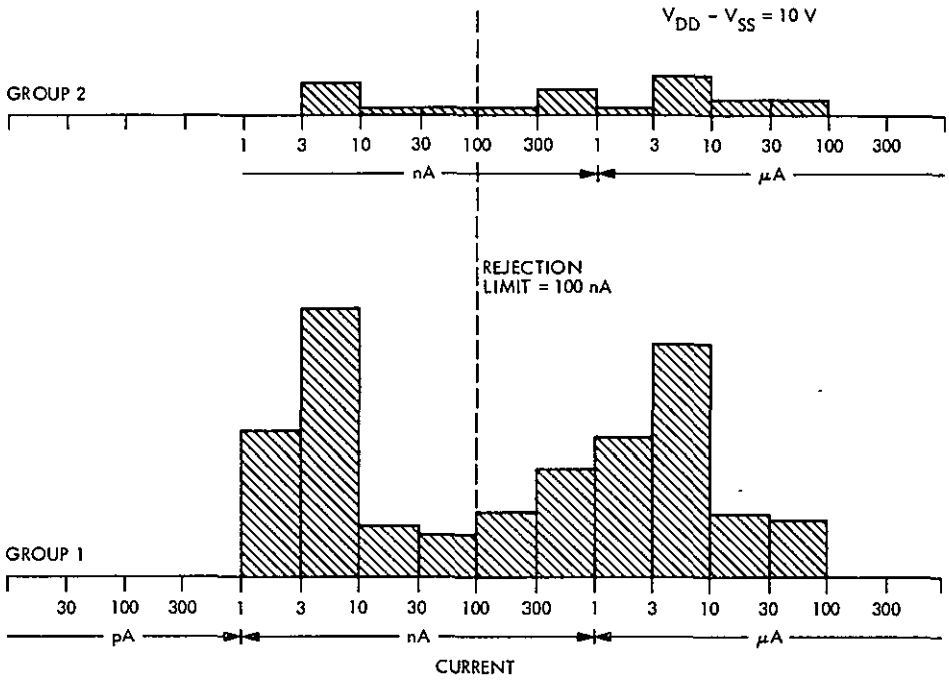

Figure 8-13. Post-irradiation Switch Leakage Current for RCA CD4052A Multiplexers with 950°C Gate Oxide Anneal in Forming Gas

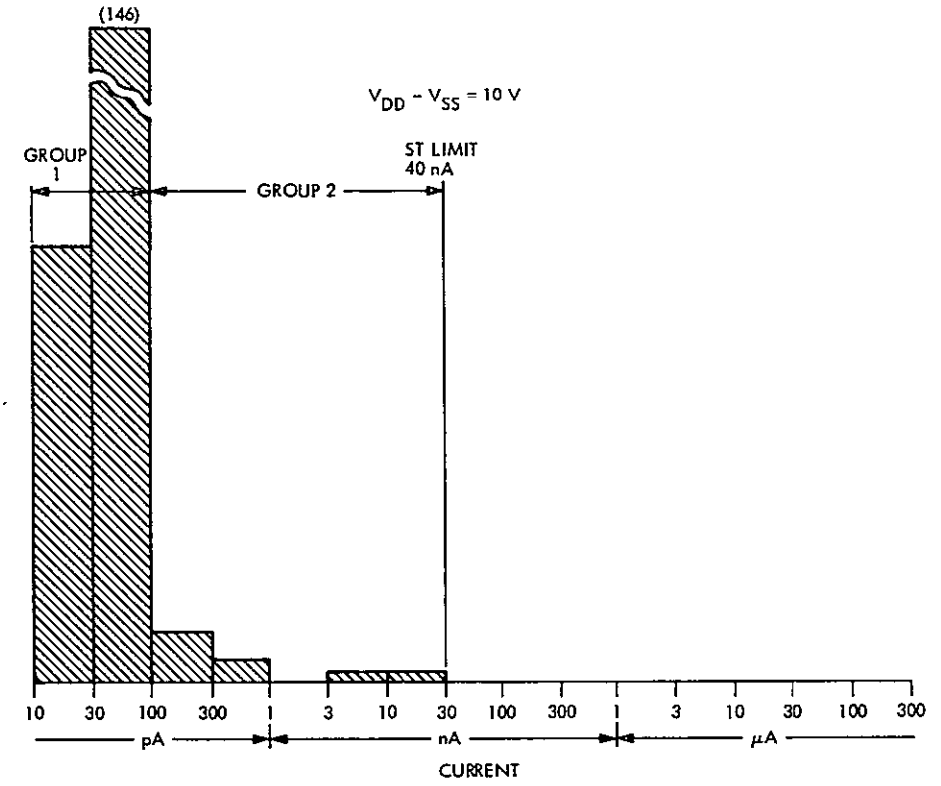

Figure 8-14. Pre-irradiation Switch Leakage Current for RCA CD4052A Multiplexers With 950°C Gate Oxide Anneal in Nitrogen

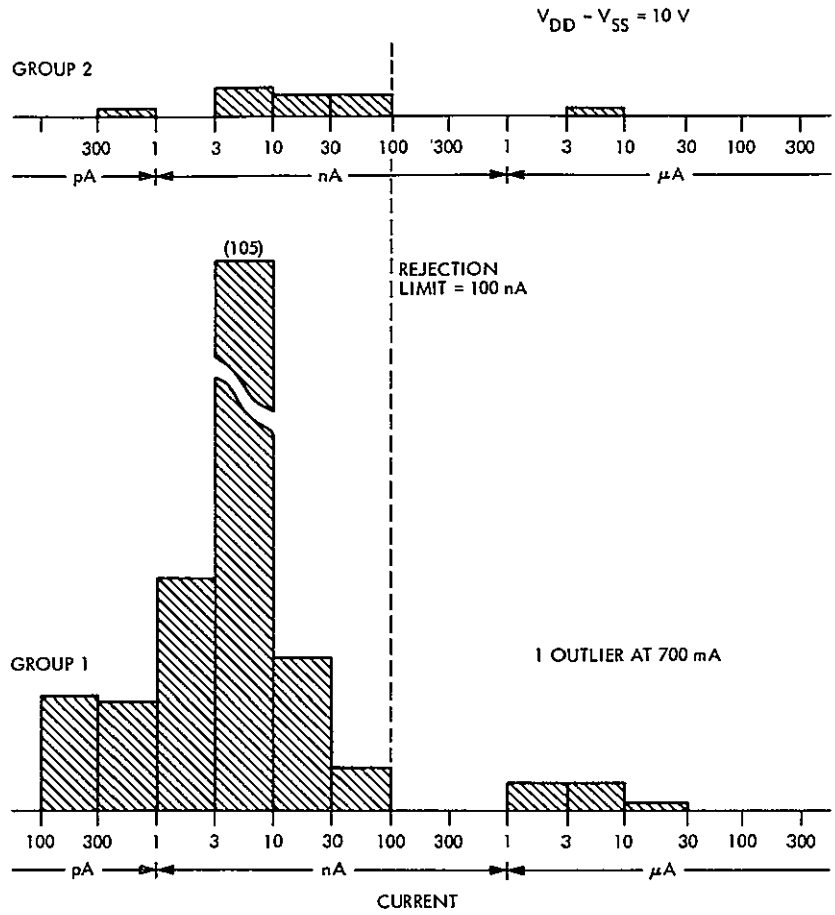

Figure 8-15. Post-irradiation Switch Leakage Current for RCA CD4052A Multiplexers With 950°C Gate Oxide Anneal in Nitrogen

3. Gate Turn-On Voltage V_{GS}

Three to five test pattern dice were selected at random from each metallization lot. The test pattern dice contain individual n- and p-channel transistors and MOS capacitors. Measurement of I_{DS} vs V_{GS} of the two transistors was made before and after a dose of 1.15×10^5 rad(Si). Figures 8-16 and 8-17 show an example of the distribution of V_{TN} before and after irradiation. Figure 8-18 and 8-19 show V_{TP}. The distribution of the relative shift in the gate turn-on voltages is shown in Figure 8-20. The figures show the 10-μA values only. The shifts were much greater at lower currents.

C-3

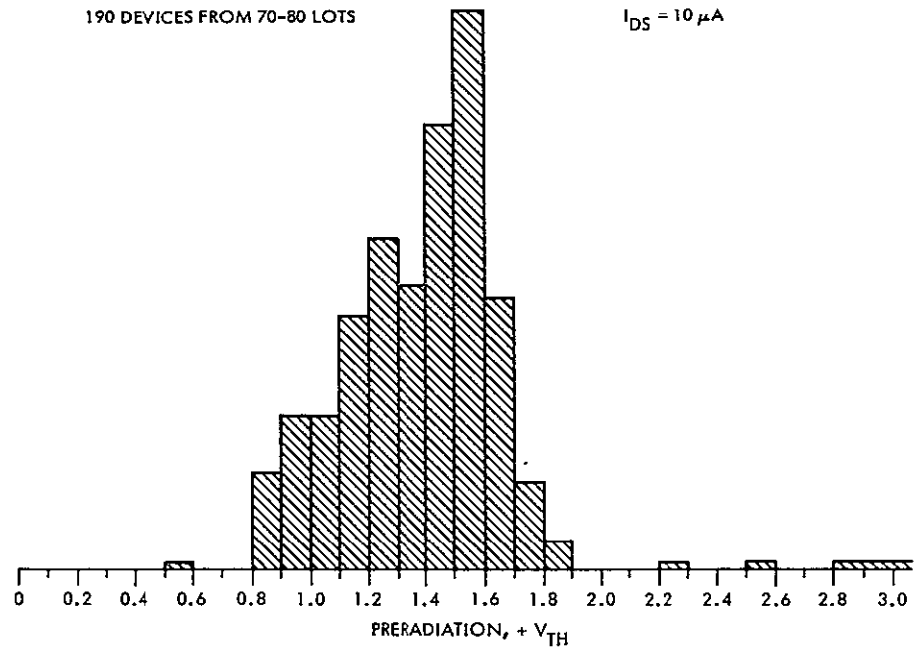

Figure 8-16. Pre-irradiation Threshold Voltage of n-Channel Transistor on Test Pattern TA 6372 With 950°C Gate Oxide Anneal in Forming Gas

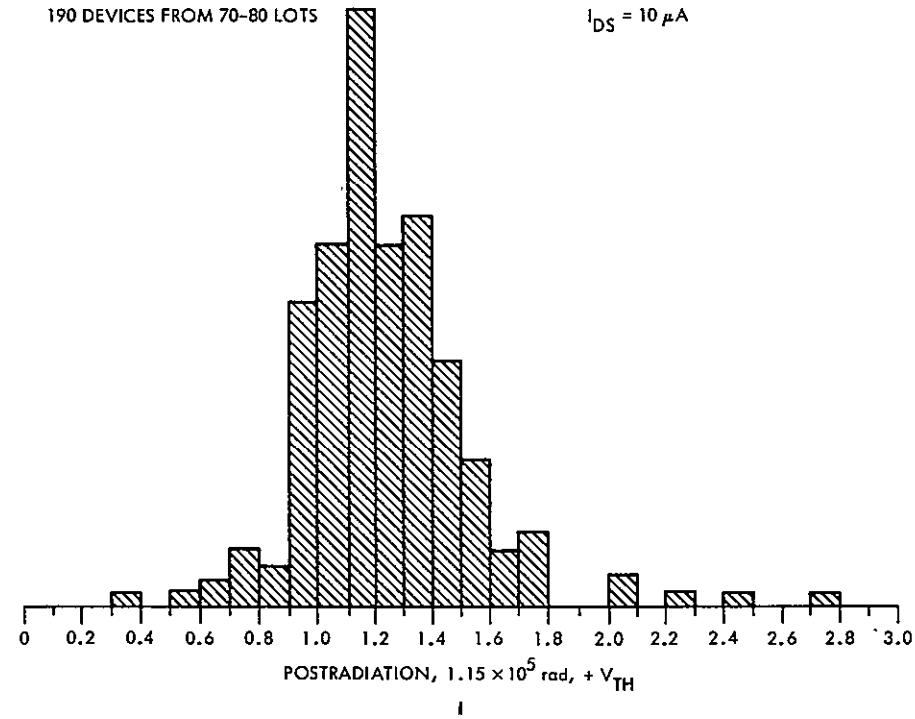

Figure 8-17. Post-irradiation Threshold Voltage of n-Channel Transistor on Test Pattern TA 6372 With 950°C Gate Oxide Anneal in Forming Gas

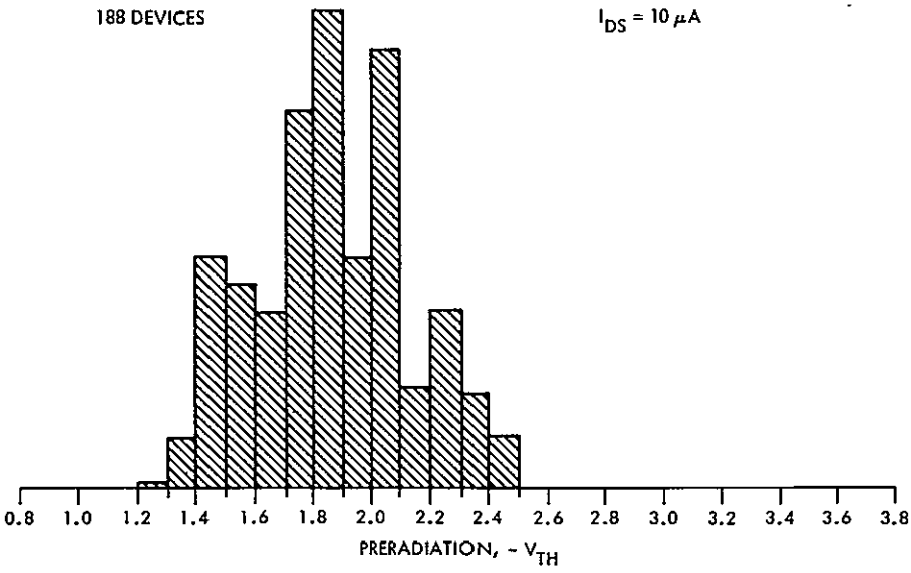

Figure 8-18. Pre-irradiation Threshold Voltage of p-Channel Transistor on Test Pattern TA 6372 With 950°C Gate Oxide Anneal in Forming Gas

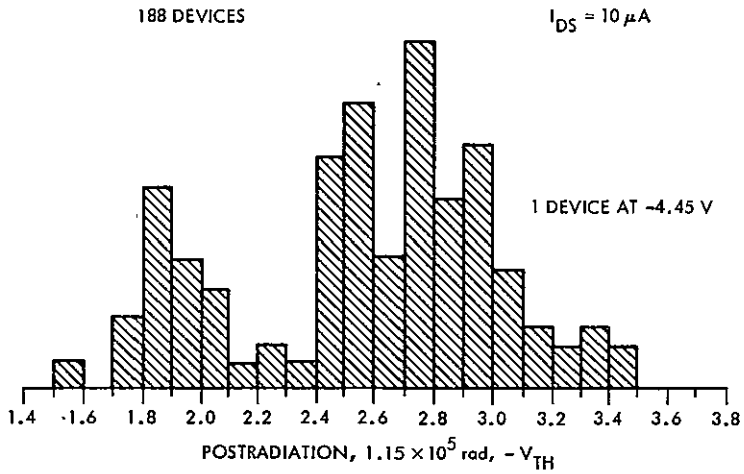

Figure 8-19. Post-irradiation Threshold Voltage of p-Channel Transistor on Test Pattern TA 6372 With 950°C Gate Oxide Anneal in Forming Gas

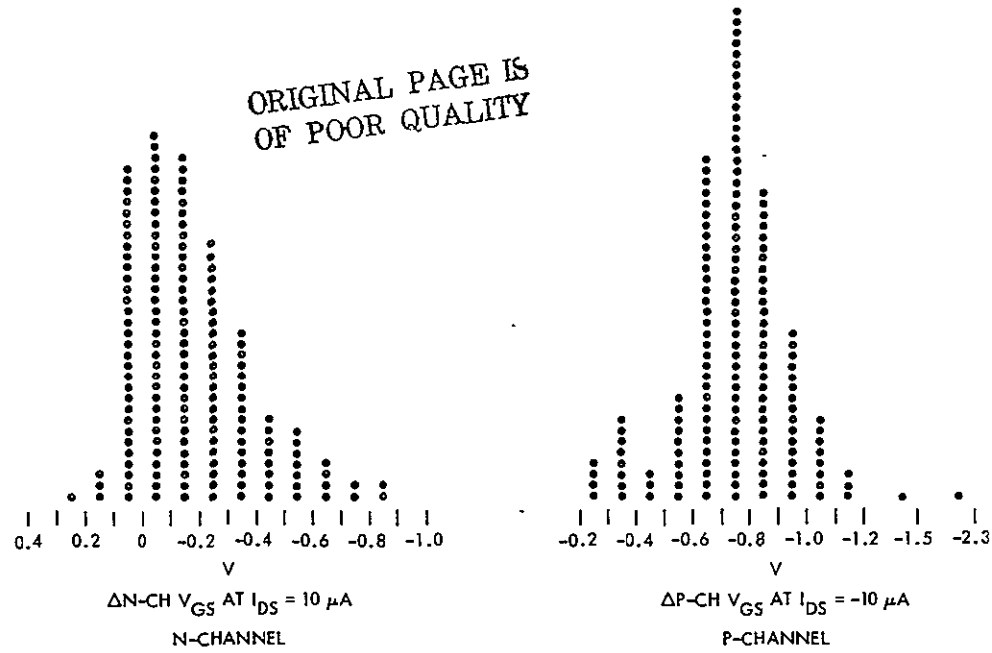

Figure 8-20. Distribution on ΔV_{GS} at I_{DS} After 1/5 x 10^{15} rad(Si)

4. Lots Screened at Less Than 150 krad(Si)

For several lots, the acceptance criterion used was a total dose of less than 150 krad(Si). Table 8-17 lists the device types, lots, conditions, and subsystems involved. Due to severe delivery problems with these device types, the subsystem cognizant engineers chose to accept the marginal devices where their requirements permitted. Run 3722 was not used, as other devices screened to 150 krad(Si) became

available prior to delivery of run 3722. Disposition of runs 3225 and 3193 were as indicated in Table 8-17. Figures 8-21 and 8-22 show the behavior of lot 3193 compared to a typical accepted lot. Both the quiescent supply current and the transmission gate leakage current were substantially worse for lot 3193.

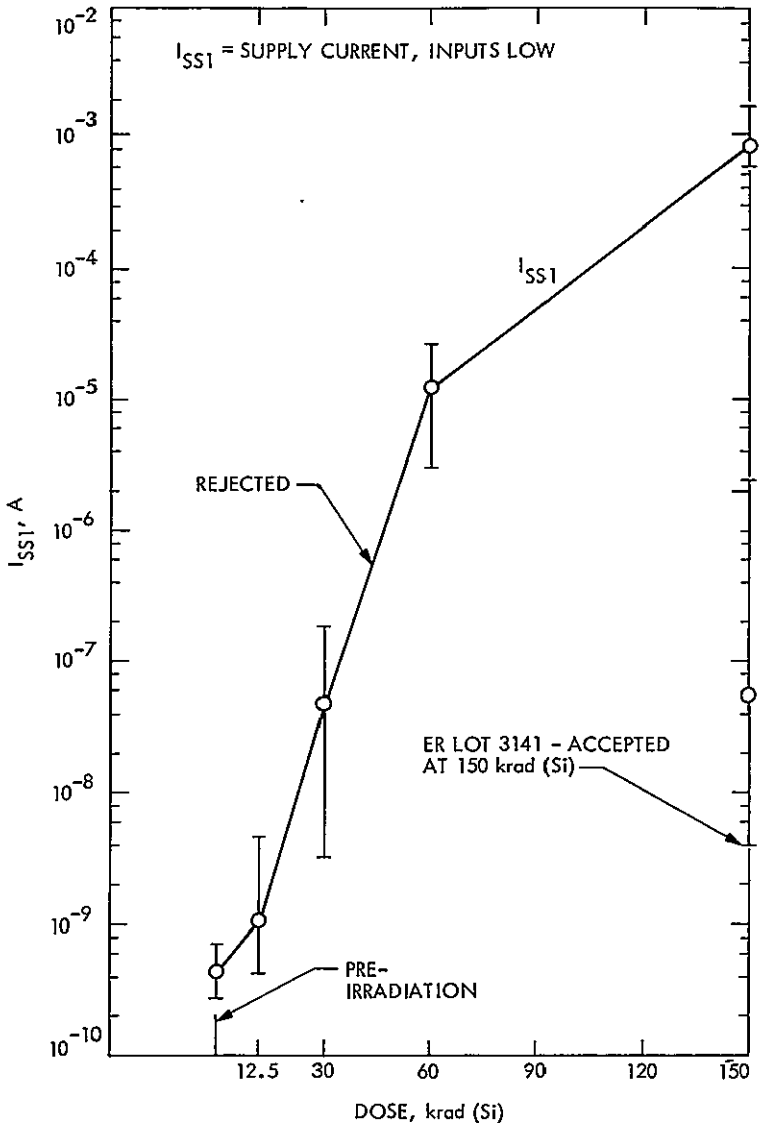

Figure 8-21. Comparison of a Rejected to an Accepted CD4053B Lot for I_{SS1}

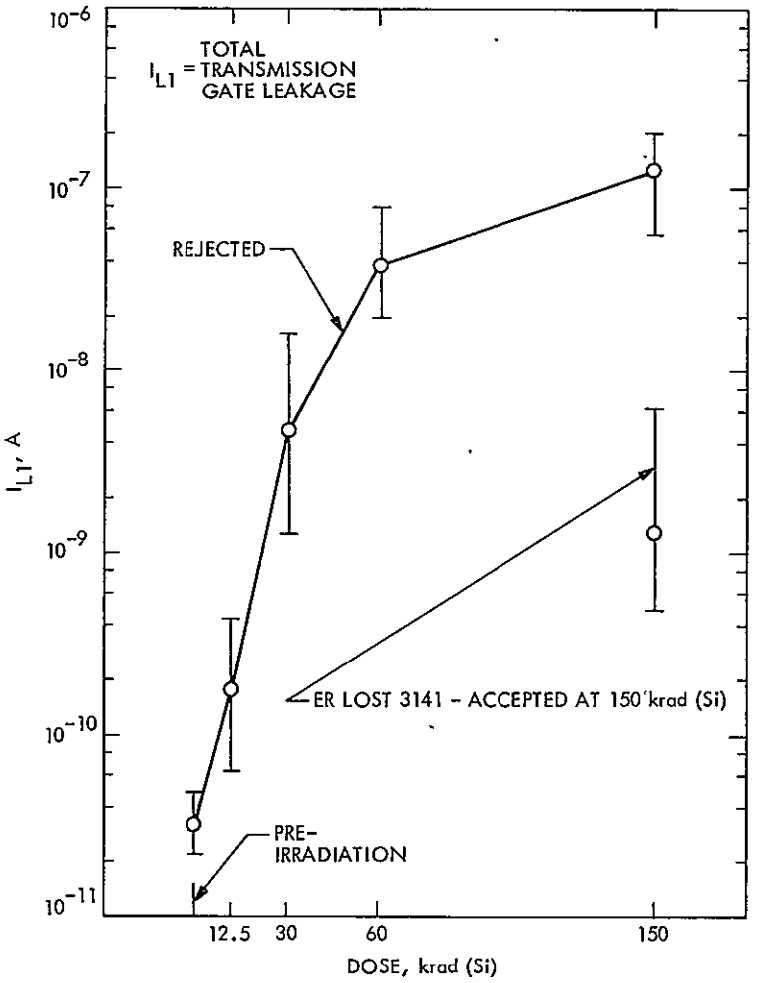

Figure 8-22. Comparison of a Rejected to an Accepted CD4053B Lot for I_{L1}

F. CRYSTAL OSCILLATORS

Crystal screening typically consisted of the manufacturer's fabricating three to six samples from a crystal bar and sending them to the JPL subsystem user. The sample crystals were then irradiated, and the crystal bar was accepted or rejected. Crystals for flight use were fabricated only from accepted bars, with no additional radiation testing. In general the crystals did not degrade significantly from the radiation environment and posed no special problems.

Table 8-17. Diffusion Lots With Acceptance Criteria for a Total Dose of Less Than 150 krad(Si)

Device Type	Diffusion Run	Dose, krad(Si)	No. of Wafers		Potential Subsystem Users[a]
			Tested	Passed	
CD4001	3722	60	19	19	No devices delivered or used.
CD4029	3225	60	18	14	MAG < 60 krad(Si) IRIS, UVS, and CRS, 2 each, Spares only. FDS -- replaced 60-krad(Si) devices with 150-krad(Si) devices through special RCA buyout MIRIS < 35 krad(Si)
CD4053	3193	30	10	10	ISS(ADC) < 15 krad(Si) IRIS < 30 krad(Si)

[a]Subsystem abbreviations are identified in the Definition of Identification Codes.

SECTION IX

CONCLUSIONS AND RECOMMENDATIONS

A. ORGANIZATION OF HARDENING EFFORT

In the Voyager program, radiation was originally not considered to be a problem. Subsequently, Pioneer Jupiter flybys indicated the presence of strong radiation belts, which led to an intensive program to harden the existing Mariner design. At this point, there was not sufficient time to undertake a device-hardening program except in the case of the LM108 and LM102 operational amplifiers and the CMOS CD4000 series, where hardening resulted in improved devices.

A radiation characterization of all sensitive device types was carried out, accompanied by a worst-case circuit analysis which led to redesign where required. However, in most cases the subsystems, because of schedule and resource constraints, were locked into the existing design and previously selected device types, so that spot shielding had to be used. In some instances the shielding level had to be as low as 10 krad(Si). In addition, some inherently very soft devices were used, e.g., the LM139 comparator, the DG181 analog switch, and the ICL 8018 analog-to-digital converter. All these devices required heavy shielding. A further essential step in ensuring survival in the Jupiter radiation belt was an extensive screening program that included wafer lot sampling of CMOS and hybrids, diffusion lot sampling of linear IC's, irradiate-anneal screening, date code lot sampling of transistors, and radiation lot sampling of flight parts.

It is possible to design systems hard to at least 10^6 rad(Si), provided this is made the objective of the program at the outset. In order to achieve such hardness, the program requires a centralized organization that rigidly enforces the following requirements:

(1) Radiation-hard circuit design, including worst-case circuit analysis that is tolerant of some device degradation caused by the radiation environment.

(2) Device selection of components that are relatively radiation-hard, coupled with a radiation characterization program.

(3) A hardness assurance program used in the procurement of devices with well-defined radiation characteristics. Radiation screening of flight parts forms an essential part of such a program.

(4) A development program for hardening soft devices that are considered essential and that cannot be adequately shielded.

B. DEVICE SELECTION

Radiation degradation can usually be improved by the judicious selection of device manufacturers and device types. This approach was severely limited on Voyager, due to time constraints and the requirement for the use of existing designs and equipment. Device type and manufacturer selection is a desirable approach on any program subject to damaging radiation environments. This is due to the fabrication techniques used by the different manufacturers and the inherent problems in CMOS and in certain linear integrated circuits.

In addition, transistors should be selected so that they can be operated near their I_C/h_{FE} peak. Although devices procured from military-controlled production lines are not necessarily harder than the commercial devices, they do have the desirable feature of lot traceability. Procuring commercial devices which are not traceable and then radiation screening them is not a desirable method.

C. HARDENING

1. Introduction

All the Voyager hardening efforts were accomplished by the manufacturer with minimum funding using empirical techniques. This approach should be avoided in future programs. In general, radiation-hardening represents a trade-off between shielding, device hardening, device selection, and circuit design.

Shielding is practicable only for essential device types that are used in very small quantities. Commonly used devices that are inherently soft must be hardened, e.g., CMOS and bipolar linear devices. All devices subject to catastrophic failure modes must be either hardened or shielded.

Surface ionization effects in semiconductor devices depend critically on the wafer fabrication process. It is therefore sometimes possible to obtain a more radiation-resistant device by substituting the product of one vendor for another. Conversely, the radiation resistance may deteriorate very suddenly because of intentional or unintentional process changes on the line. Radiation hardness assurance procedures are needed to safeguard the devices against such a possibility.

Bipolar transistors should be selected according to certain principles, giving preference to transistors with low breakdown voltages and with epitaxial construction. It is also very important to choose transistors so that they can be operated with collector currents near the maximum gain point. In order to radiation-harden circuits, it is important to apply design rules that allow for the operation of devices with degraded parameters as long as they are still functional.

2. Bipolar Linear Devices

The HA2700, LM108A and LM101A operational amplifiers, together with the LM111and LM139 comparator, have been shown to exhibit significant degradation at fluences well below 10^5 rad(Si). Both Pioneer and Voyager currently are using all of these device types and it is highly probable that they will be required on a Jupiter Orbiter.

3. CMOS Devices

It is expected that there will be an extreme desire to make widespread use of the standard 4000 series CMOS devices. The best available production devices today in terms of radiation-hardening utilize the modified oxide anneal process developed for Voyager. These devices are marginally good at 10^5 rad(Si) but fail catastrophically prior to 10^6 rad(Si).

Several hardening techniques are currently under investigation by the military; most of these efforts are directed toward developing a hard gate insulator material.

Of the many programs underway, the one that will likely benefit future programs the most is about to be initiated by the Air Force Materiel Laboratory (AFML). A manufacturing methods program is planned to be established by AFML during this calendar year. The intent is to bring into production 4000 series CMOS/bulk devices which are radiation-tolerant to 10^6 rad(Si).

4. Analog Switches

Three device types (DG129, DG133, DG141) from one analog switch family represented approximately 70 percent of the total Voyager requirements. The driver is a monolithic bipolar device containing lateral pnp transistors. N-channel JFET's are used as the switches. Radiation characterization tests have been performed up to 10^{13} e/cm^2. At that level the devices showed an increase of more than an order of magnitude in on resistance and a severe degradation in their dynamic switching characteristics dependent on the bias conditions during irradiation. The DG129 and DG133 also exhibited large increases in leakage current, which were lot dependent and resulted from inversion layer formation in the JFET's.

The DG181, which is of a different family, made up the balance of the Voyager requirement. The driver is a monolithic device containing both bipolar and MOS transistors. N-channel JFET's are used as the switches. Radiation tests for Voyager found the driver to be extremely radiation sensitive, and the devices required shielding down to 1.25×10^{12} e/cm^2.

D. RADIATION HARDNESS ASSURANCE

With respect to hardness assurance for total ionizing dose, the work done in support of Voyager is likely as large in magnitude as the total of all work done previously. The approaches taken were selected in a climate of immediacy, and although they satisfied the Voyager need, there are some shortcomings associated with them. Examples of their deficiencies are (1) degradation in radiation tolerance is not detected until devices are essentially ready for delivery, and rejection at that stage often impacts subsystem fabrication schedules, (2) bipolar transistors are not subject to sufficient lot control. Hardness assurance methods with greater rigor, as well as improved cost effectiveness, will be required for future programs.

Emphasis should be placed on utilization of methods that can be applied at the earliest possible time in the processing cycle. The final specifications should be tailored to best suit the particular device technology and the process flow of each manufacturer. All test methods, sampling procedures, and guaranteed device specifications at 10^6 rad(Si) should be included.

E. RADIATION TESTING AND DOSIMETRY

In general, the radiation test program was successful. Over 200 device types were characterized in a radiation environment, over 230 IC and transistor screening tests were conducted, and over 13,000 CMOS devices were radiation screened, using four subcontractor test organizations. The controlling test document was the Radiation Test Requirement (RTR) plan. The RTR's were extremely useful in carrying out the above-cited test programs due to the versatility of the RTR, which allowed its use for all the device types tested under the various test conditions.

F. RECOMMENDATIONS

The following recommendations would improve the effectiveness of future programs:

(1) Emphasis should be placed on radiation hardening of circuits via design during the design phase.

(2) The parts program should be started as early as possible to allow adequate time for radiation characterization and collection of degradation data to be used by circuit designers.

(3) Device radiation hardening should be initiated and preferably completed as a pre-project activity.

(4) All transistors and IC's should have diffusion lot traceability.

(5) More emphasis should be placed on detailed written radiation test procedures.

(6) Correlation between different dosimetry methods should be studied and approved.

(7) Devices for radiation characterization testing should be procured very early in the program.

REFERENCES

1-1. Stanley, A.G., Martin, K.E., and Douglas, S., Radiation Design Criteria Handbook, Technical Memorandum 33-763, Jet Propulsion Laboratory, Pasadena, Calif., Aug. 1, 1976.

2-1. Mariner Jupiter/Saturn 1977 Radiation Control Requirements Document, PD 618-229, Rev. A, Appendix A, "Radiation Models," Jet Propulsion Laboratory, Pasadena, Calif., Dec. 19, 1975 (JPL internal document).

3-1. Andrews, J., and Wallen, P., MJS77 Microcircuit Radiation Capability Study, IOM MJS R&QA 217-75, Jet Propulsion Laboratory, Pasadena, Calif., Oct. 9, 1975 (JPL internal document).

4-1. Munroe, M.E., Theory of Probability, McGraw-Hill, New York, 1951.

4-2. Arimura, I., et al., A Study of Electronics Radiation Hardness Assurance Techniques, AFWL-TR-73-134, Vol. III, The Boeing Company, Seattle, Wash., Jan. 1974.

4-3. Radiation Handbook, IOM MJS'77-WSS-75-55, Jet Propulsion Laboratory, Pasadena, Calif., Sept. 5, 1975 (JPL internal document).

4-4. Stanley, A.G., and Price, W.E., Irradiate-Anneal Screening of Total Dose Effects in Semiconductor Devices, Technical Memorandum 33-788, Jet Propulsion Laboratory, Pasadena, Calif., July 15, 1976.

4-5. Peck, D.S., "The Analysis of Data From Accelerated Stress Tests," 9th Annual Proceeding Reliability Physics, Las Vegas, Nev., Apr. 1971, IEEE Catalog No. 71-C-9-PHY, IEEE Editorial Department, 345 East 47th St., New York.

6-1. Vincoff, M., A Study of the Effects of Gate Oxide Anneal Temperature on Radiation Resistance and Reliability, RCA Interim Report, Contract No. 954049, RCA, Apr. 15, 1975.

6-2. Reiss, E.M., and Vincoff, M.N., "Effects of Variation of Gate-Oxide Anneal Temperature on Radiation Resistance and Reliability of C/MOS Devices," paper presented at the 1975 IEEE Annual Conference on Nuclear and Space Radiation Effects, Humboldt State University, Arcata, Calif., July 14-17, 1975.

6-3. Stanley, A.G., and Bergens, D., Review of CMOS Screening, IOM 365-F-70-75, Jet Propulsion Laboratory, Pasadena, Calif., July 25, 1975 (JPL internal document).

6-4. Burghard, R.A., and Gwyn, C.W., "Radiation Failure Modes in CMOS Integrated Circuits," IEEE Trans. Nucl. Sci., Vol. NS-20, No. 6, pp. 300-306, Dec. 1973.

6-5. Gregory, B.L., "Process Controls for Radiation-Hardened Aluminum Gate Bulk Silicon CMOS," IEEE Trans. Nucl. Sci., Vol. NS-22, No. 6, pp. 2295-2302, Dec. 1975.

6-6. Stanley, A.G., and McKenzie, P.F., "Effects of Electron Irradiation on Operational Amplifiers," IEEE Trans. Nucl. Sci., Vol. NS-20, No. 2, pp. 100-107, Apr. 1973.

7-1. Srour, J.R., et al., Radiation Effects on Oxides, Semiconductors, and Devices, HDL-CR-75-171-1, Northrop Research and Technology Center, Hawthorne, Calif., May 1975.

7-2. Yamakawa, K.A., Rate/Anneal Measurements in RCA CMOS, IOM 365-F-44-75, June 5, 1975.

8-1. Gregory, B.L., "Process Controls for Radiation-Hardened Aluminum Gate Bulk Silicon CMOS," paper presented at the 1975 IEEE Annual Conference on Nuclear and Space Radiation Effects, Humboldt State University, Arcata, Calif., July 14-17, 1975.

NASA — JPL — Coml , L.A., Calif